

## **INFORMATION TO USERS**

**This manuscript has been reproduced from the microfilm master. UMI films the text directly from the original or copy submitted. Thus, some thesis and dissertation copies are in typewriter face, while others may be from any type of computer printer.**

**The quality of this reproduction is dependent upon the quality of the copy submitted. Broken or indistinct print, colored or poor quality illustrations and photographs, print bleedthrough, substandard margins, and improper alignment can adversely affect reproduction.**

**In the unlikely event that the author did not send UMI a complete manuscript and there are missing pages, these will be noted. Also, if unauthorized copyright material had to be removed, a note will indicate the deletion.**

**Oversize materials (e.g., maps, drawings, charts) are reproduced by sectioning the original, beginning at the upper left-hand corner and continuing from left to right in equal sections with small overlaps.**

**ProQuest Information and Learning  
300 North Zeeb Road, Ann Arbor, MI 48106-1346 USA  
800-521-0600**

**UMI<sup>®</sup>**

**DISSERTATION**

**CHARACTERIZATION OF THE PH-RESPONSIVE STABILIZATION OF  
GLUTAMATE DEHYDROGENASE AND GLUTAMINASE MESSENGER RNAS**

**Submitted by**

**Jill M. Schroeder**

**Department of Biochemistry and Molecular Biology**

**In partial fulfillment of the requirements**

**For the Degree of Doctor of Philosophy**

**Colorado State University**

**Fort Collins, Colorado**

**Fall 2002**

UMI Number: 3075381

UMI<sup>®</sup>

---

UMI Microform 3075381

Copyright 2003 by ProQuest Information and Learning Company.  
All rights reserved. This microform edition is protected against  
unauthorized copying under Title 17, United States Code.

---

ProQuest Information and Learning Company  
300 North Zeeb Road  
P.O. Box 1346  
Ann Arbor, MI 48106-1346


COLORADO STATE UNIVERSITY

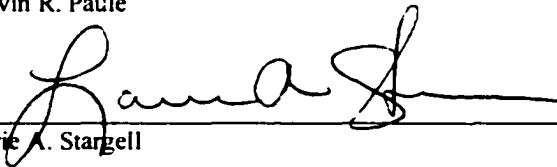
October 11, 2002

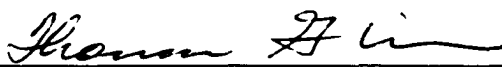
WE HEREBY RECOMMEND THAT THE DISSERTATION PREPARED UNDER OUR SUPERVISION BY JILL M. SCHROEDER ENTITLED CHARACTERIZATION OF THE PH-RESPONSIVE STABILIZATION OF GLUTAMATE DEHYDROGENASE AND GLUTAMINASE MESSENGER RNAS BE ACCEPTED AS FULFILLING IN PART REQUIREMENTS FOR THE DEGREE OF DOCTOR OF PHILOSOPHY.

Committee on Graduate Work

  
James R. Bamberg

  
Marvin R. Paule

  
Laurie A. Stargell

  
Thomas G. Wilson

  
Advisor- Norman P. Curthoys

  
Department Head- Norman P. Curthoys

## ABSTRACT OF DISSERTATION

### CHARACTERIZATION OF THE PH-RESPONSIVE STABILIZATION OF GLUTAMATE DEHYDROGENASE AND GLUTAMINASE MESSENGER RNAs

During chronic metabolic acidosis, the adaptive increase in rat renal ammoniogenesis and gluconeogenesis from glutamine is sustained, in part, by increased expression of the mitochondrial glutaminase (GA) and glutamate dehydrogenase (GDH) enzymes. The increased enzyme levels result from the pH-responsive stabilization of their respective mRNAs. GA mRNA contains a pH-response element (pHRE) within its 3'-untranslated region (3'-UTR) that contains a direct repeat of an 8-base AU-rich sequence (ARE) and binds  $\zeta$ -crystallin/NADPH:quinone reductase ( $\zeta$ -crys/Nqr) with high affinity and specificity.  $\zeta$ -crys/Nqr also binds to the full-length 3'-UTR of the GDH mRNA, but with less affinity. The 3'-UTR of GDH mRNA contains four 8-base AREs that are 88% identical to one of the GA AREs. The individual 8-base ARE from the GA pHRE bind the  $\zeta$ -crys/Nqr with high affinity. The four individual GDH AREs bind  $\zeta$ -crys/Nqr with less affinity than the GA AREs. Competition studies confirmed the relative order of affinities observed in the direct binding studies. Experiments were performed to determine whether the GDH AREs are functional pHREs. Insertion of the GDH 3'-UTR into the stable  $\beta$ -globin plasmid (p $\beta$ G) produced a chimeric mRNA that was stabilized in acidic medium. In functional studies, GDH4 was seen to function as a pHRE.

A tetracycline responsive expression system was created that can activate or inhibit transcription of a single gene within the cell so that the *in vivo* decay of the GA

mRNA could be studied. An 8C line of LLC-PK<sub>1</sub>-F<sup>+</sup> cells stably expressing the tTA protein, a recombinant transcriptional activator protein, was produced. When pTRE2-βG-GA-bGH was stably transfected into the 8C cell line, a homogeneous population of βG-GA mRNA was synthesized using a transcriptional pulse. After creating a transcriptional pulse a pH-responsive stabilization of the βG-GA mRNA was observed. The deadenylation and decay of the βG-GA mRNA over time was monitored to determine the type of decay that occurs under conditions mimicking metabolic acidosis. RNase H treatment was used to obtain a shorter RNA so deadenylation could be easily monitored. Biphasic decay of the βG-GA mRNA was observed under normal and acidic conditions using a synchronous, distributive deadenylation mechanism in the initial phase.

Jill M. Schroeder  
Department of Biochemistry  
And Molecular Biology  
Fort Collins, CO 80523  
Fall 2002

## ACKNOWLEDGMENTS

First and foremost, I would like to express my deepest gratitude to my advisor, Dr. Norm Curthoys, for being a wonderful mentor throughout my time as a graduate student. His patience, guidance, and assistance have been invaluable in completing my Ph.D.

I would also like to thank my committee, Dr. James Bamburg, Dr. Marvin Paule, Dr. Laurie Stargell, and Dr. Thomas Wilson, for helping me to find more inner strength and determination than I believed that I had. I would especially like to thank Dr. Bamburg for his enthusiasm for my research.

I would like to thank all of the members, both past and present, of the Curthoy's lab for their research advice and especially for their friendship and support.

I would like to thank two of my undergraduate advisors, Dr. Jim Platt and Dr. Dennis Barrett, for helping me find my current career path, showing me how exciting science could be, and reminding me to look at the big picture in life. I would also like to thank the many teachers I have had from kindergarten to present for providing me with the wisdom that got me to where I am today.

Special thanks must be made to my friends and above all to my family for their love, support, and encouragement throughout my life. I would like to thank Markus Gloeckler for his love and help in finishing graduate school and this thesis. I especially want to thank my Grandpa George Trapp for the many long talks about my future, his pride in my achievements, and his undying belief that I could accomplish anything in life. Last, but definitely not least, I want to thank my mom Susan Schroeder for everything. Without your assistance, advice, and love at every step throughout my life, I would not be where I am today.

## Table of Contents

<b>1 Introduction.....</b>	<b>1</b>
1.1 Glutamine.....	2
1.2 Glutaminase .....	4
1.3 Glutamate Dehydrogenase .....	5
1.4 Metabolic Acidosis .....	7
1.5 mRNA Stability .....	11
1.5.1 mRNP formation.....	12
1.5.2 Endoribonucleolytic cleavage.....	13
1.5.3 ARE-mediated decay .....	15
1.5.4 Deadenylation .....	15
1.5.5 3'-to-5' mRNA decay .....	18
1.5.6 5'-to-3' mRNA decay .....	19
1.5.7 The link between mRNA stability and translation.....	20
1.6 mRNA-binding proteins.....	23
1.7 LLC-PK <sub>1</sub> -F <sup>+</sup> cell line .....	25
1.8 Stabilization of the GA mRNA.....	26
1.8.1 pH-responsive stabilization of GA mRNA.....	26
1.8.2 Identification and analysis of a pH-responsive element in the GA 3'-UTR...	27
1.8.3 Identification and purification of ζ-crystallin .....	28

1.8.4 Proposed model for the stabilization of the GA mRNA .....	29
1.8.5 Stabilization of the GDH mRNA .....	30
<b>2 Statement of Problem .....</b>	<b>33</b>
<b>3 Materials .....</b>	<b>37</b>
3.1 Materials.....	38
3.2 Buffers and Solutions.....	39
3.2.1 Krebs-Henseleit Saline Buffer (KHS) .....	39
3.2.2 Rat Renal Cortex Cytoplasmic Extraction Buffer .....	39
3.2.3 1X Binding Buffer for FPLC .....	40
3.2.4 100X Binding Buffer for FPLC .....	40
3.2.5 1X Dialysis Buffer, pH 7.4 .....	40
3.2.6 Lower Tris Stock.....	40
3.2.7 Upper Tris stock.....	41
3.2.8 2X Sample Buffer .....	41
3.2.9 4X Reservoir Buffer Stock.....	41
3.2.10 Annealing Buffer .....	41
3.2.11 50X TAE Buffer .....	42
3.2.12 10X Stop Buffer .....	42
3.2.13 5X TBE Buffer.....	42
3.2.14 Type III Buffer (6X) .....	42
3.2.15 Elution Buffer .....	42
3.2.16 10X <i>in vitro</i> Transcription Buffer (from Promega): .....	43
3.2.17 Water-saturated Phenol .....	43

3.2.18 DEPC-treated Water .....	43
3.2.19 10X Binding Buffer .....	43
3.2.20 2X HBSP, pH 7.0.....	43
3.2.21 65 $\mu$ M 5,6-Dichlorobenzimidazole 1- $\beta$ -D-ribofuranoside (DRB).....	44
3.2.22 Solution D (Denaturing Lysis Solution) .....	44
3.2.23 10X MOPS Buffer .....	44
3.2.24 Northern Loading Buffer .....	44
3.2.25 RNA Agarose Gel Running Buffer.....	45
3.2.26 20X SSC .....	45
3.2.27 Hybridization Buffer.....	45
3.2.28 Northern Wash Solutions.....	45
3.2.29 10X RNase H Buffer.....	46
3.2.30 RNase H Denaturing Buffer.....	46
3.2.31 RNase H Gel Loading Buffer .....	46
<b>4 Methods.....</b>	<b>47</b>
4.1 Preparation of rat renal cortical cytosolic extract: .....	48
4.2 Affinity purification of $\zeta$ -crystallin and other pHRE-binding proteins: .....	49
4.3 Construction of pBSSK-GDH1-4 .....	50
4.4 Construction of transcription vectors for GA(R2-IA), GA(R2-IB), and GDH1, 2, 3, and 4: .....	50
4.5 Creation of templates .....	50
4.6 In-Vitro Transcription.....	53
4.7 RNA Electrophoretic mobility shift assay (RNA-EMSA).....	54

<b>4.8 Construction of <math>\beta</math>-Globin Constructs .....</b>	<b>55</b>
<b>4.8.1 p<math>\beta</math>G-GDH.....</b>	<b>55</b>
<b>4.8.2 p<math>\beta</math>G-GA(R2-I) and p<math>\beta</math>G-GDH4 .....</b>	<b>58</b>
<b>4.8.3 p<math>\beta</math>G-GDH4-PCK.....</b>	<b>58</b>
<b>4.9 Cell Culture.....</b>	<b>59</b>
<b>4.10 Creation of stable cell lines using p<math>\beta</math>G vectors:.....</b>	<b>59</b>
<b>4.11 mRNA half-life analysis using DRB .....</b>	<b>60</b>
<b>4.12 Isolation of total RNA.....</b>	<b>60</b>
<b>4.13 Preparation of cDNA probes.....</b>	<b>61</b>
<b>4.14 Northern Analysis .....</b>	<b>61</b>
<b>4.15 Creation of stable pTet-Off cell lines.....</b>	<b>62</b>
<b>4.16 Luciferase Assays to test pTet-Off stable cell lines:.....</b>	<b>63</b>
<b>4.17 Construction of pTRE constructs.....</b>	<b>64</b>
<b>4.17.1 pTRE2-<math>\beta</math>G-GA-bGH .....</b>	<b>64</b>
<b>4.17.2 pTRE2-<math>\beta</math>G-bGH, pTRE2-<math>\beta</math>G-GDH-bGH, pTRE2-<math>\beta</math>G-GA(R2-I)-bGH, and         pTRE2-<math>\beta</math>G-GDH4-bGH .....</b>	<b>64</b>
<b>4.18 Creation of TRE-<math>\beta</math>G-GA-bGH stable cell lines.....</b>	<b>67</b>
<b>4.19 Creation of a Transcriptional Pulse.....</b>	<b>68</b>
<b>4.20 Functional Studies using pTRE2-<math>\beta</math>G-GA-bGH .....</b>	<b>68</b>
<b>4.20.1 Half-life analysis using Dox to inhibit transcription.....</b>	<b>68</b>
<b>4.20.2 Half-life analysis using a transcriptional pulse.....</b>	<b>69</b>
<b>4.21 Preparation of bGH Northern probe.....</b>	<b>69</b>
<b>4.22 Design of RNase H deoxyoligonucleotides .....</b>	<b>69</b>

4.23 RNase H Treatment.....	70
<b>5 Binding and Functional Studies of GDH and GA AREs.....</b>	<b>72</b>
5.1 Binding and Competition Studies .....	73
5.1.1 $\zeta$ -crystallin binds the 3'-UTR of GDH in an Electrophoretic Mobility Shift Analysis (EMSA).....	73
5.1.2 $\zeta$ -crystallin binds the individual AREs from the GA and GDH 3'-UTRs .....	76
5.1.3 GA and GDH AREs compete $\zeta$ -crystallin/GA(R2-I) binding.....	80
5.2 Functional Studies.....	80
5.2.1 $\beta$ G mRNA is stable and not pH-responsive .....	86
5.2.2 pH-responsive stabilization of $\beta$ G-GA mRNA.....	86
5.2.3 GA(R2-I) is a pHRE .....	91
5.2.4 $\beta$ G-GDH mRNA contains a pHRE .....	91
5.2.5 Stability of mRNA containing the GDH4 ARE.....	98
5.2.5.1 $\beta$ G-GDH4 mRNA is not sufficiently destabilized to observe a pH- response.....	98
5.2.5.2 GDH4 functions as a weak pHRE .....	98
<b>6 mRNA Decay Studies using a Tetracycline-Responsive Expression     System.....</b>	<b>104</b>
6.1 Tetracycline-responsive expression system .....	105
6.1.1 Creation and characterization of a tTA expressing LLC-PK <sub>1</sub> -F <sup>+</sup> cell line....	106
6.1.2 Creation and characterization of cell lines stably transfected with pTRE2- $\beta$ G- GA-bGH.....	109

6.1.3 A pH-responsive stabilization of $\beta$ G-GA mRNA does not occur using Dox to inhibit transcription of the TRE- $\beta$ G-GA-bGH transgene .....	114
6.1.4 Creating a transcriptional pulse of $\beta$ G-GA .....	122
6.1.5 $\beta$ G-GA mRNA synthesized during a three hour transcriptional pulse is stabilized under acidic conditions.....	125
6.1.6 Transcription of the TRE2- $\beta$ G-GA-bGH transgene in 8C LLC-PK <sub>1</sub> -F <sup>+</sup> cells is effected by changes in the pH of the medium.....	130
6.1.7 RNase H Treatment of $\beta$ G-GA mRNA.....	133
6.1.7.1 Testing of RNase H treatment on $\beta$ G-GA mRNA.....	133
6.1.7.2 $\beta$ G-GA mRNA is deadenylated as part of a biphasic decay mechanism	136
<b>7 Discussion and Future Directions.....</b>	<b>142</b>
7.1 $\zeta$ -crystallin binding to GA and GDH AREs.....	143
7.2 pH-responsive stabilization of the GDH mRNA .....	145
7.3 The decay of GA mRNA .....	147
7.4 Future Directions.....	150
<b>8 Appendix: Preliminary Characterization of pHRE-BP2.....</b>	<b>157</b>
8.1 FPLC affinity purification of a second pHRE binding protein.....	158
8.2 Preliminary studies of pHRE-BP2 binding.....	163
8.2.1 $\zeta$ -crystallin and pHRE-BP2 bind GA(R2-I).....	163
8.2.2 Antibody analysis of pHRE-BP2 .....	168
8.2.3 GA(R2-I) versus GA(R2-H) binding to pHRE-BP2.....	168
8.3 Future Directions.....	177

## List of Figures and Tables

Fig. 1.1. Schematic representation of renal glutamine catabolism in the proximal tubule cell.....	9
Fig. 1.2. Proposed model for the mechanism by which the onset of metabolic acidosis leads to a stabilization of the renal GA and GDH mRNAs. ....	31
Fig. 4.1. Sequences of oligonucleotides that were used to construct the pBS-GDH and pBS-GA transcription vectors.....	51
Fig. 4.2. Schematic representation of the cloning of p $\beta$ G-GDH, p $\beta$ G-GA(R2-I), and p $\beta$ G-GDH4.....	56
Fig. 4.3. Schematic representation of the cloning of pTRE2- $\beta$ G-GA-bGH, pTRE2- $\beta$ G-GDH-bGH, pTRE2- $\beta$ G-GA(R2-I)-bGH, pTRE2- $\beta$ G-GDH4-bGH, and pTRE2- $\beta$ G-bGH.....	65
Fig. 5.1. $\zeta$ -crys/Nqr binds to GA(R2-I) and GDH1-4 RNAs.....	74
Fig. 5.2. $\zeta$ -crys/Nqr binds to various ribonucleotides that contain the putative AREs from the GA and GDH mRNAs. ....	78
Fig. 5.3. GA(R2-IA) and GA(R2-IB) RNAs compete binding of $\zeta$ -crys/Nqr to the GA(R2-I) RNA. ....	81
Fig. 5.4. GDH1, GDH2, GDH3, and GDH4 RNAs compete binding of $\zeta$ -crys/Nqr to the GA(R2-I) RNA. ....	83
Fig. 5.5. $\beta$ G mRNA is stable not pH-responsive. ....	87
Fig. 5.6. $\beta$ G-GA mRNA is stabilized in response to changes in pH.....	89
Fig. 5.7. GA(R2-I) stabilizes $\beta$ G-GA(R2-I) mRNA under acidic conditions.....	92
Fig. 5.8. Schematic of ARE locations within the 3'-UTRs of GA and GDH.....	94
Fig. 5.9. $\beta$ G-GDH mRNA is stabilized in response to changes in pH.....	96
Fig. 5.10. $\beta$ G-GDH4 mRNA is not sufficiently destabilized to observe a pH-response. ....	99
Fig. 5.11. GDH4 functions as a weak pHRE in $\beta$ G-GDH4-PEPCK mRNA.....	101
Fig. 6.1. Schematic of the Tet-Off System for regulating gene expression.....	107
Fig. 6.2. Characterization of stable LLC-PK <sub>1</sub> -F <sup>+</sup> transfectants expressing the tTA protein. ....	110
Fig. 6.3. Optimization of tetracycline-responsive luciferase expression in 8C cells.....	112
Fig. 6.4. Characterization of 8C LLC-PK <sub>1</sub> -F <sup>+</sup> cells stably transfected with pTRE2- $\beta$ G-GA-bGH.....	115
Fig. 6.5. A pH-responsive stabilization of $\beta$ G-GA mRNA does not occur using Dox to inhibit transcription of the TRE- $\beta$ G-GA-bGH transgene. ....	118

Fig. 6.6. $\beta$ G-GA mRNA is expressed at higher levels using a tetracycline-responsive promoter compared to a RSV promoter.....	120
Fig. 6.7. The inhibition of TRE- $\beta$ G-GA-bGH transcription using various concentrations of Doxycycline (Dox). .....	123
Fig. 6.8. Reinitiation of $\beta$ G-GA mRNA expression after removal of Doxycycline (Dox) from tetracycline-responsive cells. ....	126
Fig. 6.9. $\beta$ G-GA mRNA synthesized during a three hour transcriptional pulse is stabilized under acidic conditions.....	128
Fig. 6.10. Transcription of the TRE2- $\beta$ G-GA-bGH transgene in 8C LLC-PK <sub>1</sub> -F <sup>+</sup> cells is effected by changes in the pH of the medium.....	131
Fig. 6.11. Schematic of RNase H digestion of $\beta$ G-GA mRNA. ....	134
Fig. 6.12. RNase H treatment shortens $\beta$ G-GA mRNA.....	137
Fig. 6.13. $\beta$ G-GA mRNA is deadenylated as part of a biphasic decay mechanism. ....	139
Fig. 7.1. A model for the coordinate induction of GA, GDH, and PEPCK gene expression during metabolic acidosis through the activation of the p38 SAPK signaling pathway. ....	155
Fig. 8.1. Original protein elution profile from an FPLC affinity column for $\zeta$ -crys/Nqr. ....	159
Fig. 8.2. Protein elution profile from an FPLC affinity column.....	161
Fig. 8.3. $\zeta$ -crys/Nqr and pHRE-BP2 bind GA(R2-I). ....	164
Fig. 8.4. Analysis of binding synergism between $\zeta$ -crys/Nqr and pHRE-BP2 to GA(R2-I).....	166
Fig. 8.5. Anti- $\zeta$ -crys/Nqr antibodies do not effect pHRE-BP2 binding to GA(R2-I)....	169
Fig. 8.6. Synergistic binding to GA(R2-H) to $\zeta$ -crys/Nqr and pHRE-BP2 and the effect of RNase T1 treatment on binding.....	172
Fig. 8.7. Comparison of $\zeta$ -crys/Nqr and pHRE-BP2 binding to GA(R2-I) and GA(R2-H). ....	174
 Table 3.1. Summary of Half-life ( $t_{1/2}$ ) Values at pH 7.4 and 6.9 for Chimeric RNAs....	103

## **Abbreviations**

3'-UTR - 3'-untranslated region

5'-cap - 5'-7-methyl-guanosine cap

+/- S.D. – plus or minus the standard deviation

ARE - AU-rich element

AU-rich - adenylate- and uridylate- rich

b – base

bp – base pair

$\beta$ G –  $\beta$ -globin

bGH - bovine growth hormone

BME -  $\beta$ -Mercaptoethanol

BSA – bovine serum albumin

CMV - cytomegalovirus

DEPC - diethyl pyrocarbonate

DNA – deoxyribonucleic acid

Dox - Doxycycline

DRB - 5,6-dichlorobenzimidazole 1- $\beta$ -D-ribofuranoside

DTT - dithiothreitol

EDTA - ethylenediaminetetraacetic acid

ELAV - embryonic lethal abnormal visual

EMSA - Electrophoretic Mobility Shift Assay

ErEN - erythroid cell-enriched endoribonuclease

FBPase - fructose 1,6-bisphosphatase

FPLC - fast protein liquid chromatography

G418 - geneticin

GAPDH - glyceraldehyde-3-phosphate dehydrogenase

GDH - glutamate dehydrogenase

GA - glutaminase

GM-CSF - granulocyte-macrophage colony-stimulating factor

hnRNP - heterogeneous nuclear ribonucleoprotein

IRE - iron-responsive element

IRP - iron regulatory protein

JNK - c-jun N-terminal kinase

kb - kilobase

kDa - kilodalton

LLC-PK<sub>1</sub>-F<sup>+</sup> cells - LLC-PK<sub>1</sub>-FBPase<sup>+</sup> cells

Luc - luciferase

MAPK - mitogen-activated protein kinase

mCRD - major protein-coding-region determinant of instability

MKK - mitogen-activated protein kinase kinase

MOPS - 3-(N-morpholino)propanesulfonic acid

mRNA - messenger ribonucleic acid

**mRNP - messenger ribonucleoproteins**

**nt - nucleotide**

**oligo - oligodeoxynucleotide**

**PABP - poly (A) binding protein**

**PAIP-1 - PABP-interacting protein 1**

**p $\beta$ G -  $\beta$ -globin/growth hormone vector**

**PBS – phosphate buffered saline**

**pBSSK - pBluescript II SK (-)**

**PAN1 - PABP-dependent poly (A) nuclease**

**PCR – polymerase chain reaction**

**PEPCK - phosphoenolpyruvate carboxykinase**

**pH<sub>i</sub> - intracellular pH**

**pHRE - pH-responsive element**

**PI3-K - phosphatidylinositol 3-kinase**

**PminCMV - minimal immediate early promoter of cytomegalovirus**

**PMR-1 - polysomal ribonuclease 1**

**PMSF - phenylmethylsulfonylfluoride**

**pol II – polymerase II**

**RNA –ribonucleic acid**

**RNase – ribonuclease**

**RSV - Rous sarcoma virus long terminal repeat promoter**

**SAPK - stress-activated protein kinase**

**SDS - sodium dodecylsulfate**

**SGLT1 - Na<sup>+</sup>/glucose cotransporter**

**t<sub>1/2</sub> – half-life**

**TCA - tricarboxylic acid**

**tet - tetracycline**

**tetO - tetracycline operator sequence**

**TetR - tet repressor**

**TNF- $\alpha$  - tumor necrosis factor alpha**

**TRE - tetracycline-responsive element**

**TTP - tristetraprolin**

**U - units**

**UV – ultraviolet**

**VP16 - virion protein 16**

**$\zeta$ -crys/Nqr -  $\zeta$ -crystallin/NADPH:quinone reductase**

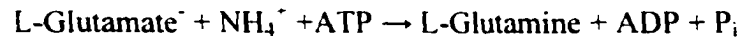
**$\zeta$ -crystallin -  $\zeta$ -crystallin/NADPH:quinone reductase**

# **1 Introduction**

## **1.1 Glutamine**

Glutamine is an abundant amino acid that accounts for over 60% of the free  $\alpha$ -amino acids in the body (Curthoys & Watford 1995). Glutamine plays many important roles in transporting carbon and nitrogen between organs of the body. The metabolism of glutamine contributes to key metabolic pathways, such as ureagenesis, ammoniogenesis, and gluconeogenesis.

Glutamine synthesis and hydrolysis in mammals were first observed by Krebs in 1935 (Krebs 1935). Glutamine synthetase uses the hydrolysis of ATP to convert glutamate and an ammonium ion into glutamine (See the equation below) (Adam & Simpson 1974).



The synthesis of glutamine occurs in the majority of tissues in the body, though the highest activities are in skeletal muscle, the lungs, and adipose tissue (Curthoys & Watford 1995).

Many of the tissues that synthesize glutamine also catabolize glutamine. The major enzyme used for the catabolism of glutamine is glutaminase (Curthoys & Watford 1995). Glutamine can be both synthesized and catabolized in liver, kidney, brain, lungs, and adipose tissue. The relative rates of the two reactions change with the metabolic conditions of the various tissues (Souba 1993).

Glutamine is also catabolized by the membrane-bound  $\gamma$ -glutamyl transpeptidase and the cytosolic glutamine aminotransferase  $\omega$ -deamidase pathway (Nissim 1999). The metabolism of glutamine provides precursors for transamination reactions, the  $\gamma$ -glutamyl

cycle, the purine nucleotide cycle, the tricarboxylic acid (TCA) cycle, and the hepatic urea cycle. Glutamine is used in these pathways to synthesize glucose, urea, purines, pyrimidines, glucosamine, and other amino acids (Curthoys & Watford 1995). However, less than 5% of glutamine present in the body is used for the synthesis of purines, pyrimidines, glucosamine, and other amino acids. The majority of the glutamine is used as a major respiratory fuel in the production of energy for cells of the intestinal epithelium, the immune system, the fetus, hair follicles, and tumors.

Glutamine was originally considered a non-essential amino acid due to its high levels of synthesis in the body (Neu et al 1996). However, it has been reclassified as a conditionally essential amino acid, since it has been shown to be effective in treating critically ill patients. Patients recovering from trauma, major surgery, or sepsis, do not synthesize and/or store sufficient glutamine to meet their metabolic needs.

Different neurons in the brain can use glutamine as a precursor for the synthesis of glutamate or  $\gamma$ -aminobutyric acid that function as excitatory or inhibitory neurotransmitters, respectively (Curthoys & Watford 1995). Glutamine synthesis in the brain occurs primarily in the glial cells. Thus, glutamine synthesis and utilization in the brain occur via an inter-cellular cycle.

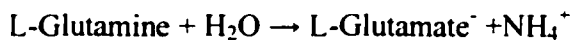
In the liver, the catabolism of glutamine by glutaminase to generate urea and glucose occurs primarily in the periportal cells (Curthoys & Watford 1995). The liver also acts as a glutamine producer. A 1-3 cell layer of hepatocytes surrounding the perivenous region of the acinus expresses high levels of glutamine synthetase. These cells trap ammonia that escaped ureagenesis and use it to generate glutamine. As a result of the separation and independent regulation of glutamine catabolism and synthesis

within the liver, this organ contributes significantly to maintenance of glutamine homeostasis.

Under normal acid-base balance, the kidneys metabolize very little glutamine (Squires et al 1976). The acute onset of metabolic acidosis causes the kidneys to extract more glutamine from the blood (Hughey et al 1980). The increased extraction of glutamine results in an increased flux through the glutaminase and glutamate dehydrogenase pathway (Curthoys & Watford 1995). The products of this catabolism are used to partially correct the metabolic acidosis.

## **1.2 Glutaminase**

Many enzymatic reactions use glutamine as a substrate. However, a true glutaminase activity generates stoichiometric amounts of glutamate and ammonium ion by deamidating glutamine (See the equation below) (Meister 1975).



The glutaminase that catalyzes this reaction is the phosphate-dependent glutaminase (GA), which is also known as mitochondrial glutaminase, phosphate-activated glutaminase and glutaminase I (Curthoys & Watford 1995).

There are two isozymes of phosphate-dependent glutaminase, which catalyze the same reaction, but have different sequences, structures, and kinetics (Curthoys & Watford 1995). The first isozyme is the liver-type enzyme, which in the rat is found solely in the mitochondrial matrix of the postnatal liver. The second isozyme is the kidney-type enzyme that is expressed at high levels in the mitochondria of kidney, brain, intestine, and fetal liver tissues and in lower levels in a wide range of other tissues. Within the

coding regions of the genes of the two isozymes, there is a >70% identity. The amino acid sequences predicted from the cDNAs of the two isoenzymes show a >75% identity. The pattern of the variation between amino acids indicates that the two types of glutaminase are products of two different genes.

The rat kidney-type glutaminase cDNA was isolated by screening rat cDNA libraries (Shapiro et al 1991). The cDNA was transcribed and translated *in vitro* to produce a 74-kDa protein (Shapiro et al 1991), which is the same size observed in *in vivo* pulse-chase experiments (Perera et al 1990; Perera et al 1991). This precursor protein is imported into mitochondria and then processed to a 72-kDa intermediate that is alternatively cleaved to yield either a 66-kDa or a 68-kDa mature subunit (Perera et al 1990; Perera et al 1991; Shapiro et al 1991). A 66-kDa protein subunit is synthesized more rapidly than a 68-kDa subunit. The slower rate of production of the 68-kDa subunit accounts for the 3:1 ratio observed for the 66- and 68-kDa subunits. Antibodies prepared against rat renal glutaminase react with both the 66- and 68-kDa subunits of glutaminase, isolated from either brain or kidney tissue (Shapiro et al 1987). The processing reactions that produce the two mature glutaminase subunits are catalyzed by the mitochondrial matrix processing peptidase (Srinivasan et al 1995).

### **1.3 Glutamate Dehydrogenase**

The oxidative deamination of glutamate to  $\alpha$ -ketoglutarate and an ammonium ion is catalyzed by the enzyme glutamate dehydrogenase (GDH) (See the equation below) (Wright & Knepper 1990).



GDH cDNAs have been isolated from human brain (Banner et al 1987; Nakatani et al 1988) and liver (Nakatani et al 1987) and from rat liver (Das et al 1989).

The cDNAs from both human and rat encode a 558-amino acid precursor protein (Kaiser et al 1992). The cDNA sequences for these proteins have a sequence identity of 91%. A comparison of the sequences of the GDH cDNAs from brain and the liver suggest that their proteins are encoded by a single gene that uses alternative polyadenylation sites to create the two distinct mRNAs. Different tissues express GDH mRNA at various levels (Banner et al 1987; Nakatani et al 1987).

The brain form of GDH plays a role in astrocytes by creating  $\alpha$ -ketoglutarate that is oxidized in the TCA cycle to supply energy and lactate (Schousboe et al 1997; Sonnewald et al 1997). This reaction is also important due to the lack of pyruvate carboxylase in neurons, which limits the de novo synthesis of TCA cycle intermediates. Therefore, the  $\alpha$ -ketoglutarate and lactate that are synthesized in astrocytes can be transported to the neurons as needed.

In the liver, the main role of GDH is to form glutamate through the reductive amination of  $\alpha$ -ketoglutarate (Nissim 1999). The glutamate is then used to synthesize glutamine. The GDH reaction in liver does not generate ammonium ions for use in ureagenesis.

In the kidneys, GDH activity is greatest in the proximal tubules, but it is found at lower levels in other parts of the kidney (Wright et al 1992). During chronic acidosis, the levels of GDH mRNA are increased only in the renal cortex. The activity of GDH is increased three-fold only in the S1 and S2 proximal tubules in chronically acidotic rats (Wright & Knepper 1990) due to an increase in total GDH protein (Seyama et al 1973).

Interestingly, mitochondrial GA (Curthoys & Lowry 1973) and cytosolic phosphoenolpyruvate carboxykinase (PEPCK) (Burch et al 1978) activity levels are also increased only in the S1 and S2 proximal tubules in rats suffering from chronic acidosis.

#### **1.4 Metabolic Acidosis**

The renal catabolism of glutamine is increased by the onset of metabolic acidosis (Tannen 1993). In normal acid-base balance, very little of the plasma glutamine is metabolized in the kidney (Brosnan et al 1988). Approximately 20% of the glutamine in the plasma is filtered by the glomeruli into the lumen of the nephron (Curthoys & Gstraunthaler 2001). The majority of the filtered glutamine is reabsorbed in the proximal convoluted tubule. The glutamine is transported across the apical brush border membrane into the proximal tubule cell and is then transported across the basolateral membrane of the cell and back into the blood. Only a small proportion of the filtered glutamine is transported into the mitochondrial matrix, where it is catabolized by GA and GDH.

However, during acute metabolic acidosis, 30% of the plasma glutamine is extracted and metabolized as it travels through the kidney (Curthoys & Gstraunthaler 2001). Thus, more plasma glutamine is extracted into the proximal tubule cell than can be accounted for by the amount of plasma glutamine that is filtered by the glomeruli. This indicates that glutamine is also being removed from the blood due to a reversal of the basolateral transporter. During chronic acidosis, one-third of the total plasma glutamine is extracted and metabolized in a single pass through the kidney.

Ammoniogenesis and gluconeogenesis are coupled to the maintenance of acid-base balance (Goodman et al 1966). Thus, the levels of glutaminase (GA), glutamate

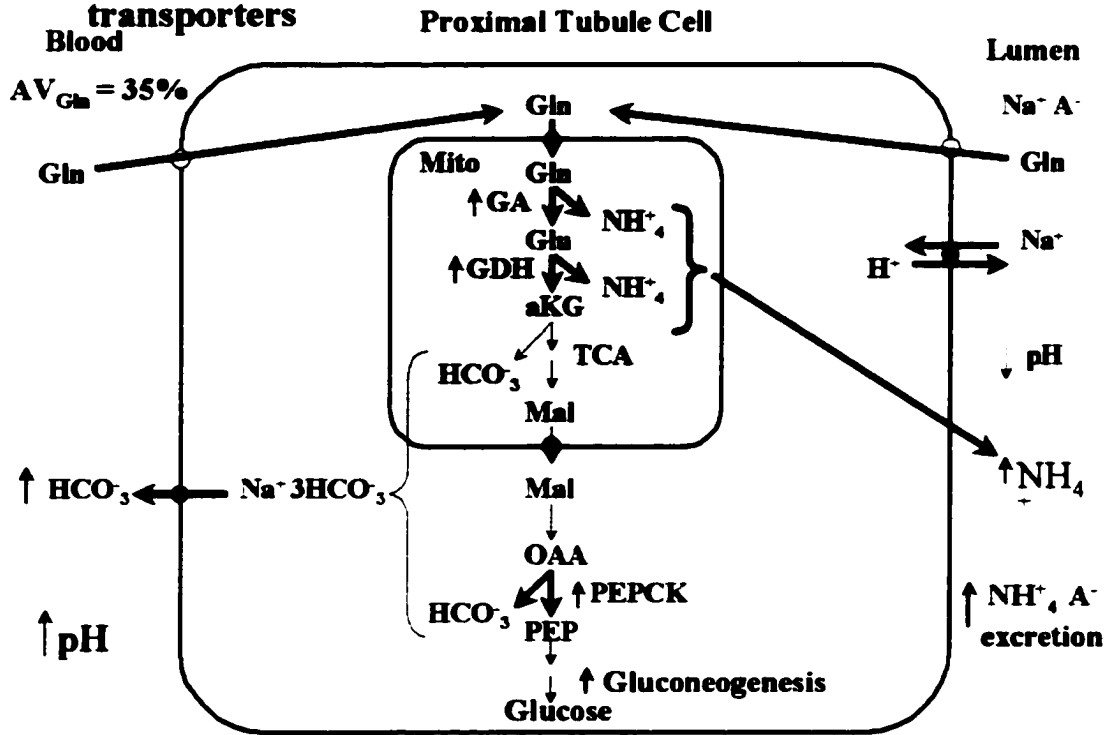
dehydrogenase (GDH), and phosphoenolpyruvate carboxykinase (PEPCK) are increased during acidosis (Fig. 1.1). The increased rates of reactions catalyzed by these enzymes yield a greater level of metabolites, which helps compensate for the decrease in blood pH (Curthoys & Gstraunthaler 2001). In rats suffering from chronic acidosis, the amount of GA is increased seven to twenty fold within the S1 and S2 segments of the renal proximal convoluted tubule (Curthoys & Lowry 1973). The amount of GDH in the kidney is also increased three fold in the S1 and S2 segments of the proximal convoluted tubules (Wright & Knepper 1990). The increase of GA and GDH activity levels causes an increased production of ammonium ions (Curthoys & Watford 1995). These ions function as expendable cations that facilitate excretion of titratable acids in the urine while conserving  $\text{Na}^+$  and  $\text{K}^+$  ions. This is accomplished by increasing the activity of the apical  $\text{Na}^+/\text{H}^+$  antiporter causing an acidification of the fluid in the lumen of the proximal tubule that ensures the excretion of ammonia (Preisig & Alpern 1988).

The level of PEPCK is increased six fold (Hwang & Curthoys 1991) in the S1 and S2 segments of the proximal convoluted tubule during chronic acidosis (Burch et al 1978). PEPCK is a key regulatory enzyme in the catabolism of  $\alpha$ -ketoglutarate to phosphoenolpyruvate and it catalyzes the rate-limiting step in renal gluconeogenesis (Curthoys & Watford 1995). The increase in PEPCK activity also leads to an increased synthesis of bicarbonate ions. The bicarbonate ions are exported into the venous blood by the  $\text{Na}-3\text{HCO}_3^-$  symporter. This process partially compensates the decrease in blood pH caused by the metabolic acidosis (Preisig & Alpern 1988). The increase in the level of PEPCK is caused by an increased rate of transcription of the PEPCK mRNA (Hanson & Reshef 1997).

**Fig. 1.1. Schematic representation of renal glutamine catabolism in the proximal tubule cell.**

During chronic acidosis, there is an increase in the levels of glutaminase (GA), glutamate dehydrogenase (GDH), phosphoenolpyruvate carboxykinase (PEPCK), the mitochondrial glutamine transporter, the apical  $\text{Na}^+/\text{H}^+$  exchanger, and the basolateral  $\text{Na}^+-3\text{HCO}_3^-$  cotransporter. The increased activity in ammoniagenic and gluconeogenic pathways during metabolic acidosis is shown with thicker arrows.

**Chronic Acidosis - ↑ GA, GDH, PEPCK and transporters**



The increase in the activity of GA during metabolic acidosis is due to an increased synthesis of GA (Tong et al 1986) caused by a rise in the level of total and translatable GA mRNA (Hwang & Curthoys 1991; Tong et al 1987). The increase in the levels of GA mRNA is not due to an increased rate of transcription (Hwang & Curthoys 1991; Hwang et al 1991), as is seen with PEPCK, but rather it is due to a selective stabilization of the GA mRNA (Hansen et al 1996; Laterza & Curthoys 2000; Laterza et al 1997). The increase in GDH mRNA during metabolic acidosis occurs with similar kinetics, suggesting that GDH may also be increased by a pH- responsive stabilization of the mRNA (Kaiser et al 1992). This is an important way of controlling the level of mRNA, and thus the level of enzyme, since the levels of an mRNA can increase or decrease by several fold due to a change in half-life without any change in transcription levels (Ross 1995).

### **1.5 mRNA Stability**

Knowledge of how an mRNA is stabilized and destabilized is rapidly expanding, but there remains much to be learned. The stability of an mRNA, which is determined by measuring its half-life, can vary over a broad range. Some mRNAs have a short half-life of less than 30 min, while others are very stable with a half-life of over 30 h (Ross 1995). Furthermore, the half-life of an mRNA can be modulated by a variety of endogenous and exogenous signals (Ross 1995; van Hoof & Parker 2002). This modulation of half-life plays an important role in the post-transcriptional regulation of gene expression since the abundance of an mRNA can fluctuate several fold due to a change in half-life. Cells utilize this mechanism during growth and differentiation and to respond to various environmental changes and stresses.

The stability of an mRNA is determined by the presence of a cis-acting element within the mRNA (Ross 1995). These elements are either specific sequences or structures found in the RNA. Some common cis-acting elements are the 7-methyl-guanosine cap at the 5'-end of the mRNA (5'-cap), stem-loop structures, adenylate- and uridylate- rich (AU-rich) elements (ARE), and the poly (A) tail. Stabilization or destabilization can be regulated by trans-acting factors, usually mRNA binding proteins, which interact with the cis-acting elements.

Three known mRNA decay pathways control the level of an mRNA within a eukaryotic cell (Hanson & Schoenberg 2001). These are 1) specific endoribonucleolytic cleavage followed by exoribonuclease activity, 2) mRNA deadenylation followed by decapping and 5'-to-3' exoribonuclease activity, and 3) mRNA deadenylation followed by 3'-to-5' exosome mediated decay. All of these decay pathways breach the protective ends of the mRNA and facilitate exoribonucleolytic degradation. In this section, the various pathways that mediate degradation and elements that regulate mRNA stability will be discussed.

### **1.5.1 mRNP formation**

The 5'-cap and the poly (A) tail are known to protect mRNA from degradation in the cell. The resulting stabilization is accomplished by the formation of messenger ribonucleoproteins (mRNPs) (Wells et al 1998). In these RNA/protein complexes, the 5'-cap, the poly (A) tail, poly (A) binding protein (PABP), eIF4G, and eIF4E interact with each other to protect the RNA from degradation. The mRNPs are also believed to play a role in protein translation (Gao et al 2000). Experiments conducted by the Wilusz laboratory suggest the presence of two distinct mRNP degradation pathways, one of

which is dependent on translation and one that is independent of translation (Gao et al 2000).

In both pathways, eIF4E is bound to the 5'-cap and PABP is bound to the poly (A) tail with eIF4G acting as a bridging protein between eIF4E and PABP (Gao et al 2000; Gao et al 2001). In the translation independent pathway, the interaction between the 5'-cap and eIF4E is either inhibited or reversed. This allows a 3'-to-5' poly (A) specific deadenylase (DAN/PARN), which is associated with the 5'-cap, to shorten or remove the poly (A) tail. DAN/PARN then recruits a decapping protein and/or a 3'-to-5' exonuclease(s) to degrade the remaining RNA. The deadenylation and subsequent degradation of the mRNA can be averted by the recruitment of a stabilizing ARE-binding protein, such as HuR. However, the recruitment of other ARE-binding proteins, such as TTP, can enhance mRNA turnover by recruiting a ribonuclease or disrupting the protective RNA/protein complexes. The translation dependent pathway is discussed in the section regarding the link between mRNA stability and translation.

### **1.5.2 Endoribonucleolytic cleavage**

Endoribonucleolytic cleavage of an mRNA bypasses the need to remove the 5'-cap or the poly (A) tail in order to degrade the mRNA (Cunningham et al 2001). An endonuclease cleaves the mRNA at a specific sequence and thus produces two unprotected fragments of mRNA that can be degraded by exonucleases. Specific examples that elucidate the role of endonucleolytic cleavage in the degradation of an mRNA are discussed below.

The most well characterized example of this type of decay involves the iron-responsive element (IRE). The IRE that contains five homologous stem-loop structures

within the 3'-UTR, controls the stability of the transferrin receptor mRNA (Ross 1995). The binding of an iron regulatory protein (IRP) to the IRE stabilizes the mRNA by preventing the recruitment of an endonuclease that cleaves within the IRE region of the 3'-UTR. The formation of the IRE/IRP complex occurs when the cellular levels of iron are low so that an increased amount of the transferrin receptor is synthesized. The cytosolic aconitase has been shown to function as an IRP (Haile et al 1992). This enzyme contains an essential iron-sulfur center that also functions as a sensor of iron availability within the cell.

The  $\alpha$ -globin mRNA is protected from endonucleolytic cleavage by formation of a protective complex that requires the poly (A) tail (Wang & Kiledjian 2000). The necessity of the poly (A) tail for stabilization is not observed for the degradation of some mRNAs that are initiated by endonucleolytic cleavage. However, in this system, the mRNA is protected by the formation of a complex that links the endonucleolytic cleavage site and the poly (A) tail through the interactions of the PABP and two  $\alpha$ CP proteins. When this complex is disrupted, the sequence specific erythroid cell-enriched endoribonuclease (ErEN) gains access to the cleavage site and initiates degradation of the  $\alpha$ -globin mRNA.

While some endonucleases recognize structural elements, such as stem-loops, others cleave mRNAs at a specific sequence. The latter sites can be protected by the binding of a stabilizing protein. An example is a U-rich region of the p27kip1 mRNA, which encodes an inhibitor of cyclin-dependent kinases (Zhao et al 2000). The HuR protein stabilizes this mRNA by binding to the U-rich element, and inhibits its cleavage by a unidentified endonuclease.

### **1.5.3 ARE-mediated decay**

Elements found within the 3'-UTR dictate the half-life of most mRNAs (Chen & Shyu 1995; Ross 1995). AREs are frequently found in the 3'-UTR of many unstable mRNAs and are the most well characterized determinant of mRNA half-life (Chen & Shyu 1995). AU-rich elements serve as the binding site for a number of mRNA (or ARE)-binding proteins. These proteins effect turnover by recruiting or by blocking the recruitment of a ribonuclease to the mRNA (Chen et al 2001; Chen & Shyu 1995).

Interestingly, ARE-mediated decay can be inhibited by activation of a signaling pathway. For example, the proinflammatory cytokine induced activation of the p38 mitogen-activated protein kinase (MAPK) pathway leads to an inhibition of ARE-mediated decay of the IL-1 mRNA (Winzen et al 1999). The IL-3 interleukin mRNA containing a Class II ARE (explained below) is stabilized by ionomycin-induced activation of the c-jun N-terminal kinase (JNK)-stress-activated kinase pathway in mast cells, however stabilization does not occur if the Class II ARE is replaced with a Class I ARE (Ming et al 1998).

Deadenylation is the initial step in the degradation of the majority of mRNAs (Chen & Shyu 1995; van Hoof & Parker 2002). After the poly (A) tail has been shortened, the mRNA can be degraded from the 3'-end or it can be decapped and degraded from the 5'-end. This type of biphasic degradation is a prominent method of decay found in eukaryotes.

### **1.5.4 Deadenylation**

Deadenylation is the first step in the biphasic decay of mRNAs in both yeast (Decker & Parker 1993) and mammals (Ross 1995). Under normal conditions, the

binding of PABP to the poly (A) tail protects the mRNA from deadenylation (Ross 1995). However, when PABP is not associated, the poly (A) tail is shortened or removed by a deadenylase. At this point, the second phase of decay occurs, degrading the mRNA body. The deadenylation of an mRNA is carried out by a 3'-to-5' poly (A) specific deadenylase, DAN/PARN, in mammals (Gao et al 2000) and by a 3'-to-5' PABP-dependent poly (A) nuclease (PAN1) in yeast (Lowell et al 1992).

Biphasic degradation in which a deadenylation phase precedes a general decay phase was initially observed using transcriptional pulse-chase experiments (Chen et al 1995; Xu et al 1998). Synchronous and asynchronous deadenylation phases, which are indicative of distributive (non-processive) or processive ribonucleolytic deadenylation, have been classified into the three distinct patterns of deadenylation, Class I, II, and III (Chen & Shyu 1995; Peng et al 1996; Wilson & Treisman 1988). These deadenylation types are controlled by different AREs. mRNA decay, using Class I or II degradation, is seen in molecules containing one or more copies of an AUUUA sequence within the 3'-UTR (Xu et al 2001). In Class I deadenylation, there are 1 to 3 copies of the sequence AUUUA scattered throughout a U-rich region of the 3'-UTR. Class I AREs are found in mRNAs such as, c-fos and c-myc. Class II AREs are found solely in the mRNAs encoding cytokines, such as granulocyte-macrophage colony-stimulating factor (GM-CSF) and tumor necrosis factor alpha (TNF- $\alpha$ ). These AREs contain 5 to 8 overlapping copies of the AUUUA motif within the 3'-UTR. Class III AREs usually contain a U-rich region and may encode other unidentified elements, but do not contain the AUUUA sequence. Class III sequences are found in mRNAs such as, c-jun.

mRNAs containing Class I or III AREs display a biphasic decay that is initiated by synchronous poly (A) shortening of the mRNA population and is followed by the rapid decay of the mRNA body (Chen et al 1994; Chen & Shyu 1994). Synchronous deadenylation is consistent with a mechanism of distributive or non-processive ribonucleolytic removal of the poly (A) tail. In this type of decay, while the poly (A) tail is shortened to 30-60-nt, the concentration of mRNA remains fairly constant (Chen & Shyu 1995; Peng et al 1996). However, once the shortening of the poly (A) tail is complete, the body of the mRNA is rapidly degraded. The decay of the mRNA body following deadenylation follows first-order kinetics.

In mRNAs containing Class II AREs, degradation is preceded by asynchronous or processive deadenylation of the mRNA (Chen & Shyu 1995; Peng et al 1996). This mechanism produces several kinetic intermediates, the smallest of which is the poly (A)<sup>-</sup> mRNA. The poly (A)<sup>-</sup> mRNA species is present in extremely low quantities while the various poly (A)<sup>+</sup> mRNA intermediates may be present at high levels. This pattern is consistent with the rapid degradation of the mRNA body immediately following removal of the poly (A) tail. Therefore, the Class II ARE-containing mRNAs may recruit a different ribonuclease that catalyzes a processive deadenylation (Wilson & Treisman 1988).

The absence of the poly (A) tail drastically destabilizes an mRNA (Ross 1995). Two degradation pathways are possible following deadenylation: the first involves the removal of the 5'-cap followed by 5'-to-3' degradation of the mRNA body and the second involves the recruitment of a 3'-exonuclease or in most cases an exosome to degrade the remaining mRNA (van Hoof & Parker 2002). Both yeast and mammals

utilize these two pathways. However, 5'-to-3' degradation is the more predominate pathway in yeast, while the 3'-to-5' pathway appears to be the major pathway in mammals.

### **1.5.5 3'-to-5' mRNA decay**

The exosome is a collection of ribonucleases that degrades mRNAs (van Hoof & Parker 1999). This ribonuclease complex has been identified and purified in yeast and more recently in humans (Chen et al 2001; van Hoof & Parker 1999; Wang & Kiledjian 2000). The exosome consists of at least ten essential proteins and several auxiliary proteins, such as RNA helicases and decapping enzymes that are associated with, but are not integral components of the exosome. All ten of the essential subunits appear to function as ribonucleases (van Hoof & Parker 1999). Some of the enzymes are phosphorolytic enzymes that use phosphate as the attacking group to cleave RNA and produce nucleotide 5' diphosphates, while some are hydrolases that release nucleotide 5' monophosphates. The exosome is located in both the nucleus and the cytoplasm (Chen et al 2001). In the nucleus, the exosome is utilized in the processing of small nuclear and nucleolar RNAs, ribosomal RNAs, and the degradation of pre-rRNA spacers and unspliced pre-mRNAs. However, in the cytoplasm, the exosome functions in mRNA turnover.

AREs can recruit the exosome to the mRNA following the deadenylation of an mRNA. Specific destabilizing ARE-binding proteins copurify with the exosome suggesting that the ARE-binding proteins may recruit the exosome (Chen et al 2001). Alternatively, the ARE itself may recruit the exosome since the PM-Scl75 subunit of the exosome can bind specifically to ARE-containing mRNAs (Mukherjee et al 2002).

The exosome is hypothesized to form for a variety of reasons (van Hoof & Parker 1999). The first is that the exosome prevents the cleavage of the wrong substrates since the active sites are located within the complex and are not accessible to all macromolecules. This may also prevent early termination of degradation. Some of the ribonucleases in the exosome may be inactivated under various conditions. The exosome allows several ribonucleases that have varying functions to be recruited to the appropriate RNA as a single unit and thus provide the RNA a broad range of degradative options depending on the conditions of the cell.

The auxiliary proteins associated with the exosome perform several functions that assist in the degradation of the mRNA (Wang & Kiledjian 2001). The RNA helicases are hypothesized to eliminate RNA secondary structure and/or disrupt RNA/protein interactions. Thus, the helicase may convert the RNA into an unprotected substrate for the exosome. RNA degradation by the exosome primarily degrades the body of the mRNA. However, the exosome may also contain a "scavenger" decapping enzyme that functions solely on short 5'-fragments of mRNA that remain after exosome-mediated mRNA degradation.

### **1.5.6 5'-to-3' mRNA decay**

The 5'-cap of an mRNA contains a unique 5'-5' phosphodiester bond that is resistant to exoribonucleases and thus protects the RNA from degradation (Sachs 1993). mRNAs that do not have a 5'-cap were observed to be 4-fold less stable than their counterparts containing a 5'-cap (Ross 1995). The formation of the mRNP complex containing eIF4E was initially thought to stabilize the mRNA from deadenylation and decapping (Gao et al 2001; Wells et al 1998). However, more recent studies indicate that

decapping may be independent of eIF4E binding (Gao et al 2001). Thus, decapping may be prevented by a direct interaction between the 5'-cap and PABP, instead of by the formation of a complex containing the 5'-cap, eIF4E, eIF4G, PABP, and the poly (A) tail.

In yeast, the 5'-cap is removed by the decapping enzyme, Dcp1p, after the removal of the poly (A) tail (Muhlrad et al 1994). This decapping activity is regulated by a number of factors such as, Dcp2p, a complex of Lsm1-7 proteins, Vps16p, and Mrt1p/Pat1p (Gao et al 2001). The decapped mRNAs are then degraded by a 5'-to-3' exonuclease, Xrn1p (Hsu & Stevens 1993). In mammals, no decapping proteins were identified by searching protein databases for sequences that are homologous to Dcp1p (Gao et al 2001). However, a decapping activity similar to that of yeast Dcp1p has been reported. The mammalian decapping activity cleaves the 5'-cap from the mRNA in an ATP-independent, Mg<sup>2+</sup>-dependent manner and plays a similar role in mRNP interactions. However, this activity works effectively on short transcripts, which differs from what is observed in yeast.

### **1.5.7 The link between mRNA stability and translation**

A connection between mRNA stability and translation has been seen in a variety of cases. The finding that translational inhibitors that block either the initiation or elongation of translation are potent stabilizers of mRNA was one of the first indications of a link between translation and mRNA turnover (Ross 1995). When a chimeric construct with a stem-loop inserted into the 5'-UTR of an ARE-containing mRNA was transfected into monkey kidney cells, translation initiation was stalled and the mRNA was stabilized (Chen & Shyu 1995; Ross 1995). However, when a picornavirus internal

ribosome entry site was added to the mRNA downstream of the stem-loop, translation could occur and the mRNA was destabilized. When similar experiments were repeated using different cell lines, stem-loops, and AREs, a variety of results were observed indicating that mRNA stability may be uncoupled from translation under varying conditions. It is also interesting to note that the poly (A) tail can stimulate translation initiation (Gao et al 2000) and that changes in the length of the poly (A) tail during development can regulate the translational efficiency of some mRNAs (Richter 1999).

The IRE/IRP complex is used in iron homeostasis to affect both the stability and the translation of mRNAs containing an iron response element (Ross 1995). Iron is imported into cells via the transferrin receptor and stored by binding to ferritin. The stability of the transferrin receptor mRNA increases when the IRE/IRP complex is formed under low iron conditions in the cell and thus the level of transferrin receptor is increased. At the same time, the IRP also binds a single IRE in the 5'-UTR of the ferritin mRNA and blocks translation, so that the amount of ferritin protein is decreased. The two reactions regulate the level of free iron in the cell by producing different effects on the two iron responsive mRNAs.

Further insight into the link between stability and translation was established by studying the previously discussed mRNP complexes. In the translation-dependent mRNA stability pathway, the eIF4E/eIF4G/PABP complex of the mRNP can recruit eIF3 and the small ribosomal subunit to begin protein synthesis (Gao et al 2000; Gao et al 2001). As the ribosome travels down the mRNA, the eIF4E/eIF4G/PABP complex is temporarily disrupted, allowing for the recruitment of the deadenylation machinery by the

5'-cap and the mRNA can be degraded using one of the decay mechanisms discussed above.

Other mRNA elements also play a role in translation-coupled mRNA stability. The purine-rich major protein-coding-region determinant of instability (mCRD), found in the c-fos coding region, interacts with the poly (A) tail by the formation of a protein bridging complex (Grosset et al 2000). This complex is made up of Unr, which binds the mCRD, PABP, which binds the poly (A) tail, and PABP-interacting protein 1 (PAIP-1), NSAP-1, and hnRNP D, which form a bridging complex. This complex of proteins prevents deadenylation of the c-fos mRNA. However, these interactions are disrupted by ribosomal transit and the degradation machinery is recruited to the RNA. Unr is also involved in internal translation initiation. Thus, it may pull the bridging complex and/or the 5'- and 3'-ends of the mRNA into the correct formation for the initiation of translation. It is still unknown whether this mCRD bridging complex makes a three-way interaction between the mCRD, the 5'-cap, and the poly (A) tail, or if it functions to protect the mRNA from deadenylation in the absence of mRNP formation. These experiments demonstrate that the interactions between the various regions of the mRNA, which stabilize the mRNA, can be altered by translation in a way that enhances mRNA stability turnover.

Another link between translation and mRNA stability was found in the study of polysomal ribonuclease 1 (PMR-1). PMR-1 normally binds an inhibitor and exists in a latent state that is associated with polysomes (Cunningham et al 2001). When estrogen levels rise the inhibitor dissociates from PMR-1 and the active ribonuclease cleaves the albumin mRNA after its translation. In this case, translation and a change in cellular

conditions cause the degradation of the mRNA. This process is facilitated by the association between the polysomes and PMR-1.

## **1.6 mRNA-binding proteins**

mRNA-binding proteins have a wide range of functions in the cell, from stabilization to destabilization of the mRNA. Some of these proteins can perform either function depending on the cell type, the conditions of the cell, or the position or the type of element within the RNA.

The binding of proteins, such as HuR, to an ARE protects the mRNA from degradation (Chen et al 2001). However, the mRNA is rapidly degraded by ribonucleases when the binding protein dissociates from the ARE. The HuR protein is believed to stabilize an mRNA by blocking access to an endonuclease recognition site (Zhao et al 2000). HuR is a member of the embryonic lethal abnormal visual (ELAV) family of mRNA binding proteins that stabilizes a variety of ARE-containing mRNAs (Peng et al 1998). HuR also shuttles between the nucleus and the cytoplasm (Fan & Steitz 1998). Therefore, HuR may bind to the appropriate mRNAs in the nucleus. The RNA/HuR complex binds four proteins that participate in translocation through the nuclear pore complex and/or are phosphorylase inhibitors; HuR remains bound to the mRNA after translocation into the cytoplasm and protects the mRNA from degradation. Binding of the HuR protein to an mRNA is regulated by three protein phosphatase 2A inhibitors (Brennan et al 2000) and the binding of HuR to the Na<sup>+</sup>/glucose cotransporter (SGLT1) mRNA is dependent upon its level of phosphorylation (Loflin & Lever 2001). The ability of HuR to bind to an ARE and stabilize the mRNA is mediated by the phosphatidylinositol 3-kinase (PI3-K) or the p38 MAPK signaling pathways (Ming et al

2001). This indicates that phosphorylation of proteins involved in HuR binding plays an important role in mRNA stabilization (Loflin & Lever 2001).

There are other ARE-binding proteins, such as tristetraprolin (TTP) and KSRP, a K-type RNA binding protein, which bind to an ARE and recruit a ribonuclease to degrade the mRNA (Chen et al 2001). TTP is a known stimulator of *in vivo* mRNA turnover (Lai et al 1999; Ming et al 2001; Stoecklin et al 2000). KSRP was previously identified as part of a protein complex required for neuronal-specific splicing when assembled on an intronic c-src enhancer (Min et al 1997). These proteins also bind to an ARE and interact with the exosome to mediate mRNA decay (Chen et al 2001). It is interesting to note, that the destabilization of the IL-3 mRNA caused by the binding of TTP to the ARE can be blocked by p38 MAPK-mediated activation of HuR binding to the mRNA (Ming et al 2001).

Finally, there are ARE-binding proteins, such as AUF1, which can act as stabilizers or destabilizers depending on the mRNA and the cellular conditions (Chen et al 2001). AUF1, also known as hnRNP D, acts in a cell-dependent manner. It stabilizes ARE-containing mRNAs in NIH 3T3 cells (Xu et al 2001) and destabilizes them in K562 cells (Loflin et al 1999; Zhang et al 1993). Heterogeneous nuclear ribonucleoproteins (hnRNPs) participate in the translocation of mRNAs from the nucleus to the cytoplasm. They may function to protect the mRNA during the transport process (Shyu & Wilkinson 2000). hnRNP D also plays several roles in mRNA turnover in the cytoplasm. Its ability to participate in multiple processes may be due to alternative splicing of the hnRNP D mRNA that yields four different protein isoforms (Xu et al 2001). All isoforms of hnRNP D can associate with the c-fos mCRD bridging complex that stabilizes the c-fos

mRNA (Grosset et al 2000; Xu et al 2001), while only two isoforms increase stability of Classes I and II (AUUUA) ARE-containing mRNAs but have little effect on Class III (non-AUUUA) ARE-containing mRNAs (Xu et al 2001). The AUUUA ARE motif is a common binding site for hnRNP D, but is not required for binding of hnRNP D to an mRNA (Wilson & Brewer 1999). The different stabilizing functions of the various isoforms make it possible to control the stabilization of a single type of ARE-containing mRNAs under various cellular conditions without affecting the levels of other mRNAs (Xu et al 2001).

### **1.7 LLC-PK<sub>1</sub>-F<sup>+</sup> cell line**

A renal cell line that retained pH-responsive cellular adaptations in response to metabolic acidosis was needed to characterize the molecular mechanisms that mediate the effects of metabolic acidosis. The LLC-PK<sub>1</sub> cell line exhibits a pH-responsive increase in glutamine catabolism but these cells lack fructose 1,6-bisphosphatase (FBPase) and thus cannot synthesize glucose from lactate or pyruvate. Therefore, a gluconeogenic subline of LLC-PK<sub>1</sub> cells was isolated (Gstraunthaler & Handler 1987). The LLC-PK<sub>1</sub> cells were adapted to medium low in glucose (<0.5 mM) and then selected in medium that in essence lacked glucose, but was supplemented with 10 mM sodium pyruvate. The selected cells produced large amounts of FBPase even when maintained in medium with 5 mM glucose, and thus were named LLC-PK<sub>1</sub>-FBPase<sup>+</sup> (LLC-PK<sub>1</sub>-F<sup>+</sup>) cells. These cells also exhibit an enhanced rate of glutamine catabolism and ammonia production (Curthoys & Watford 1995). When the LLC-PK<sub>1</sub>-F<sup>+</sup> cells are transferred to acidic medium (pH 6.9, 9 mM HCO<sub>3</sub><sup>-</sup>), the level of ammonium ion production is increased, which correlates to an increase in GA activity. There is also a pH-induced increase in the

levels of GDH mRNA in this cell line (Kaiser et al 1992). There is a 10-fold higher level of PEPCK activity in the LLC-PK<sub>1</sub>-F<sup>+</sup> cells compared to the parental LLC-PK<sub>1</sub> cells (Holcomb et al 1995). The level of PEPCK mRNA is also increased 3-fold when the LLC-PK<sub>1</sub>-F<sup>+</sup> cells are treated with acidic medium (Hwang & Curthoys 1991). This data shows that the gluconeogenic LLC-PK<sub>1</sub>-F<sup>+</sup> strain is a pH-responsive proximal tubule-like cell line.

The largest difference between the cell culture system and the rat renal system is in the metabolism of glutamate. Glutamate created by mitochondrial GA in the cell culture system is primarily transaminated to pyruvate to form alanine and  $\alpha$ -ketoglutarate and thus only a single ammonium ion is produced per glutamine consumed (Curthoys & Watford 1995). However, in the rat renal system, GDH is used to deaminate glutamate, producing  $\alpha$ -ketoglutarate. This pathway generates two ammonium ions per catabolized glutamine.

## **1.8 Stabilization of the GA mRNA**

### **1.8.1 pH-responsive stabilization of GA mRNA**

The 3'-UTR of GA was subjected to functional analysis to determine whether it contains a pH-responsive element (Hansen et al 1996). The 3'-UTR of the GA cDNA was cloned into a  $\beta$ -globin/growth hormone (p $\beta$ G) vector and transfected into the LLC-PK<sub>1</sub>-F<sup>+</sup> cells. The parent  $\beta$ G mRNA is expressed at high levels in cells grown in normal medium and the stability and levels of the  $\beta$ G mRNA are unaffected when the cells are transferred to acidic medium mimicking metabolic acidosis. However, the chimeric  $\beta$ G-GA mRNA containing the GA 3'-UTR was destabilized and thus expressed at lower

levels in cells grown in normal medium. Furthermore, the  $\beta$ G-GA mRNA was stabilized and increased when the cells were transferred to an acidic medium.

### **1.8.2 Identification and analysis of a pH-responsive element in the GA 3'-UTR**

The pH-responsive stabilization of the GA mRNA was thought to be caused by a unique sequence within the 3'-UTR of the mRNA that functioned as a pH-responsive element. Electrophoretic Mobility Shift Assays (EMSAs) were performed to map an element within the 3'-UTR of GA, that was bound by a specific protein contained in rat renal cortical cytosolic extracts (Laterza et al 1997). The binding element was mapped to an 29-base region of the GA 3'-UTR (GA(R2-I)) that contains a direct repeat of two 8-base AREs, UUAAAUA and UUUAAAUA. Mutation of the GA(R2-I) probe to increase the GC content of either of the 8-base elements caused a significant decrease in the formation of the RNA-protein complex. When both elements were mutated, no binding was observed.

Functional studies were performed to test whether this AU-rich binding element also functions as a pH-responsive element (pHRE). In the p $\beta$ G-GA(R2-H)-PCK plasmid, only 76-nt of the GA 3'-UTR including the two AREs was added to the  $\beta$ G construct and placed upstream of the PEPCK 3'-UTR. The PEPCK sequence contains an instability element that is only slightly pH-responsive (Laterza & Curthoys 2000). It was added to sufficiently destabilize the mRNA, so that a pH-responsive stabilization of the mRNA could be observed. In this experiment, a five-fold pH-responsive stabilization of the  $\beta$ G-GA(R2-H)-PCK mRNA was produced (Laterza & Curthoys 2000). These data show that the direct repeat of the AREs acts as a pHRE and is sufficient to cause a pH-responsive

stabilization. When the two AREs of the GA 3'-UTR were mutated by site-directed mutagenesis of p $\beta$ G-GA, the pH-responsive stabilization of the mRNA was abolished (Laterza & Curthoys 2000). This indicates that the pHRE is necessary to create a pH-responsive stabilization of the GA mRNA.

### **1.8.3 Identification and purification of $\zeta$ -crystallin**

A single protein in cytosolic extracts of rat renal cortex was observed to specifically bind the GA pHRE in an EMSA. When this protein was UV-crosslinked to the GA pHRE, a 48-kDa complex was formed and visualized through SDS-PAGE (Laterza et al 1997). Affinity purification of the protein from rat renal cortex cytosolic extracts was accomplished using a biotinylated oligoribonucleotide as a ligand (Tang & Curthoys 2001). The resulting complex was bound to avidin agarose packed into a fast protein liquid chromatography (FPLC) column. The eluted protein was microsequenced using mass spectroscopy and was identified as  $\zeta$ -crystallin/NADPH:quinone reductase ( $\zeta$ -crys/Nqr or  $\zeta$ -crystallin). The 36-kDa purified protein reacted with anti- $\zeta$ -crys/Nqr antibodies and formation of the  $\zeta$ -crystallin/RNA complex was blocked in an EMSA, further indicating that the binding protein is  $\zeta$ -crystallin.

$\zeta$ -crystallin accounts for 10% of the total protein found in the lens of hystricomorph rodents (Rao et al 1992) and camelids (Garland et al 1991). This overexpression of  $\zeta$ -crystallin in the lens of these species is caused by the use of an additional  $\zeta$ -crystallin promoter (Gonzalez et al 1994b; Lee et al 1994). Enzymatic levels of  $\zeta$ -crystallin are produced in various tissues of other species (Gonzalez et al 1994a; Rao & Zigler 1992). The  $\zeta$ -crystallin protein also has an enzymatic activity as a

novel NADPH:quinone reductase. This activity reduces various quinones by a sequential transfer of single electrons (Rao et al 1992).

Some proteins have been characterized as functioning both as an enzyme and as an RNA-binding protein (Hentze 1994). A well-characterized example is the iron regulatory protein, which is an RNA binding protein and cytoplasmic aconitase. Further examples of dual functioning proteins include GDH, glyceraldehyde-3-phosphate dehydrogenase (GAPDH), lactate dehydrogenase, thymidylate synthetase, dihydrofolate reductase, and catalase. By having two different activities, the protein can function as both a post-transcriptional RNA regulator and a metabolic catalyst. Most of the dual function enzymes mentioned above utilize pyridine nucleotides as substrates and RNA competes with the dinucleotide for the enzyme's binding site. There is no previous evidence that  $\zeta$ -crystallin functions as an RNA-binding protein, however it is known to bind to Z-form DNA and single stranded DNA (Gagna et al 1998; Rao et al 1997). The DNA is thought to interact with  $\zeta$ -crystallin in its dinucleotide-binding site, since the DNA binding is effectively competed by the addition of NADPH (Rao et al 1997).

#### **1.8.4 Proposed model for the stabilization of the GA mRNA**

A previously proposed model for the stabilization of renal GA mRNA at the onset of metabolic acidosis involves the binding of  $\zeta$ -crys/Nqr to the GA pHRE (Curthoys & Gstraunthaler 2001). During normal acid-base balance, the pHRE is not bound by  $\zeta$ -crys/Nqr and the pHRE recruits a specific endoribonuclease to degrade the mRNA. However, during metabolic acidosis,  $\zeta$ -crys/Nqr binds to the GA pHRE with greater affinity, thus protecting the mRNA from ribonucleolytic digestion. Therefore, the stability of the GA mRNA is increased during metabolic acidosis, since the binding

activity of  $\zeta$ -crys/Nqr to the GA mRNA is increased (Fig. 1.2). This model fits the data that has been gathered, however it is likely to be an oversimplification of the actual mechanism.

### **1.8.5 Stabilization of the GDH mRNA**

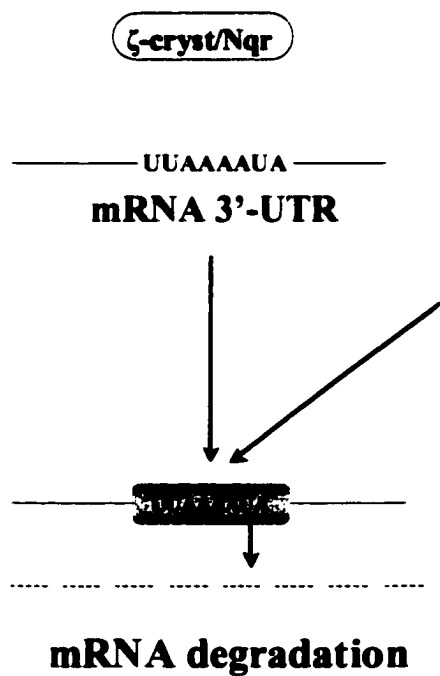
GDH mRNA is induced with kinetics similar to those observed for GA mRNA during the onset of acute metabolic acidosis (Kaiser et al 1992). For both mRNAs, there is an 8-10 h lag between the onset of metabolic acidosis and the increased production of mRNA. In addition, when LLC-PK<sub>1</sub>-F<sup>+</sup> cells, are transferred to acidic conditions and treated with actinomycin D to inhibit transcription, a three-fold stabilization of the endogenous GDH mRNA is observed. These data suggest that the GDH mRNA is stabilized by a pHRE within the 3'-UTR of GDH.

The 3'-UTR of GDH contains four 8-base AREs that are 88% identical to those found in the GA pHRE (Das et al 1989). However, these AREs are distributed throughout the 3'-UTR, unlike the direct repeat found in GA mRNA. The sequences and their location in within the GDH cDNA are given to illustrate the relative distances between the elements: element 1: UUUAAGUA (located 1973-1980 bp), element 2: CUAAAAUA (2313-2320 bp), element 3: UUCAAAUA (2537-2544 bp), and element 4: UUUAUUA (2749-2756 bp). The presence of similar ARE sequences in its 3'-UTR suggest that the GDH mRNA may also be stabilized during acidosis.

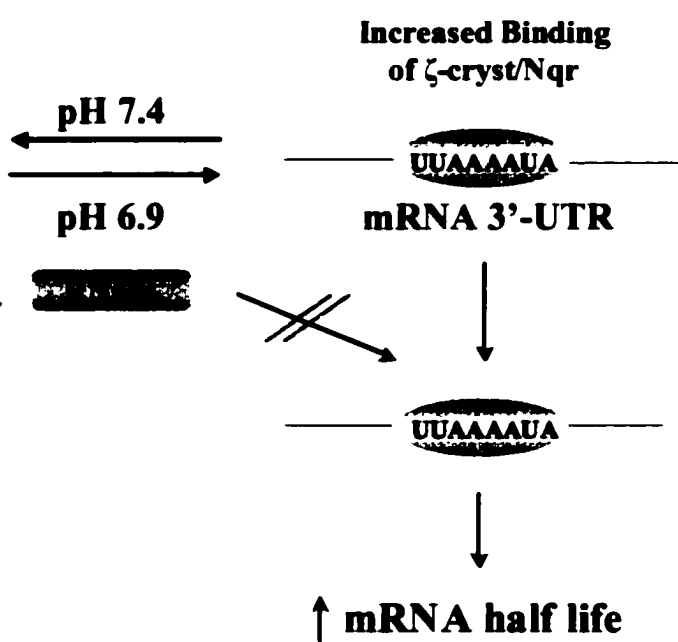
**Fig. 1.2. Proposed model for the mechanism by which the onset of metabolic acidosis leads to a stabilization of the renal GA and GDH mRNAs.**

An 8-base AU-rich pHRE serves as a binding site for  $\zeta$ -crys/Nqr and recruits a specific endoribonuclease. In normal acid-base balance, the weak binding of the pHRE allows for the more rapid initiation of degradation of the GA or GDH mRNA. However, during metabolic acidosis, the increased binding of  $\zeta$ -crys/Nqr blocks recruitment of the endoribonuclease and leads to stabilization of the GA or GDH mRNA.

### Normal Acid-Base Balance



### Metabolic Acidosis



## **2 Statement of Problem**

Ammoniogenesis and gluconeogenesis are coupled to the maintenance of acid-base balance. At the onset of metabolic acidosis, there is increased catabolism of glutamine in the kidneys. The levels of GA, GDH, and PEPCK are also increased during acidosis. The increased rates of reactions catalyzed by these enzymes yield an increased level of ammonium and bicarbonate ions that help compensate the decrease in blood pH while preserving the plasma levels of sodium and potassium ions. The increase in PEPCK is caused by an increased rate of transcription of the PEPCK mRNA. However, the increases in GA and GDH are caused by a pH-responsive stabilization of their respective mRNA.

A protein in rat renal cortical cytosolic extracts, later identified as  $\zeta$ -crystallin, was observed to bind to the 3'-UTR of GA. The binding element was mapped to a 29-nt sequence that contained a direct repeat of two 8-nt AREs. A 76-nt GA mRNA segment containing the direct repeat was observed to stabilize the  $\beta$ G-GA(R2-H)-PEPCK mRNA in cells treated with acidic medium. Furthermore, when the pHRE within the  $\beta$ G-GA mRNA was mutated the pH-responsive stabilization was abolished.

These data provide a basic understanding of the mechanisms of pH-responsive gene expression, but there are still questions that remain to be answered. A major question that arises is whether an element(s) within the 3'-UTR of the GDH mRNA is also responsible for the pH-responsive stabilization of this mRNA. Such a response may be mediated by the presence of four AREs within the 3'-UTR that are 88% identical to the GA AREs. To test this hypothesis, binding and competition assays will be performed to determine if the 3'-UTR of GDH and the individual GDH AREs exhibit specific binding of  $\zeta$ -crystallin. The 3'-UTR of GDH and a representative GDH ARE will be

cloned into a stable p $\beta$ G plasmid to determine whether these sequences also act as pHREs. Control experiments must also be done to determine how well the individual AREs in GA bind  $\zeta$ -crystallin. The data obtained for the individual GA AREs can then be compared to the data obtained for the binding of the direct repeat in GA and the individual GDH AREs. Functional studies using a p $\beta$ G plasmid containing only the 29-nt GA element encoding the direct ARE repeat will be conducted to verify that short sequences can function as a pHRE.

The next major question involves the mechanism of GA mRNA decay. It is hypothesized that GA mRNA undergoes a biphasic decay that is initiated by deadenylation. The presence of AREs within the GA 3'-UTR support this hypothesis since ARE-mediated mRNA decay is usually biphasic. The GA mRNA is hypothesized to undergo distributive deadenylation in the initial phase of decay consistent with the fact that the GA pHRE is a Class III ARE. These hypotheses can be tested by creating a tetracycline-responsive expression system. The deadenylation and decay of a homogeneous population of a single mRNA can be monitored using this system. Studies conducted using this system should reveal whether an mRNA containing the 3'-UTR of GA is initially deadenylated and if so, what type of deadenylation occurs. This system can also be used to determine whether the mechanism of decay is altered in response to metabolic acidosis to produce a pH-responsive stabilization.

This body of work will provide further insight into how metabolic acidosis affects the stability and decay of the GDH and GA mRNAs. The information will also shed light on the mechanisms of cellular regulation that activate renal catabolism of glutamine and ammoniogenesis during metabolic acidosis. These experiments may provide information

**that will eventually lead to improved pharmacological approaches for stimulating renal ammoniogenesis and/or gluconeogenesis to more effectively treat the chronic metabolic acidosis caused by starvation, dietary stress, renal nephropathies, genetically determined acidurias, and diseases such as diabetes mellitus.**

### **3 Materials**

### **3.1 Materials**

Male Sprague-Dawley rats (140-160 g) were purchased from Charles River. Slide-a-lyzer cassettes were obtained from Pierce. Microcon columns were obtained from Millipore. [ $\alpha$ -<sup>32</sup>P]UTP and [ $\alpha$ -<sup>32</sup>P]dCTP (specific activity 3000 Ci/mmol) were purchased from ICN Biochemicals or Amersham Pharmacia Biotech. Oligolabelling kit was from Pharmacia Biotechnology. Restriction enzymes, RNase T1, T7 RNA polymerase, an RNA standard, and yeast tRNA were acquired from Roche. New England Biolabs and MBI Fermentas. GENE CLEAN kits were obtained from Bio101, Inc. The PCRScript cloning kit was obtained from Stratagene. Chemicals for acrylamide gels, Micro Bio-spin chromatography columns, and protein standards were purchased from Bio-Rad. RNasin was obtained from Promega. GelBond PAG films were purchased from Intermountain Scientific. DNA preparation kits were from Promega or Qiagen. GeneScreen Plus was purchased from New England Nuclear. Gel-blotting paper was purchased from Schleicher and Schuell. An RNA standard, DMEM/F12, DME base medium, and Geneticin (G418) were products of Gibco-BRL. Tissue culture plates were purchased from Dow Corning. RNase H was purchased from Epicentre Technologies. Guanidine thiocyanate and sodium-N-lauryl sarcosine were obtained from Fluka. MOPS was obtained from Research Organics. Other chemicals were acquired from Sigma, Mallinckrodt, or Fisher.

## **3.2 Buffers and Solutions**

### **3.2.1 Krebs-Henseleit Saline Buffer (KHS)**

118 mM Sodium Chloride

4.8 mM Potassium Chloride

1.2 mM Sodium Phosphate

1.2 mM Magnesium Phosphate

2.5 mM Calcium Chloride

25 mM Sodium Bicarbonate

5.5 mM Glucose

1.0 mM Acetoacetate

1.0 mM Alanine

0.1 mM Myoinositol

1.0 mM Glutamine

pH to 7.4

### **3.2.2 Rat Renal Cortex Cytoplasmic Extraction Buffer**

40 mM Hepes

100 mM Potassium Acetate

10 mM Magnesium Acetate

1 mM Dithiothreitol (DTT)

0.01 mM Leupeptin

0.01 mM Antipain

5 µg/ml Phenylmethylsulfonylfluoride (PMSF)

pH to 7.4

### **3.2.3 1X Binding Buffer for FPLC**

10 mM Hepes

1 mM DTT

0.5% Igepal CA630

pH to 7.4

### **3.2.4 100X Binding Buffer for FPLC**

10 mM Hepes

1 mM DTT

0.5% Igepal CA630

0.5 M Potassium Acetate

50 mM Magnesium Acetate

pH to 7.4

### **3.2.5 1X Dialysis Buffer, pH 7.4**

10 mM Hepes

25 mM Potassium Acetate

2.5 mM Magnesium Acetate

1 mM DTT

pH to 7.4

### **3.2.6 Lower Tris Stock**

18.17 g Tris Base

4 ml 10% Sodium Dodecylsulfate (SDS)  
pH to 8.6, adjust to 100 ml

### **3.2.7 Upper Tris stock**

6.06 g Tris Base  
4 ml 10% SDS  
pH to 6.6, adjust to 100 ml

### **3.2.8 2X Sample Buffer**

10 ml Glycerol  
5 ml  $\beta$ -Mercaptoethanol (BME)  
30 ml 10% SDS  
12.5 ml Upper Tris Stock  
5 ml 0.05% Bromophenol Blue  
adjust to 100 ml

### **3.2.9 4X Reservoir Buffer Stock**

12 g Tris base  
57.6 g Glycine  
pH to 8.5, adjust to 1 L  
After dilution add 1/100 volume of 10% SDS

### **3.2.10 Annealing Buffer**

50 mM Sodium Chloride  
66 mM Tris-HCl  
6.6 mM Magnesium Chloride  
pH to 7.5

### **3.2.11 50X TAE Buffer**

2.0 M Tris-acetate, pH 8.0

100 mM Ethylenediaminetetraacetic acid (EDTA)

### **3.2.12 10X Stop Buffer**

2 ml 0.25 M EDTA

2.5 ml Glycerol

0.5 ml Nanopure Water

25 mg Bromophenol Blue

### **3.2.13 5X TBE Buffer**

450 mM Tris, pH 8.2

550 mM Boric Acid

10 mM EDTA

### **3.2.14 Type III Buffer (6X)**

0.25% Bromophenol Blue

0.25% Xylene Cyanol

30% Glycerol

### **3.2.15 Elution Buffer**

0.5 M Ammonium Acetate

10 mM Magnesium Acetate

1 mM EDTA

0.1% SDS

### **3.2.16 10X *in vitro* Transcription Buffer (from Promega):**

200 mM Tris-HCl, pH 7.9

30 mM Magnesium Chloride

10 mM Spermidine

50 mM Sodium Chloride

### **3.2.17 Water-saturated Phenol**

0.1% 8-Hydroxyquinoline (v/v) to phenol was added and thoroughly mixed with an equal volume of nanopure water and dissolved and equilibrated at 50°C

### **3.2.18 DEPC-treated Water**

0.1% (v/v) Diethyl Pyrocarbonate (DEPC)

Incubate at 37 °C overnight and autoclave

### **3.2.19 10X Binding Buffer**

100 mM HEPES

25 mM Magnesium Acetate

250 mM Potassium Acetate

pH to 7.4

### **3.2.20 2X HBSP, pH 7.0**

1.5 mM Sodium Phosphate

10 mM Potassium Chloride

280 mM Sodium Chloride

12 mM Glucose

50 mM Hepes

### **3.2.21 65 $\mu$ M 5,6-Dichlorobenzimidazole 1- $\beta$ -D-ribofuranoside (DRB)**

4.2 mg/ml dissolved in 95% ethanol

Use 40  $\mu$ l 4.2 mg/ml DRB/8ml medium to obtain 65  $\mu$ M

### **3.2.22 Solution D (Denaturing Lysis Solution)**

4.0 M Guanidine Thiocyanate

25 mM Sodium Citrate, pH 7.0

0.5% w/v Sodium-N-lauryl Sarcosine

0.1 M  $\beta$ -mercaptoethanol

0.033% v/v Antifoam

### **3.2.23 10X MOPS Buffer**

0.2 M MOPS (3-(N-morpholino)propanesulfonic acid)

10 mM Sodium Acetate

10 mM EDTA, pH to 7.0

### **3.2.24 Northern Loading Buffer**

33.75% Formaldehyde (37% v/v)

10% Glycerol

10% 0.1 % Bromophenol Blue

20% 10X MOPS

### **3.2.25 RNA Agarose Gel Running Buffer**

10% v/v 10X MOPS

8% v/v Formaldehyde (37% v/v)

### **3.2.26 20X SSC**

3.0 M Sodium Chloride

0.1 M Sodium Citrate

### **3.2.27 Hybridization Buffer**

250 mM Sodium Chloride

50% v/v Formamide

25 mM Sodium Phosphate, pH 7.2

1 mM EDTA

7% w/v SDS

### **3.2.28 Northern Wash Solutions**

Wash 1: 2X SSC

0.5% w/v SDS

Wash 2: 25 mM Sodium Phosphate, pH 7.2

0.5% w/v SDS

1 mM EDTA

Wash 3: 25 mM Sodium Phosphate, pH 7.2

5% w/v SDS

1 mM EDTA

### **3.2.29 10X RNase H Buffer**

0.5 M Tris, pH 7.4

1.0 M Sodium Chloride

20 mM Magnesium Chloride

10 mM DTT

### **3.2.30 RNase H Denaturing Buffer**

20  $\mu$ l Formazol

3  $\mu$ l 10X MOPS

6  $\mu$ l Formaldehyde (37% v/v)

### **3.2.31 RNase H Gel Loading Buffer**

50% Glycerol

1mM EDTA

0.25% Bromophenol Blue

0.25% Xylene Cyanol

25  $\mu$ l/ml of 10 mg/ml Ethidium Bromide

## **4 Methods**

#### **4.1 Preparation of rat renal cortical cytosolic extract:**

Male Sprague-Dawley rats were anesthetized with 1 mg pentobarbital/kg body mass and a midline incision was made. The kidneys were perfused *in situ* with Krebs-Henseleit Solution and removed. The kidneys were immediately decapsulated, sliced longitudinally, and placed in ice-cold Krebs-Henseleit Solution. The cortex was dissected away from the papilla and the medulla. The cortical kidney tissue was cut into small pieces and suspended in an equal volume of buffer (40 mM HEPES, pH 7.4, with 100 mM potassium acetate, 10 mM magnesium acetate, 1 mM dithiothreitol, 10  $\mu$ M leupeptin, 10  $\mu$ M antipain, and 5  $\mu$ g/ml phenylmethylsulfonyl fluoride). The tissue was homogenized using a Dounce homogenizer, and an aliquot was examined microscopically for released nuclei. The homogenate was then centrifuged at 1,000 x g for 10 min to pellet intact cells and nuclei. The supernatant was centrifuged at 10,000 x g for 10 min to pellet the mitochondria and then for 90 min at 100,000 x g to pellet the membrane-bound organelles and polyribosomes. The final supernatant was aliquoted and frozen at -70°C. The protein concentration was determined by a Lowry assay using bovine serum albumin as a standard (Lowry et al 1951). When an acidotic extract was needed, rats were made acutely acidotic by stomach loading them with 20 mmol  $\text{NH}_4\text{Cl}$  per kg of body weight, followed by giving them 0.28 mM  $\text{NH}_4\text{Cl}$  as the sole source of drinking water for 16-24 h.

## **4.2 Affinity purification of $\zeta$ -crystallin and other pHRE-binding proteins:**

Before application to a fast protein liquid chromatography (FPLC) column, 1 ml of rat renal cortical cytosolic extract was dialyzed overnight against 1X binding buffer containing 10 mM Hepes, pH 7.4, 25 mM potassium acetate, and 1 mM dithiothreitol. After dialysis, 40  $\mu$ l 10% Igepal CA 630, 0.25 mg yeast tRNA, 12  $\mu$ l of 0.2M dithiothreitol, and 20  $\mu$ l RNAsin (40 units/ $\mu$ l) were added and incubated at 4°C for 10 min. The GA(R2-H) complimentary biotinylated RNA ligand was centrifuged through a Bio-Rad Micro Bio-spin P6 column. Approximately 3  $\mu$ g of purified RNA ligand was added to the mixture and incubated at 4°C for another 20 min. A FPLC column was packed with 0.5 ml of avidin agarose (10-fold excess with respect to the RNA ligand) and was washed extensively using the 1X binding buffer. The sample was loaded onto the column at a flow rate of 0.1 ml/min and the column was washed at 0.5 ml/min with 110 ml binding buffer in which the concentrations of the potassium acetate and magnesium acetate were increased 4-fold. The binding activity was eluted with 4.5 ml of buffer, in which the potassium acetate and magnesium acetate concentrations were linearly increased from 4X to 20X, and collected in 0.5 ml fractions. The column was then washed with another 2.5 ml of buffer containing a 20X salt concentration and the eluant was collected as 5-0.5 ml fractions. Fractions were examined for the presence of  $\zeta$ -crystallin and to assess purity: 8  $\mu$ l of protein and the Bio-Rad Prestained SDS-PAGE Low Range standards were separated on a 10% polyacrylamide gel containing 1% SDS and stained with 0.1% silver nitrate. Fractions containing a major 36 kDa-protein band were pooled and dialyzed overnight versus 1X binding buffer using a Slide-A-Lyzer cassette from Pierce. The solution was concentrated 5-10 fold using a Microcon-30

column from Millipore. The purified protein was tested in a RNA-EMSA for binding affinity and specificity.

### **4.3 Construction of pBSSK-GDH1-4**

The rat liver cDNA (Das et al 1989) was digested with XmnI and EcoRI to obtain the 1178-nt 3'-UTR of GDH. This fragment was then cloned into pBluescript II SK (-) (pBSSK) that had been previously digested with Asp718, blunted, and then cut with EcoRI (prepared by R. Gallien).

### **4.4 Construction of transcription vectors for GA(R2-IA), GA(R2-IB), and GDH1, 2, 3, and 4:**

Transcription vectors containing only one of the two GA AREs, GA(R2-IA) and GA(R2-IB), and the individual GDH AREs, GDH1, 2, 3, and 4, were constructed by annealing two complimentary oligonucleotides, synthesized by Macromolecular Resources (Fort Collins, CO). The resulting double-stranded DNA encode the ARE sequence and form Asp718 and XbaI overhangs (Fig. 4.1). The annealed oligonucleotides were inserted into pBSSK that had been restricted with Asp718 and XbaI.

### **4.5 Creation of templates**

A DNA transcription template containing a T7 promoter was created by digesting the pBSSK plasmid with BssHII, which flanks the T7 promoter and the end of the ARE. The GDH1-4 template was prepared using only this digestion. The creation of all other templates required the addition of XbaI and SacI to the digestion. XbaI digests the

**Fig. 4.1. Sequences of oligonucleotides that were used to construct the pBS-GDH and pBS-GA transcription vectors.**

Bold letters indicate partial Asp718 and XbaI sites respectively. Underlined letters are the putative pHREs.

pBS-GDH1

**5'-GTACCGTTTCGC TT TTAAGTAAAGTTTCT T-3'**

pBS-GDH2

**5'-GTACCGTGAACGCCTAAAATATAGGAAATT-3'**

pBS-GDH3

**5'-GTACCAACCATACTTCAAATAGAGTGTCCT-3'**

pBS-GDH4

**5'-GTACCAGACATTATTTTATATAAGAATGAGT-3'**

pBS-GA(R2-I)

**5'-GTACCTCTTTAAATATTAATAAT TACTACTAAT-3'**

pBS-GA(R2-IA)

**5'-GTACCTGTGACTCT TAAATAATTACTACT-3'**

pBS-GA(R2-IB)

**5'-GTACCTGTGACTCT TAAATAATTAC TACT-3'**

DNA at the end of the ARE sequence and SacI digests the similarly sized non-template DNA into two pieces so that the template and promoter-less DNA can be separated on an 8% native polyacrylamide gel.

The template was purified from the gel using the crush and soak method (Sambrook et al 1989). The gel slice containing the DNA template was excised from the gel and crushed. The DNA was eluted from the gel in 0.5 ml of elution buffer by shaking overnight at 37°C. The gel and buffer is spun through a disposable plastic column with a frit, which acts as a filter to separate the gel from the eluate when centrifuged at 1,000 x g for 5 sec. The eluted DNA is precipitated with two volumes of 100% ethanol and incubated at -20°C for 30 min. The DNA is pelleted at 14,000 x g for 10 min at 4°C, and the pellet is washed with 200 µl 70% ethanol and centrifuged for 10 min at 14,000 x g at 4°C. The pellet is briefly dried at room temperature and resuspended in 11 µl Diethyl pyrocarbonate (DEPC)-treated water.

#### **4.6 In-Vitro Transcription**

A modified version of the standard method of in-vitro transcription was used (Melton et al 1984), in which a 10 µl reaction contains: 0.1 µg DNA template, 10 µCi [ $\alpha$ -<sup>32</sup>P] UTP, 0.5 mM ATP, CTP, and GTP, 50 µM unlabelled UTP, 20 units RNAsin, 1X transcription buffer, 10 mM dithiothreitol, and 10 units of T7 RNA polymerase. After a 1 h incubation at 37°C, 1 unit of RNase-free DNase was added and incubated at 37°C for 15 min. The volume of the reaction was increased to 50 µl with DEPC-treated water and the product was purified using a Bio-Rad Micro Bio-Spin chromatography column. The

final product was quantified using a scintillation counter and DEPC-treated water was added to adjust the sample to the desired concentration.

Synthesis of unlabeled RNA was performed in a 50  $\mu$ l reaction mixture lacking [ $\alpha$ - $^{32}$ P] UTP, but containing 0.5 mM of each ribonucleotide. The RNA was purified using the Bio-Rad Micro Bio-Spin chromatography column and then extracted using a 25:24:1 mixture of phenol:chloroform:isoamyl alcohol and 2M sodium acetate (pH 4.0). The extracted RNA was then precipitated by adding an equal volume of isopropanol at -20°C. The RNA pellet was washed with 80% ethanol and dried. The RNA pellet was resuspended in 20-100  $\mu$ l of DEPC-treated water. The absorbance at 260 nm was measured to determine the concentration of the RNA transcripts. The appropriate extinction coefficient was calculated from the nucleotide composition.

#### ***4.7 RNA Electrophoretic mobility shift assay (RNA-EMSA)***

This assay was performed using a modified RNA-EMSA protocol (Alberta et al 1994). Either 3  $\mu$ g of protein from rat renal cytosolic extract or 10-50 ng of purified  $\zeta$ -crystallin was incubated for 10 min at room temperature in a 10  $\mu$ l reaction containing, 10 mM HEPES, pH 7.4, 25 mM potassium acetate, 2.5 mM magnesium acetate, 2  $\mu$ g yeast tRNA, 0.5% Nonidet-P40, 5% glycerol, 1 mM dithiothreitol and 10 units RNAsin. Then approximately 10-40 fmol of labeled RNA was added and the sample was incubated at room temperature for 20 min. RNAsin is added to the reaction to protect the integrity of the RNAs during the incubations with the protein.

For the competition studies, a 30-, 100-, or 300-fold excess of unlabeled RNA competitors was added into the appropriate reactions at the same time as the labeled RNA.

For the RNA-EMSA comparing the binding of GDH1-4 and GA(R2-I) RNAs, the samples were also incubated for 10 min with 15 units of RNase T1, to reduce the length of the GDH1-4 RNA.

The samples were subjected to electrophoresis for approximately 2 h on a 5% polyacrylamide gel at 170 V using a 90 mM Tris, 110 mM boric acid, 2 mM EDTA running buffer. Gels were then dried and exposed to a PhosphorImager screen.

## **4.8 Construction of $\beta$ -Globin Constructs**

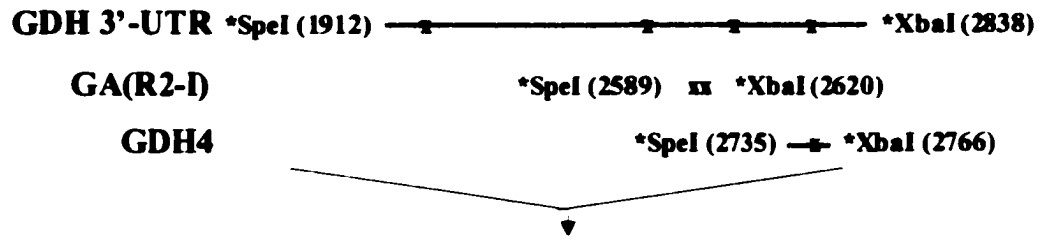
$\beta$ G constructs were created which contained either the 3'-UTR of GDH or an individual pHRE. These vectors were used in functional studies to determine whether binding elements identified in the GA and GDH 3'-UTRs function as elements that cause a pH-responsive stabilization.

### **4.8.1 p $\beta$ G-GDH**

The 930-nt segment of 3'-UTR of GDH was PCR-amplified from the pBSSK-GDH1-4 using primers that add SpeI and XbaI sites to the 5' and 3' ends, respectively. The PCR product was cloned into the SrfI site of pCR-Script SK (+) and the SpeI/XbaI fragment was excised from the plasmid and inserted into the XbaI site within the multicloning site of p $\beta$ G, between the genomic  $\beta$ -Globin sequence and the sequence that encodes the 3'-UTR and polyadenylation signal of bovine growth hormone (Fig. 4.2).

**Fig. 4.2. Schematic representation of the cloning of p $\beta$ G-GDH, p $\beta$ G-GA(R2-I), and p $\beta$ G-GDH4.**

The p $\beta$ G plasmid contains a promoter derived from the Rous sarcoma virus long terminal repeat (RSV-LTR), a transcription start site, the  $\beta$ G coding region from rabbit  $\beta$ -globin genomic DNA containing three exons (open boxes) and two introns (shaded boxes), a multicloning site (MCS), and a polyadenylation site from the bovine growth hormone cDNA (bGH-pA). The sequence encoding the 3'-UTR of the GDH mRNA was PCR amplified from pBS-GDH using primers that add SpeI and XbaI sites to the 5' and 3' ends, respectively. The PCR product was cloned into the SrfI site of pCR-Script SK (+) and an SpeI/XbaI fragment was excised from the plasmid and inserted into the XbaI site within the MCS of p $\beta$ G.  $\beta$ G-GA(R2-I) and  $\beta$ G-GDH4 were constructed by annealing complimentary oligonucleotides that encode the GA(R2-I) or the GDH4 sequence and form SpeI and XbaI overhangs and inserting them into the XbaI site of p $\beta$ G. X indicates the location of the ARE.



#### 4.8.2 pβG-GA(R2-I) and pβG-GDH4

The pβG-GA(R2-I) and pβG-GDH4 vectors were constructed by annealing complimentary oligonucleotides, synthesized by Macromolecular Resources (Fort Collins, CO), that encode the GA(R2-I) or the GDH4 sequence and form SpeI and XbaI overhangs and inserting them into the XbaI site of pβG (Fig. 4.2). The sequence of the GA(R2-I) oligonucleotides are: 5'-**CTAGTTCTTTAAATATTAAAATAATTCTAAT**-3' and 5'-**CTAGATTAGTAATTATTTAATATTTAAAGAA**-3'. The GDH4 oligonucleotides are: 5'-**CTAGTAGACATTATTTATATAAGAATGAGT**-3' and 5'-**CTAGACTCATTCTTATATAAATAATGTCTA**-3'. The boldface letters in the oligonucleotide sequences designate the partial SpeI and XbaI sites, respectively. The italicized letters in the oligonucleotide sequences designate the pHRE.

#### 4.8.3 pβG-GDH4-PCK

pβG-GDH4-PCK was constructed by K. Propst in two cloning steps. Complimentary oligonucleotides, synthesized by Macromolecular Resources (Fort Collins, CO), that encode the GDH4 sequence and form XbaI and NheI overhangs were annealed and inserted into the XbaI and NheI sites of pGEM4Z-PCK. The GDH4 oligonucleotides are: 5'-**CTAGATATCAGACATTATTTATATAAGAATGAGG**-3' and 5'-**GCTAGCCTCATTCTTATATAAATAATGTCTGATAT**-3'. The boldface letters in the oligonucleotide sequences designate the partial NheI and XbaI sites, respectively and the bold italicized letters designate an EcoRV site that was used to detect the presence of

the sequence within the cloned plasmid. The italicized letters in the oligonucleotide sequences designate the pHRE.

The pGEM4Z-GDH4-PCK vector was digested with XbaI and SpeI to obtain the GDH4-PCK sequence that was inserted into XbaI/SpeI digested pβG to produce pβG-GDH4-PCK.

#### **4.9 Cell Culture**

LLC-PK<sub>1</sub>-F<sup>+</sup> cells obtained from Gerhard Gstraunthaler were cultured as previously described (Gstraunthaler & Handler 1987). Cells were grown in a 50:50 mixture of Dulbecco's modified Eagle's and Ham's F-12 medium containing 5 mM glucose and 10% fetal bovine serum at 37°C in a 5% CO<sub>2</sub> atmosphere. Normal medium (pH 7.4) contains 25 mM sodium bicarbonate, whereas acidic medium (pH 6.9) contains 10 mM sodium bicarbonate supplemented with 15 mM sodium chloride to maintain an equivalent osmolarity and sodium ion concentration.

#### **4.10 Creation of stable cell lines using pβG vectors:**

LLC-PK<sub>1</sub>-F<sup>+</sup> cell lines expressing the various chimeric mRNAs were produced by transfection of 3-day post-split cells with calcium phosphate precipitated DNA (Chen & Okayama 1987). Fresh medium was added 1 h before the addition of 20 μg of calcium phosphate precipitated DNA. After 24 h, the transfection medium was removed, and the cells were washed two times with phosphate-buffered saline before fresh pH 7.4 medium containing 0.8 mg/ml G-418 was added. The medium was changed every two days. After 14-21 days, 3 plates containing multiple colonies were combined onto one plate and

grown. Following the next split of cells, the cells were grown in pH 7.4 medium containing 0.2 mg/ml G-418.

#### **4.11 mRNA half-life analysis using DRB**

The various transfected LLC-PK<sub>1</sub>-F<sup>+</sup> cell lines were generally split 1:10 and grown for 7-10 days in pH 7.4 medium containing 0.2 mg/ml G-418. They were then maintained in pH 7.4 medium without G-418 for 24 h and subsequently treated for 12 h in normal or acidic medium. At time zero, 65  $\mu$ M 5,6-dichloro-1- $\beta$ -ribofuranosylbenzimidazole (DRB), a specific inhibitor of RNA polymerase II transcription (Dubois et al 1994), dissolved in 95% ethanol, was added to each plate. An equivalent amount of 95% ethanol was added to control plates. The volume of ethanol never exceeded 0.5% of the total volume of medium on the plates. At 0, 3, 6, and 9-h post-DRB treatment, total cellular RNA was isolated.

#### **4.12 Isolation of total RNA**

Total RNA was isolated using the method of Chomczynski and Sacchi (Chomczynski & Sacchi 1987). 1.8 ml of Solution D (Denaturing Lysis Solution) was added to 100 mm plates of cells. Cellular lysates were mixed and distributed evenly between two 2-ml microcentrifuge tubes. Then, 80  $\mu$ l of 2.0 M sodium acetate (pH 4.0) was mixed with the lysates and 0.8 ml of water-saturated phenol and 200  $\mu$ l of chloroform:isoamyl alcohol (24:1) were added and vigorously vortexed. The samples were incubated at 4°C for 15 min or until phase separation could be seen. The samples were centrifuged at 10,000 x g for 20 min at 4°C and the aqueous phase was transferred to a new microcentrifuge tube. Isopropanol was added in an equal volume to the amount

of aqueous phase and after mixing, the sample was incubated at -20°C for at least 30 min and then centrifuged at 10,000 x g for 15 min at 4°C. RNA pellets were resuspended in 400 µl of Solution D then heated at 60°C for 10 min to redissolve the pellets. Then duplicate samples were combined. The RNA was reprecipitated by adding 800 µl of isopropanol and incubating at -20°C for at least 30 min followed by a 15 min centrifugation at 10,000 x g at 4°C. The RNA pellets were washed with 80% ethanol followed by a 5 min centrifugation at 4°C at 10,000 x g. The pellets were resuspended in 110 µl of Formazol and dissolved by heating at 60°C for 15 min. The RNA concentration was determined by measuring the absorbance of the RNA at 260 nm.

#### **4.13 Preparation of cDNA probes**

A 507-bp fragment of rabbit β-globin cDNA was excised by restricting pRSV-βG (Gorman et al 1983) with Hind III and Bgl II. A 2.0-kb fragment of the 18 S ribosomal RNA cDNA from *Acanthamoeba castellanii* was excised by restricting pAr2 with Hind III and Eco RI (D'Alessio et al 1981). The fragments were separated on 1% agarose gels, excised, and purified by using the GENECLEAN kit.

#### **4.14 Northern Analysis**

The samples containing 15 µg of total RNA were combined with 2X loading buffer and 1.5 µl of 0.4 mg/ml ethidium bromide. The RNAs were heated at 70°C for 10 min and then placed on ice. The samples were loaded onto a 1% agarose gel containing 20 mM MOPS, 1 mM EDTA, and 1 mM sodium acetate, pH 7.0. The samples were electrophoresed for either 2.5 h at 150 V or for approximately 16 h at 20 V. The gel was washed with nanopure water for 20 min, then washed with a 50 mM sodium hydroxide

solution for 20 min, and then neutralized in 0.25 M sodium phosphate, pH 6.5, for 30 min. RNA was transferred to GeneScreen Plus by standard capillary transfer protocols using 25 mM sodium phosphate, pH 6.5. The completeness of transfer was determined by UV-illumination. The transferred RNA was cross-linked to the GeneScreen Plus membrane by UV-irradiation for 3 min.

The membrane was prehybridized for 1-5 h at 43°C in hybridization solution prepared as previously described (Amasino 1986) in a Biometra hybridization oven. An oligolabeled cDNA probe ( $>10^9$  cpm/mg) was added and hybridized to the membrane under the same conditions for 20-26 h. Blots were washed two times for 15-20 min at 53°C in each of the three Northern washing solutions described in the Materials section. The blots were exposed to a PhosphorImager screen and the intensity of the resulting digital image of each band was quantified by Molecular Dynamics Software. The level of experimental mRNA was divided by the corresponding level of 18S rRNA (determined by hybridizing the same blot with the 18S cDNA probe, using the same method used for the initial cDNA probe) to correct for errors in sample loading.

For half-life studies, the log of normalized data was then plotted versus the time of treatment with DRB or Dox. The values are averages of data obtained from replicate experiments. The line represents the best-fit of the data points as determined by the KaleidaGraph program that weights each data point based upon its standard deviation.

#### **4.15 Creation of stable pTet-Off cell lines**

LLC-PK<sub>1</sub>-F<sup>+</sup> cell lines expressing the tTA protein were produced by transfection of 3-d post-split cells with calcium phosphate precipitated DNA (Chen & Okayama 1987), with the assistance of E. Anderson and N.P. Curthoys. Eleven clonal cell lines

were made by stably transfecting the pTet-off plasmid, encoding the tTA protein, into LLC-PK<sub>1</sub>-F<sup>+</sup> cells. Fresh medium was added 1 h before the addition of 20 µg of calcium phosphate precipitated DNA. After 24 h, the transfection medium was removed, and the cells were washed two times with phosphate-buffered saline before fresh pH 7.4 medium containing 0.8 mg/ml G-418 was added. The medium was changed every two days. After 14-21 days, individual colonies were isolated and grown on plates of increasing size. Following the split of cells onto 100 mm plates, the cells were grown in pH 7.4 medium containing 0.2 mg/ml G-418. Eleven tTA expressing cell lines were cloned.

#### **4.16 Luciferase Assays to test pTet-Off stable cell lines:**

The stably transfected cell lines were grown on 6-well plates using pH 7.4 medium containing 0.2 mg/ml G-418 and half of the wells contained 1 µg/ml Dox. The cells were transiently transfected by calcium phosphate precipitation of pTRE2-Luc (CLONTECH Laboratories Inc. 1999) at 3 days post-split. Approximately 16 h later, the medium was removed and fresh medium with or without 1 µg/ml Dox was added. The cells were cultured for an additional 32 h and washed twice with PBS. Cell extracts were prepared and assayed using the reagents contained in the Luciferase Assay System (E1500, Promega). The firefly luciferase activities obtained for the various stable Tet-Off clonal lines were standardized per µg of protein. The protein concentrations of the extracts were determined by Lowry assay and the fold-induction of TRE2-Luc protein was calculated by dividing the luciferase activity measured in cells –Dox by the activity in cells +Dox. Values shown are the mean +/- S.D. of experiments performed in triplicate.

## **4.17 Construction of pTRE constructs.**

### **4.17.1 pTRE2- $\beta$ G-GA-bGH**

A segment of the p $\beta$ G-GA construct (Hansen et al 1996) containing the  $\beta$ -globin coding region and the GA 3'-UTR was PCR amplified with primers containing unique MluI and XbaI sites. This fragment was cloned into pCR-Script SK (+) at the SrfI site. The pTRE2 plasmid encodes a tetracycline-responsive element (TRE), containing seven direct repeats of a 42-bp sequence containing the tet operator (tetO) positioned upstream of a minimal CMV promoter, a multicloning site, and the 3'-coding and 3'-untranslated regions of the rabbit  $\beta$ -globin gene. The pTRE2 vector was digested with MluI and XbaI and the  $\beta$ G-GA fragment was ligated into pTRE2, creating pTRE2- $\beta$ G2-GA.

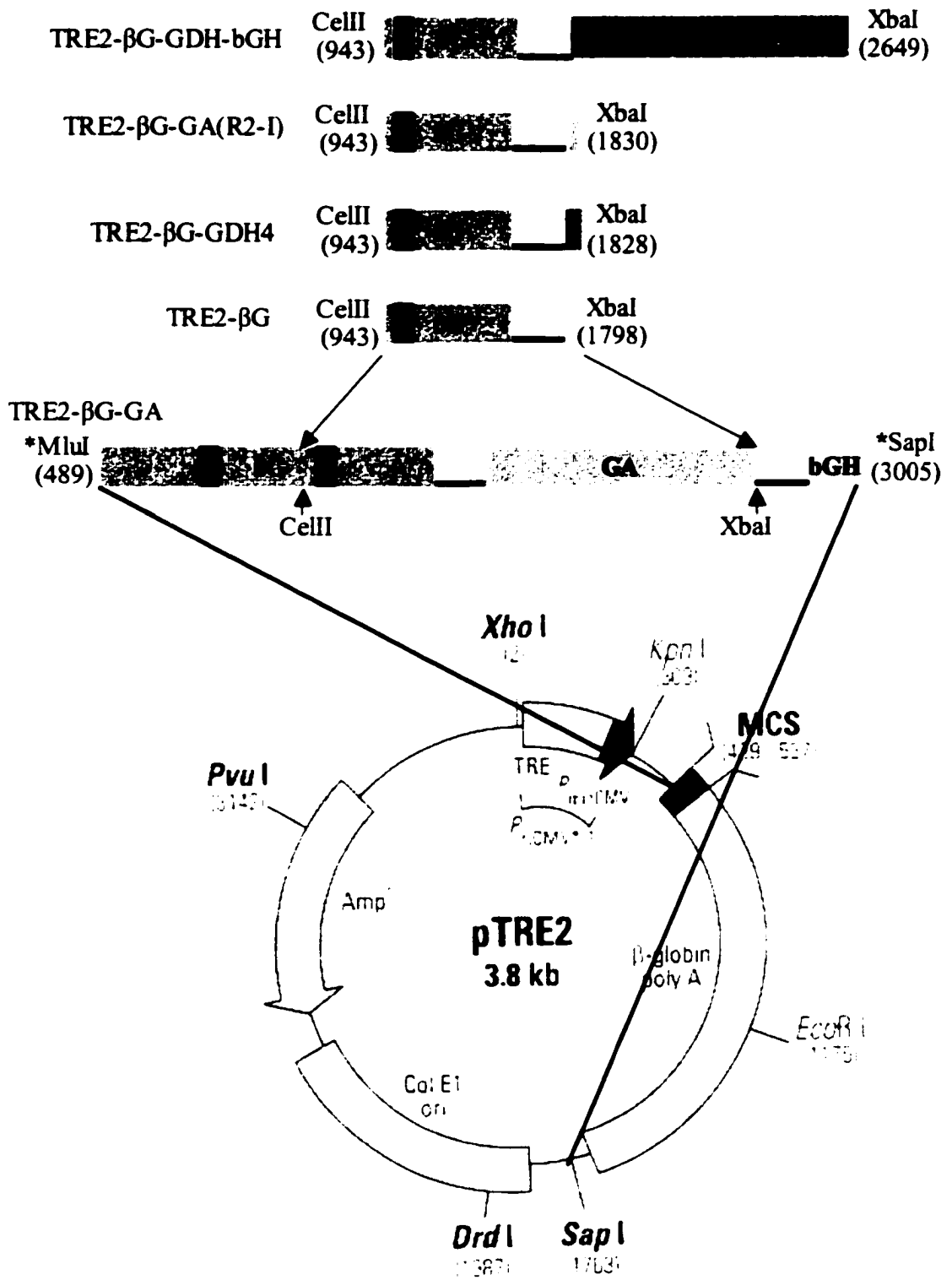
A segment of p $\beta$ G-GA encoding the bovine growth hormone (bGH) 3'-UTR and polyadenylation signal was PCR amplified using primers containing unique XbaI and SapI sites and cloned into pCR-Script SK (+) at the SrfI site. The bGH fragment was inserted into pTRE- $\beta$ G2-GA that was digested with XbaI and SapI to remove the duplicated  $\beta$ -globin sequence from TRE- $\beta$ G2-GA (Fig. 4.3).

### **4.17.2 pTRE2- $\beta$ G-bGH, pTRE2- $\beta$ G-GDH-bGH, pTRE2- $\beta$ G-GA(R2-I)-bGH, and pTRE2- $\beta$ G-GDH4-bGH**

p $\beta$ G-GDH, p $\beta$ G-GA(R2-I), and p $\beta$ G-GDH4 were digested with CeuII and XbaI and the isolated fragments were inserted into pTRE- $\beta$ G-GA-bGH that had been digested with CeuII and XbaI. This procedure removed the GA sequence or replaced it with the other GA and GDH sequences (Fig. 4.3).

**Fig. 4.3. Schematic representation of the cloning of pTRE2- $\beta$ G-GA-bGH, pTRE2- $\beta$ G-GDH-bGH, pTRE2- $\beta$ G-GA(R2-I)-bGH, pTRE2- $\beta$ G-GDH4-bGH, and pTRE2- $\beta$ G-bGH.**

The pTRE2 vector contains a tetracycline-responsive element (TRE) upstream of a minimal CMV promoter ( $P_{\text{minCMV}}$ ), a multicloning site (MCS), and the 3'-coding and 3'-untranslated regions of the rabbit  $\beta$ -globin gene ( $\beta$ -globin poly A). To generate pTRE2- $\beta$ G-GA-bGH, the  $\beta$ G coding region, the GA 3'-UTR, and the bovine growth hormone polyadenylation signal were PCR amplified from p $\beta$ G-GA with primers that add MluI and SapI sites on to the 5' and 3' ends of the PCR fragment, respectively. The PCR fragment was cloned into the SrfI site of pCR-Script SK (+) and an MluI/SapI fragment was excised and inserted into the MluI and SapI sites of pTRE2. Thus, the cloning of pTRE2- $\beta$ G-GA-bGH removed the 3'-coding and 3'-untranslated regions of the rabbit  $\beta$ -globin gene that were present in the pTRE2 vector. p $\beta$ G -GDH, p $\beta$ G -GA(R2-I), p $\beta$ G -GDH4 and p $\beta$ G were restricted with CclII and XbaI and the resulting fragments were inserted into pTRE2- $\beta$ G-GA-bGH previously digested with CclII and XbaI to create the corresponding pTRE2 plasmids. This cloning scheme removed the GA 3'-UTR and replaced it with the appropriate 3'-UTR fragment.



#### **4.18 Creation of TRE- $\beta$ G-GA-bGH stable cell lines**

Eight clonal cell lines (1A, 2A, 3A, 1B, 2B, 3B, 4B, and 5B) and two mixed cell lines (Mix and DoxMix) were made by stable transfection of pTRE2- $\beta$ G-GA-bGH and pTK-Hyg, which confers antibiotic resistance to Hygromycin B, into the 8C line of LLC-PK<sub>1</sub>-F<sup>+</sup> cells. Fresh medium, containing 0.2 mg/ml G-418 and 1  $\mu$ g/ml Dox, was added 1 h before the addition of 20  $\mu$ g of calcium phosphate precipitated DNA. After 24 h, the medium was removed, and the cells were washed two times with phosphate-buffered saline before fresh pH 7.4 medium containing 0.2 mg/ml G-418 was added (half of the plates contained 1  $\mu$ g/ml Dox). Then 48 h post-transfection, pH 7.4 medium containing 0.2 mg/ml G-418 and 0.5 mg/ml Hygromycin B was added (half of the plates contained 1  $\mu$ g/ml Dox). The medium was changed every two days. After 14-21 days, individual colonies were isolated and grown on plates of increasing size (colonies from a plate grown in the presence of 1  $\mu$ g/ml Dox died) and 3 plates containing multiple colonies were combined onto one plate (Mix or DoxMix) and grown. Mix cells were grown in the absence of Dox and DoxMix cells were grown in the presence of 1  $\mu$ g/ml Dox. Following the split of cells onto 100 mm plates, all cells were grown in pH 7.4 medium containing 0.2 mg/ml G-418 and 0.5 mg/ml Hygromycin B.

These cell lines were tested for tetracycline-responsiveness by maintaining the cells for 48 h in pH 7.4 medium in the presence or absence of 0.5  $\mu$ g/ml Dox. Total RNA was harvested from the cells and used in a Northern blot. The level of  $\beta$ G-GA mRNA was divided by the corresponding level of 18S rRNA to correct for errors in sample loading. For each cell, the reported data were normalized to the +Dox values.

## **4.19 Creation of a Transcriptional Pulse**

The minimal amount of Dox needed to shut off transcription was determined by maintaining 8C/2A LLC-PK<sub>1</sub>-F<sup>+</sup> cells in pH 7.4 medium containing 0.2 mg/ml G-418 and 0.2 mg/ml Hygromycin B for 48 h with a range of Dox concentrations from 10-1000 ng/ml. The isolated RNAs were analyzed on a Northern blot as previously described.

The length of time needed to reinitiate transcription was determined by maintaining 8C/2A LLC-PK<sub>1</sub>-F<sup>+</sup> cells in pH 7.4 medium containing 0.2 mg/ml G-418 and 0.2 mg/ml Hygromycin B for 48 h in the presence or absence 25 ng/ml Dox for 48 h. The cells grown in the absence of Dox were harvested and cells grown in the presence of Dox were washed two times with 1X PBS and then grown for 1-3 h in fresh medium containing 0.2 mg/ml G-418 and 0.2 mg/ml Hygromycin B and the RNAs were isolated. The RNAs were subjected to Northern blot analysis as previously described. The values were obtained by dividing the level of RNA present in the presence of Dox by the level of RNA present in the absence of Dox and expressing the number as a percentage.

## **4.20 Functional Studies using pTRE2-βG-GA-bGH**

### **4.20.1 Half-life analysis using Dox to inhibit transcription**

The 8C/2A LLC-PK<sub>1</sub>-F<sup>+</sup> cell line was generally split 1:10 and grown for 5-7 days in pH 7.4 medium containing 0.2 mg/ml G-418 and 0.2 mg/ml Hygromycin B. They were then maintained in pH 7.4 medium without G-418 and Hygromycin B for 12 h and subsequently treated for 12 h in normal or acidic medium. At time zero, 1 μg/ml Dox was added to each plate. At 0, 3, 6, and 9 h post-Dox treatment, total cellular RNA was

isolated. Control plates containing no Dox were harvested 9 h post-mock Dox treatment. RNAs were subjected to Northern blot analysis as previously described.

#### **4.20.2 Half-life analysis using a transcriptional pulse**

The 8C/2A LLC-PK<sub>1</sub>-F<sup>+</sup> cell line was generally split 1:10 and grown for 5-7 days in pH 7.4 medium containing 0.2 mg/ml G-418 and 0.2 mg/ml Hygromycin B. They were then maintained in pH 7.4 or pH 6.9 medium with antibiotics and 25 ng/ml Dox for 48 h. The cells were washed two times with 1X PBS and incubated in medium with antibiotics, but without Dox for 3 h to create a transcriptional pulse. The fresh medium containing antibiotics and 1 µg/ml Dox was added and RNA was isolated at 0, 3, 6, and 9-h after Dox readdition. Controls grown in the presence or absence of Dox were harvested after the initial 48 h time point. RNAs were subjected to Northern blot as previously described.

#### **4.21 Preparation of bGH Northern probe**

A 228-nt bGH fragment was excised from pCR-Script SK (+)-bGH with SphI. The fragment was separated on a 1% agarose gel, excised, and purified by using the GENECLAN kit.

#### **4.22 Design of RNase H deoxyoligonucleotides**

A 26-nt RNase H deoxyoligonucleotide (GA oligo) was designed to specifically bind to the 3'-end of the GA sequence of pTRE2-βG-GA-bGH and synthesized by the Macromolecular Resources (Fort Collins, CO). The GA oligo encodes the template strand of the DNA from 2514-2539 bp. The sequence is:

5'-GACCGACAGCTACACACCAAGAGAG-3'

An oligo dT deoxyoligonucleotide was also designed as a 30-mer of thymidine residues, which can bind specifically to the poly (A) tail of an mRNA.

#### **4.23 RNase H Treatment**

RNAs isolated from the previously described transcriptional pulse experiments are used in these assays. An RNase H treatment (Porter & Curthoys 1997) was performed after RNAs were precipitated from Formazol with 4 volumes of ethanol and a final concentration of 0.2 M sodium chloride for 5 min at room temperature. The RNA was pelleted by centrifugation at 10,000 x g for 10 min. The pellets were resuspended in 25  $\mu$ l DEPC-treated water. In a 12.5  $\mu$ l reaction, 10  $\mu$ g RNA, 1.0  $\mu$ l RNase H deoxyoligonucleotide (for untreated RNAs, this is omitted), 1.0  $\mu$ l oligo dT (if needed), and DEPC-treated water were combined. The mixture was incubated at 55°C for 60 sec, then 1.5  $\mu$ l of 10X RNase H buffer, pre-warmed to 62°C, (0.5 M Tris, pH 7.4, 1.0 M sodium chloride, 20 mM magnesium chloride, and 10 mM dithiothreitol) was added to the reaction and the reaction was incubated at 62°C. 1.0 U of RNase H (freshly diluted to 1U/ $\mu$ l with 1X RNase H buffer) was added and incubated at 62°C for 15 min. Then 29  $\mu$ l of denaturing buffer (20  $\mu$ l Formazol, 3  $\mu$ l 10X MOPS, and 6  $\mu$ l 37% formaldehyde solution) was added to stop the reaction and it is incubated at 55°C for 5 min, followed by incubation on ice. RNase H-treated RNAs were subjected to Northern blot analysis as previously described, except a 1.2% agarose gel containing 20 mM MOPS, 1 mM EDTA, and 1 mM sodium acetate, pH 7.0, was used and 10  $\mu$ l of a RNase H gel loading buffer (50% glycerol, 1mM EDTA, 0.25% bromophenol blue, and 0.25% xylene cyanol and 25

$\mu$ /ml of 10 mg/ml ethidium bromide) was added to the samples instead of the 2X loading buffer. The blot was probed with the bGH probe.

## **5 Binding and Functional Studies of GDH and GA AREs**

## **5.1 Binding and Competition Studies**

GA mRNA contains a pH-responsive element within its 3'-UTR (Hansen et al 1996). GA(R2-I) which contains two 8-base AREs in a direct repeat, is the minimal region of the GA 3'-UTR that acts as a binding element for  $\zeta$ -crystallin and also functions as a pHRE (Laterza & Curthoys 2000; Laterza et al 1997). The 3'-UTR of GDH contains four AREs that are 88% identical to one of the two AREs of the GA pHRE. Therefore, direct binding and competitions studies were performed to determine whether  $\zeta$ -crystallin binds to the 3'-UTR of GDH and whether the binding occurs using the individual AREs.

The binding and competition experiments presented here are examples of data obtained from multiple replicates of each experiment. The numerical data obtained varied between the replicates. However, the trends observed in these experiments were reproducible throughout the studies.

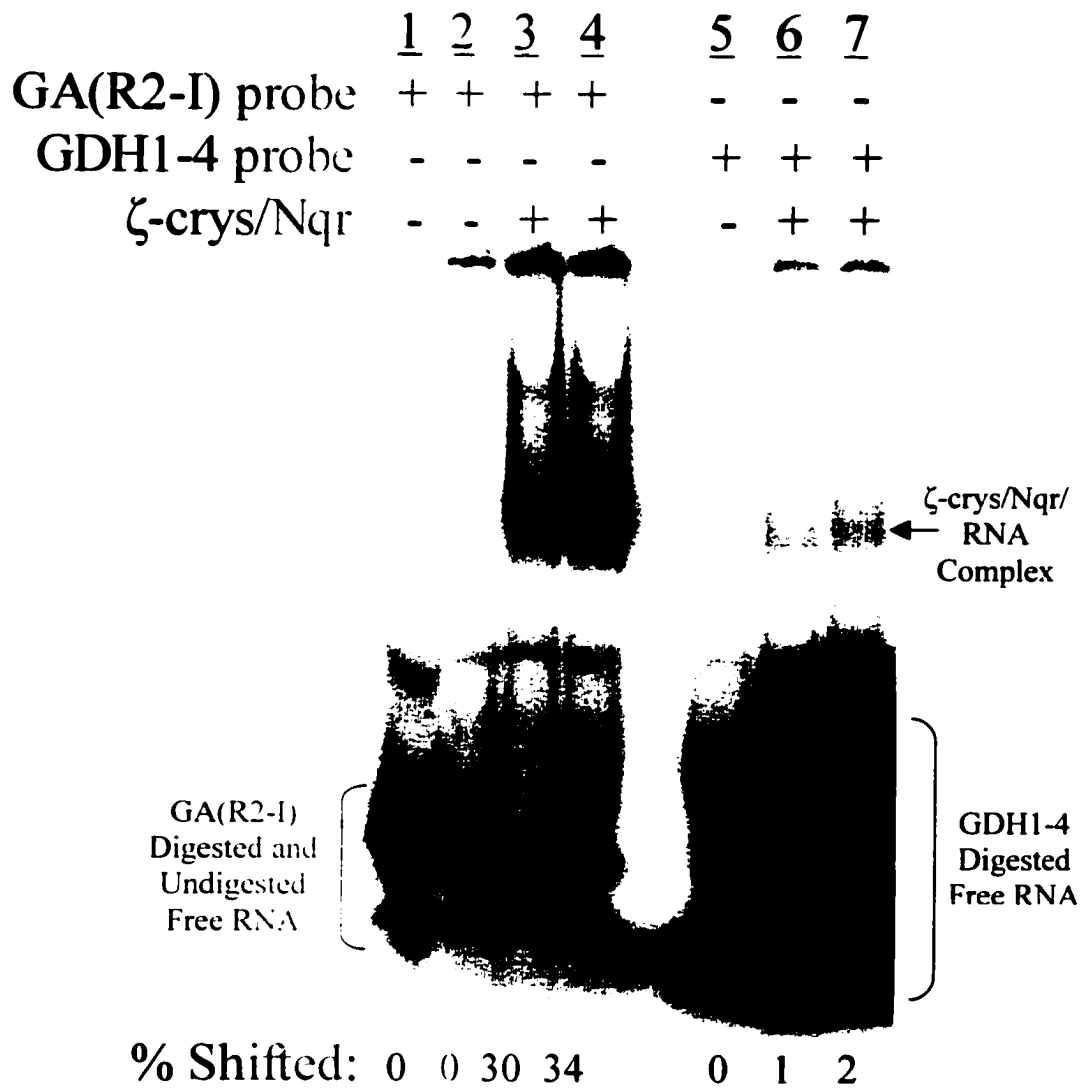
### **5.1.1 $\zeta$ -crystallin binds the 3'-UTR of GDH in an Electrophoretic Mobility Shift Analysis (EMSA)**

A segment or segments of the GDH1-4 RNA, which contained the 3'-UTR of the GDH mRNA (1696-2874 bp), formed an RNA/protein complex when incubated with  $\zeta$ -crystallin. This shifted complex has the same mobility as the 29-nt GA(R2-I) and  $\zeta$ -crystallin complex. However, the amount of radioactivity contained in the GDH1-4/ $\zeta$ -crystallin complex is relatively small compared to that contained in the GA(R2-I)/ $\zeta$ -crystallin complex (Fig. 5.1).

Much of this difference is due to the relative sizes of the two RNAs. Due to the length of the GDH1-4 RNA (~1.2 kb), the binding reactions were treated with a

**Fig. 5.1.  $\zeta$ -crys/Nqr binds to GA(R2-I) and GDH1-4 RNAs.**

The GA(R2-I) RNA (29 nt) contains the direct repeat of the two 8-base AREs from the 3'-UTR of GA mRNA. The GDH1-4 RNA (1.2 kb) contains the entire 3'-UTR of the GDH mRNA. Purified  $\zeta$ -crys/Nqr was added to lanes 3, 4, and 6 (2  $\mu$ l of protein) and lane 7 (4  $\mu$ l of protein). Samples in lanes 2 and 4-7 were treated with RNase T1 to digest the unbound RNA. The RNA-protein complexes were resolved on a non-denaturing polyacrylamide gel. The gel was then dried and imaged with a PhosphorImager screen. Several replicates of this experiment were conducted, data shown here is from a single experiment.



ribonuclease, RNase T1, to digest unbound RNA after guanine residues. This treatment is necessary to resolve the unbound GDH1-4 RNA from the shifted complex on a gel. Thus, the apparent difference in binding of GDH1-4 to  $\zeta$ -crystallin may be due to the fact that only 32-bases within the 1.2 kb of GDH1-4 mRNA are protected from digestion, while 16 of the 29 bases in the GA(R2-I) RNA are protected from digestion. Therefore most of the GDH1-4 probe is digested and appears as free probe whereas the majority of the GA(R2-I) probe is bound to  $\zeta$ -crystallin.

### **5.1.2 $\zeta$ -crystallin binds the individual AREs from the GA and GDH 3'-UTRs**

The binding of  $\zeta$ -crystallin in rat renal cytosolic extracts to the individual AREs of the GA 3'-UTR was studied using GA(R2-I) RNAs in which one of the two 8-base AREs was mutated to guanine or cytosine residues (Laterza et al 1997). In an EMSA, RNAs in which only one ARE was mutated showed reduced binding affinity to  $\zeta$ -crystallin compared to the wild-type GA(R2-I) RNA. When both of the AREs were mutated, binding was abolished.

The decreased binding affinity observed with the mutated constructs could be caused by the increase in the GC content of the mRNAs and not the missing AREs. Therefore, new constructs were prepared which contained only one of the two AREs. The GA(R2-IA) RNA contained the U U U A A A U A element (2596-2603 bp) and GA(R2-IB) RNA contained the U U A A A A U A element (2604-2611 bp) in the context of surrounding 3'-UTR sequence of the GA mRNA (Fig. 4.1). The binding studies were also performed using purified  $\zeta$ -crystallin instead of the rat renal cytosolic extracts.

An EMSA using GA(R2-IA) and GA(R2-IB) RNAs, containing a single ARE from the GA 3'-UTR, shows that  $\zeta$ -crystallin binds to the individual AREs with only slightly lower affinity than is observed for GA(R2-I).  $\zeta$ -crystallin exhibits slightly greater binding to GA(R2-IB) than GA(R2-IA) (Fig. 5.2).

This illustrates that  $\zeta$ -crystallin binding in the presence of two GA elements is greater than the binding seen with a single GA element. This EMSA (Fig. 5.2) also indicates that  $\zeta$ -crystallin binds to individual AREs with greater affinity than previously indicated using the mutated GA(R2-I) RNAs (Laterza et al 1997).

Experiments were designed to test the binding affinity and specificity of the individual 8-base AREs from the GDH 3'-UTR to  $\zeta$ -crystallin. This was done since the binding properties of full-length GDH1-4 RNA were difficult to determine in EMSAs due to the length of the RNA. The sequences and locations of the AREs within the 3'-UTR of GDH are GDH 1: UUUAAGUA (1973-1980 bp); GDH 2: CUAAAAUA (2313-2320 bp); GDH 3: UUCAAAUA (2537-2544 bp); and GDH 4: UUUAUAUA (2749-2756 bp) (Fig. 4.1).

$\zeta$ -crystallin binds to each of the RNAs containing a single 8-base ARE from the GDH 3'-UTR, but with lower affinities than observed for the GA(R2-I) RNA or the individual GA AREs. Of the GDH AREs, the GDH2 and GDH4 RNAs demonstrate the highest affinity for  $\zeta$ -crystallin while GDH1 and GDH3 show very weak binding (Fig. 5.2). This indicates that the individual GDH AREs function as binding elements for  $\zeta$ -crystallin. These elements may function alone or cooperatively to create a pH-responsive stabilization of the GDH mRNA as observed with the AREs in the GA mRNA.

**Fig. 5.2.  $\zeta$ -crys/Nqr binds to various ribonucleotides that contain the putative AREs from the GA and GDH mRNAs.**

The following [ $^{32}$ P]-labeled RNAs were incubated in the absence (-) or presence (+) of 2  $\mu$ l of purified  $\zeta$ -crys/Nqr: GA(R2-I) (lanes 1 and 2); GA(R2-IA) (lanes 3 and 4); GA(R2-IB) (lanes 5 and 6); GDH1 (lanes 7 and 8); GDH2 (lanes 9 and 10); GDH3 (lanes 11 and 12); and GDH4 (lanes 13 and 14). The samples were resolved on a non-denaturing polyacrylamide gel. The gel was then dried and imaged with a PhosphorImager screen. Several replicates of this experiment were conducted, data shown here is from a single experiment.

	<u>1</u>	<u>2</u>	<u>3</u>	<u>4</u>	<u>5</u>	<u>6</u>	<u>7</u>	<u>8</u>	<u>9</u>	<u>10</u>	<u>11</u>	<u>12</u>	<u>13</u>	<u>14</u>
$\zeta$ -crys/Nqr	-	+	-	+	-	+	-	+	-	+	-	+	-	+
% Shifted:	0	24	0	10	0	23	0	1	0	4	0	1	0	4



### **5.1.3 GA and GDH AREs compete $\zeta$ -crystallin/GA(R2-I) binding**

Competition studies were performed to determine whether the individual GA and GDH AREs exhibit specific binding to  $\zeta$ -crystallin. [<sup>32</sup>P]-labeled GA(R2-I) was bound to  $\zeta$ -crystallin and increasing amounts of unlabeled RNAs were added as competitors.

Competition studies demonstrated that a 300-fold excess of unlabeled GA(R2-IA) and GA(R2-IB) competitor is required to produce the same level of competition observed with a 30-fold excess of GA(R2-I). The competition observed with GA(R2-IB) is slightly greater than with GA(R2-IA) (Fig. 5.3). The data obtained in the competition studies are consistent with results observed in the binding studies. Both experiments indicate that a single GA ARE does not bind as well as the direct ARE repeat within the GA 3'-UTR that constitutes the pHRE.

The individual GDH ARE-containing RNAs were tested as competitors for the labeled GA(R2-I) RNA. GDH2 and GDH4 RNAs were more effective competitors of labeled GA(R2-I). A 300-fold excess of the GDH2 or GDH4 RNA does not compete as well as a 100-fold excess of GA(R2-I) RNA and the GDH3 and GDH1 RNAs are less effective competitors (Fig. 5.4). The competition pattern observed with the individual GDH elements (Fig. 5.4) confirms the results of the direct binding studies (Fig. 5.2).

## **5.2 Functional Studies**

Functional studies were performed to determine whether an element from the 3'-UTR of an mRNA is capable of creating a pH-responsive stabilization of the mRNA. This was determined by measuring the half-life of an mRNA containing the putative pHRE in cells treated with either normal or acidic medium. Cells that were stably

**Fig. 5.3. GA(R2-IA) and GA(R2-IB) RNAs compete binding of  $\zeta$ -crys/Nqr to the GA(R2-I) RNA.**

[<sup>32</sup>P]-labeled GA(R2-I) RNA (all lanes) was incubated with purified  $\zeta$ -crys/Nqr (lanes 2-10). A 30-, 100-, or 300-fold excess of an unlabeled RNA competitor was added as indicated: GA(R2-I) (lanes 3 and 4); GA(R2-IA) (lanes 5 through 7); and GA(R2-IB) (lanes 8 through 10). The samples were resolved on a non-denaturing gel. The gel was then dried and imaged with a Phosphorimager screen. Several replicates of this experiment were conducted. data shown here is from a single experiment.

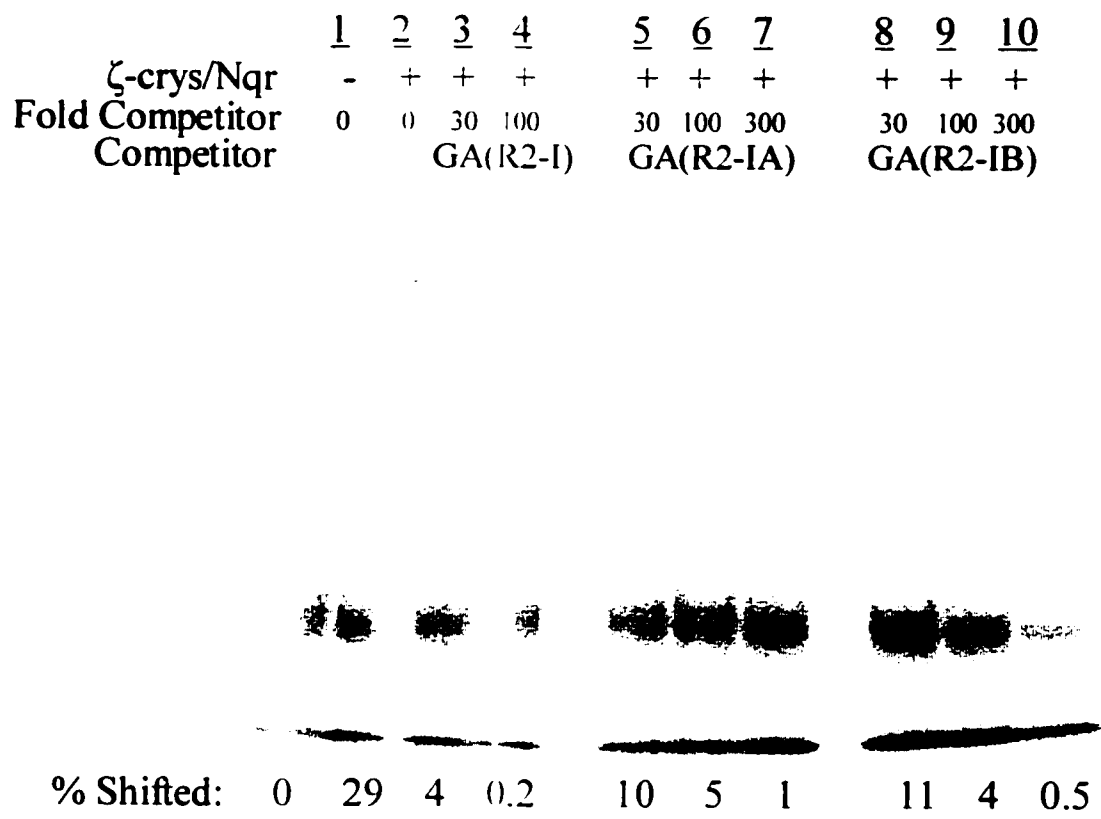
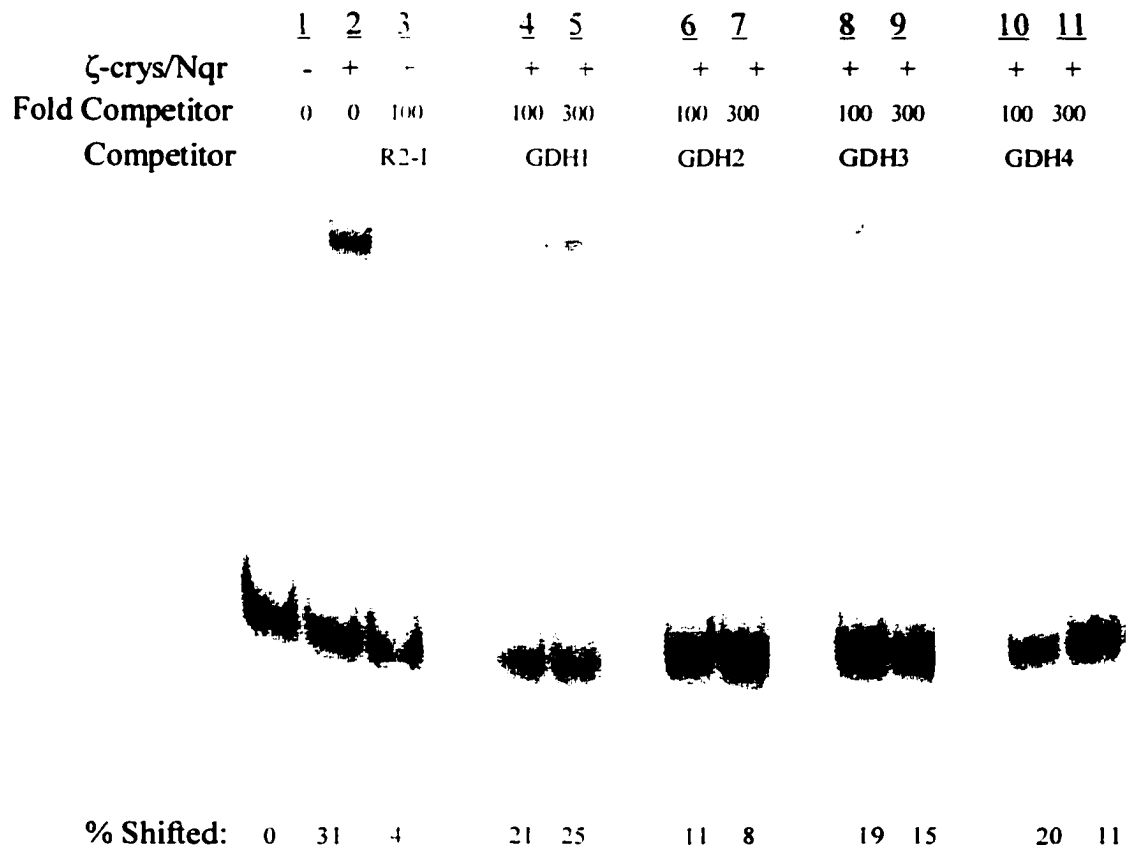


**Fig. 5.4. GDH1, GDH2, GDH3, and GDH4 RNAs compete binding of  $\zeta$ -crys/Nqr to the GA(R2-I) RNA.**

[<sup>32</sup>P]-labeled GA(R2-I) RNA (all lanes) was incubated with purified  $\zeta$ -crys/Nqr (lanes 2-10). A 30-, 100-, or 300-fold excess of an unlabeled RNA competitor was added as indicated: GA(R2-I) (lane 3); GDH1 (lanes 4 and 5); GDH2 (lanes 6 and 7); GDH3 (lanes 8 and 9); and GDH4 (lanes 10 and 11). The samples were resolved on a non-denaturing gel. The gel was then dried and imaged with a PhosphorImager screen. Several replicates of this experiment were conducted, data shown here is from a single experiment.



transfected with the p $\beta$ G plasmid that encodes a very stable and non-pH-responsive mRNA were used as the control for this analysis. The p $\beta$ G vector is composed of a promoter derived from the Rous sarcoma virus long terminal repeat (RSV-LTR), a transcription start site, the  $\beta$ G coding region from rabbit  $\beta$ -globin genomic DNA containing three exons and two introns, a multicloning site, and a 3'-UTR and polyadenylation site from the bovine growth hormone cDNA (Hansen et al 1996). When LLC-PK<sub>1</sub>-F<sup>+</sup> cells are stably transfected with a p $\beta$ G construct containing a pHRE inserted within the multicloning site, the resulting chimeric mRNA is stabilized when the cells are transferred from normal medium (pH 7.4, 25 mM HCO<sub>3</sub><sup>-</sup>) to acidic medium (pH 6.9, 10 mM HCO<sub>3</sub><sup>-</sup>).

Functional studies were performed previously to illustrate the pH-responsive stabilization of various mRNAs. The stabilization of  $\beta$ G-GA mRNA under acidic conditions results from the presence of the 955-nt GA 3'-UTR (Hansen et al 1996). When the pHRE element, containing two 8-base AREs in a direct repeat, within the  $\beta$ G-GA mRNA was altered by site directed mutagenesis, the pH-responsive stabilization of the mRNA was abolished (Laterza & Curthoys 2000). This indicated that the pHRE sequence is necessary to create a pH-responsive stabilization.

The 3'-UTR of PEPCK imparts only a slight pH-responsive stabilization of the mRNA (~ 1.3 fold) (Hansen et al 1996; Laterza & Curthoys 2000). However, the PEPCK 3'-UTR contains an instability element that decreases the stability of  $\beta$ G-PEPCK mRNA. Therefore, to test the pH-responsiveness of small segments of the GA 3'-UTR that may not produce a sufficiently unstable RNA to monitor a pH-responsive stabilization, the putative pHRE was cloned into the p $\beta$ G vector upstream of the PEPCK

3'-UTR. The p $\beta$ G-GA(R2-H)-PEPCK plasmid contains a 76-nt segment of the GA 3'-UTR, R2-H, that encodes the pHRE. The chimeric mRNA transcribed from this plasmid exhibits a five-fold pH-responsive stabilization. This indicates that the 76-nt sequence containing the pHRE is sufficient to impart a pH-responsive stabilization to the reporter mRNA (Laterza & Curthoys 2000).

### **5.2.1 $\beta$ G mRNA is stable and not pH-responsive**

It is important to test p $\beta$ G as a control in order to verify that the vector alone does not confer a pH-responsive stabilization of the mRNA. This experiment had been done previously (Hansen et al 1996), but was repeated along with an experiment using p $\beta$ G-GA in order to provide a complete set of data using cells that were treated and grown under the same conditions.

$\beta$ G mRNA is stable in LLC-PK<sub>1</sub>-F<sup>+</sup> cells with a half-life ( $t_{1/2}$ ) of over 30 h when cells are treated with either normal or acidic medium. There is also no change in the level of the mRNA expressed in cells grown in either type of medium (Fig. 5.5). This indicates that  $\beta$ G mRNA is stable and not pH-responsive.

### **5.2.2 pH-responsive stabilization of $\beta$ G-GA mRNA**

The p $\beta$ G-GA plasmid contains 955-nt of the GA 3'-UTR (Fig. 5.6.A). p $\beta$ G-GA produced an unstable mRNA with a  $t_{1/2}$  of approximately 12 h under normal growth conditions at pH 7.4. The  $\beta$ G-GA mRNA showed a pH-responsive stabilization ( $t_{1/2} > 30$  h) when the cells were transferred into acidic medium (Fig. 5.6). These observations confirm the previous conclusion that the 3'-UTR of the GA mRNA contains an instability element and imparts a pH-responsive stabilization to the  $\beta$ G mRNA (Hansen et al 1996).

**Fig. 5.5.  $\beta$ G mRNA is stable not pH-responsive.**

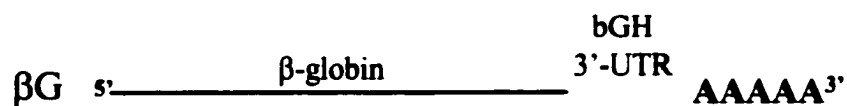
**Panel A.** A schematic of the  $\beta$ G mRNA.

**Panel B.** Northern blot of  $\beta$ G mRNA isolated from LLC-PK<sub>1</sub>-F<sup>+</sup> cells stably transfected with p $\beta$ G. Cells were either maintained in normal (pH 7.4) medium or transferred to acidic (pH 6.9) medium for 12 h and then treated with 65  $\mu$ M 5-6-dichloro-1- $\beta$ -ribofuranosylbenzimidazole (DRB) for 0, 3, 6, and 9 h.

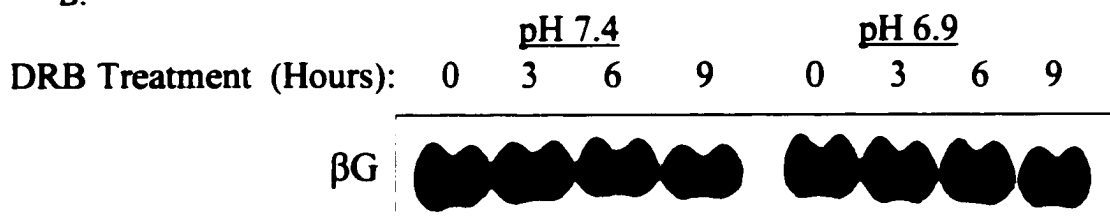
**Panel C.** Relative levels of  $\beta$ G mRNA were determined by PhosphorImager analysis. The level of  $\beta$ G mRNA was divided by the corresponding level of 18S rRNA to correct for errors in sample loading. The log of normalized data was then plotted versus the time of treatment with DRB. Values are averages of data obtained from 2 separate determinations. The line represents the best-fit of the data points as determined by the KaleidaGraph program that weights each data point based upon its standard deviation.

## Half-life Analysis of $\beta$ G mRNA

A.



B.



C.

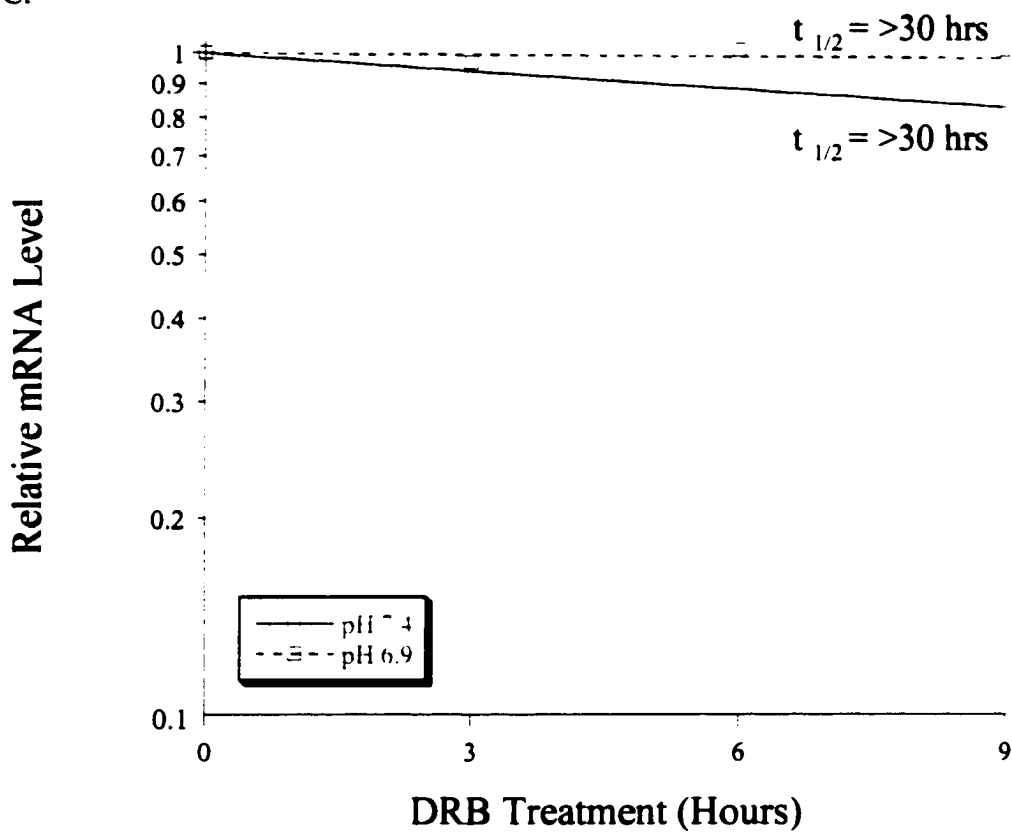


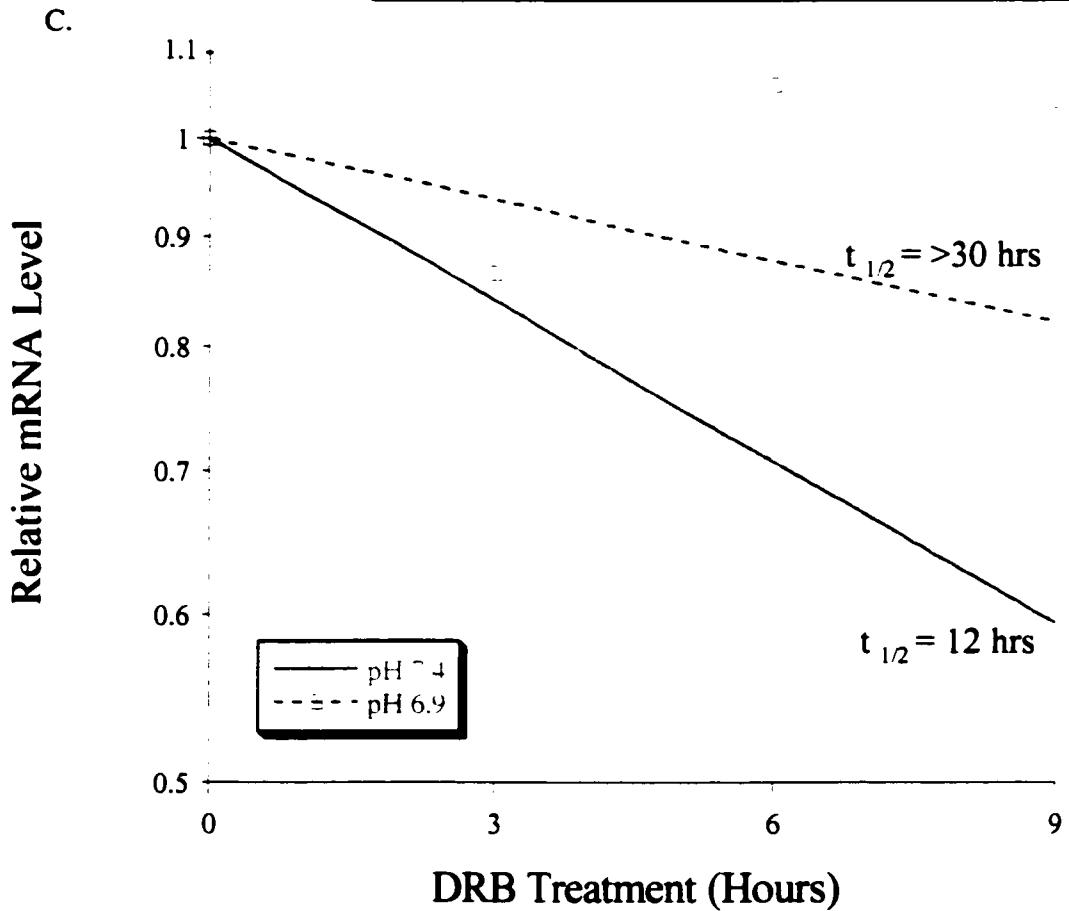
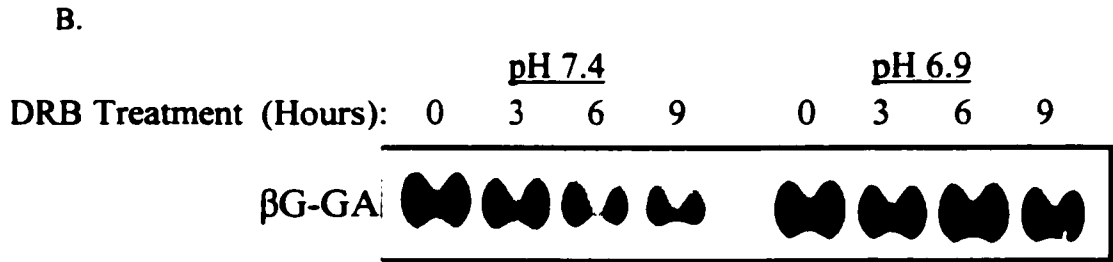
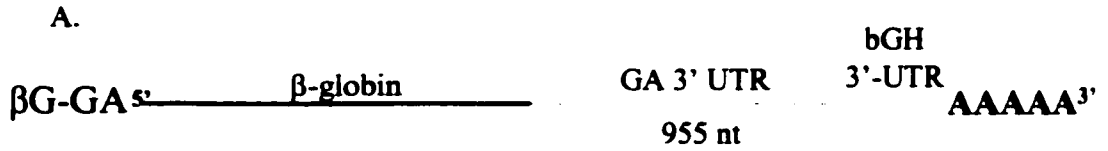
**Fig. 5.6.  $\beta$ G-GA mRNA is stabilized in response to changes in pH.**

**Panel A.** A schematic of the  $\beta$ G-GA mRNA.

**Panel B.** Northern blot of  $\beta$ G-GA mRNA isolated from LLC-PK<sub>1</sub>-F<sup>+</sup> cells stably transfected with p $\beta$ G-GA. Cells were either maintained in normal (pH 7.4) medium or transferred to acidic (pH 6.9) medium for 12 h and then treated with 65  $\mu$ M 5-6-dichloro-1- $\beta$ -ribofuranosylbenzimidazole (DRB) for 0, 3, 6, and 9 h.

**Panel C.** Relative levels of  $\beta$ G-GA mRNA were determined by PhosphorImager analysis. The level of  $\beta$ G-GA mRNA was divided by the corresponding level of 18S rRNA to correct for errors in sample loading. The log of normalized data was then plotted versus the time of treatment with DRB. Values are averages of data obtained from 2 separate determinations. The line represents the best-fit of the data points as determined by the KaleidaGraph program that weights each data point based upon its standard deviation.

# Half-life Analysis of $\beta$ G-GA mRNA



### **5.2.3 GA(R2-I) is a pHRE**

A 32-nt fragment of the GA 3'-UTR, containing the direct repeat of the two 8-base AREs that make up the pHRE, was cloned into p $\beta$ G (Fig. 4.2, Fig. 5.7.A). This construct lacks the 3'-UTR of PEPCK. Therefore, it was used to determine whether this sequence can function as a pHRE in the absence of the destabilizing effect of the PEPCK 3'-UTR. When LLC-PK<sub>1</sub>-F<sup>+</sup> cells were stably transfected with p $\beta$ G-GA(R2-I) and grown in normal medium, the  $\beta$ G-GA(R2-I) RNA decayed with a  $t_{1/2}$  of 19 h. When the same cells were transferred to acidic medium, the chimeric RNA was degraded with a  $t_{1/2}$  of over 30 h (Fig. 5.7). This indicates that the sequence contained within the GA(R2-I) region of the GA 3'-UTR is sufficient to function as a pH-responsive element. However, the  $\beta$ G-GA(R2-I) mRNA has a longer half-life at pH 7.4 than that of  $\beta$ G-GA mRNA. Therefore, additional destabilizing element(s) may be present elsewhere in the 3'-UTR of the mRNA.

### **5.2.4 $\beta$ G-GDH mRNA contains a pHRE**

Since GA and GDH mRNA exhibit the same kinetics of induction during an acute onset of acidosis (Hwang & Curthoys 1991; Kaiser et al 1992) and since the GDH 3'-UTR contains four 8-base AREs that are 88% identical to the AREs from the GA pHRE, functional studies were performed to determine if GDH mRNA levels are also increased due to a pH-responsive stabilization of the mRNA by the 3'-UTR. The p $\beta$ G-GDH vector encodes the 930-nt 3'-UTR of GDH mRNA with its four 8-base AREs (Fig. 5.8, Fig. 5.9.A). The  $\beta$ G-GDH mRNA has a  $t_{1/2}$  of approximately 14 h in cells grown in normal medium. When the cells were transferred to acidic medium, the  $t_{1/2}$  of the  $\beta$ G-GDH

**Fig. 5.7. GA(R2-I) stabilizes  $\beta$ G-GA(R2-I) mRNA under acidic conditions.**

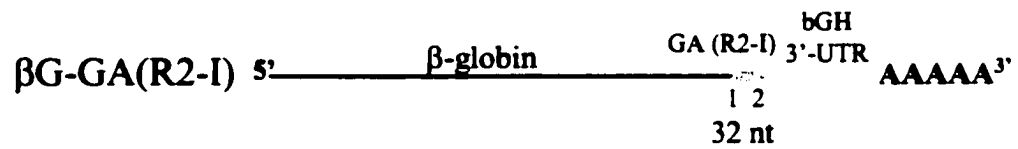
**Panel A.** A schematic of the  $\beta$ G-GA(R2-I) mRNA.

**Panel B.** Northern blot of  $\beta$ G-GA(R2-I) mRNA isolated from LLC-PK<sub>1</sub>-F<sup>+</sup> cells stably transfected with p $\beta$ G-GA(R2-I). Cells were either maintained in normal (pH 7.4) medium or transferred to acidic (pH 6.9) medium for 12 h and then treated with 65  $\mu$ M 5-6-dichloro-1- $\beta$ -ribofuranosylbenzimidazole (DRB) for 0, 3, 6, and 9 h.

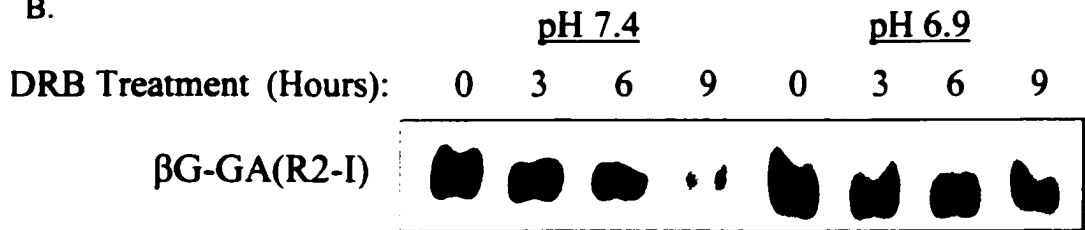
**Panel C.** Relative levels of  $\beta$ G-GA(R2-I) mRNA were determined by PhosphorImager analysis. The level of  $\beta$ G-GA(R2-I) mRNA was divided by the corresponding level of 18S rRNA to correct for errors in sample loading. The log of normalized data was then plotted versus the time of treatment with DRB. Values are averages of data obtained from 3 separate determinations. The line represents the best-fit of the data points as determined by the KaleidaGraph program that weighs each data point based upon its standard deviation.

## Half-life Analysis of $\beta$ G-GA(R2-I) mRNA

A.



B.



C.

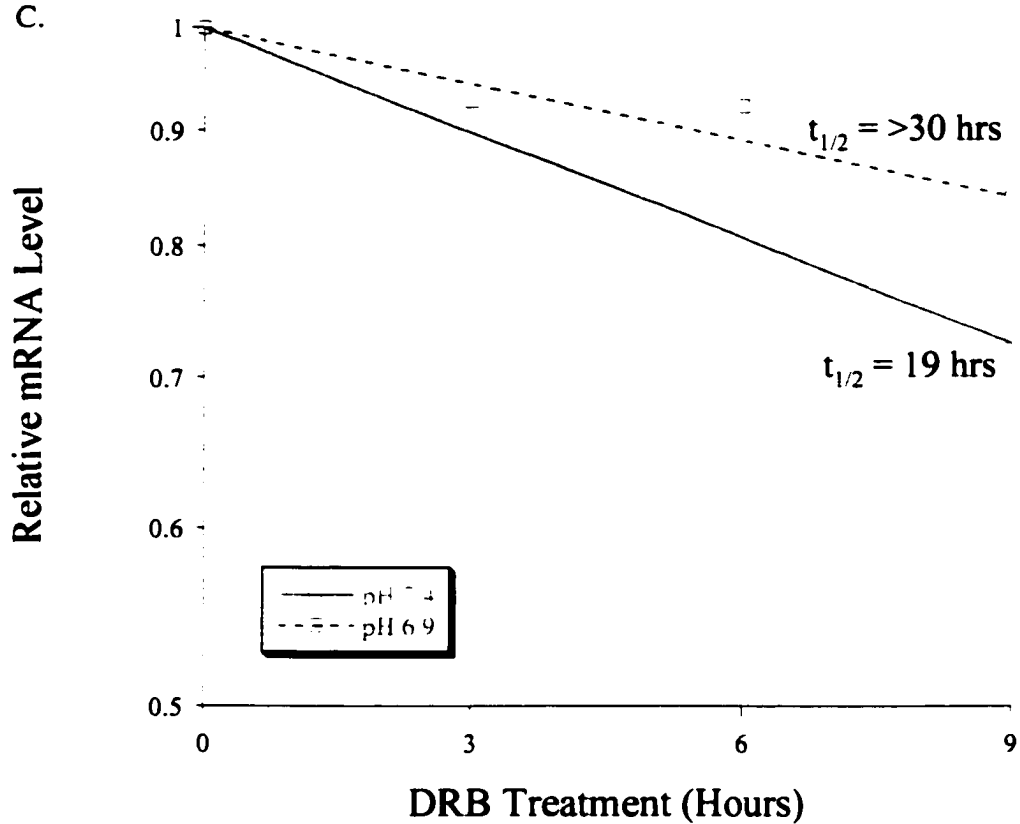


**Fig. 5.8. Schematic of ARE locations within the 3'-UTRs of GA and GDH.**

The GDH AREs 1, 3, and 4 are 88% identical to the first GA ARE (black x's) and GDH 2 is 88% identical to the second GA ARE (red, italicized x's). The nucleotide that differs between the GA and GDH sequences is underlined.

**GA 3'-UTR**  **Xc** 

**GA(R2-I):** UUAAAUAUUUUUUUUUU

**GDH 3'-UTR** 

**GDH1:** UUUAAGUA

**GDH2:** UUUUUUUU

**GDH3:** UUCAAAUA

**GDH4:** UUUAUAUA

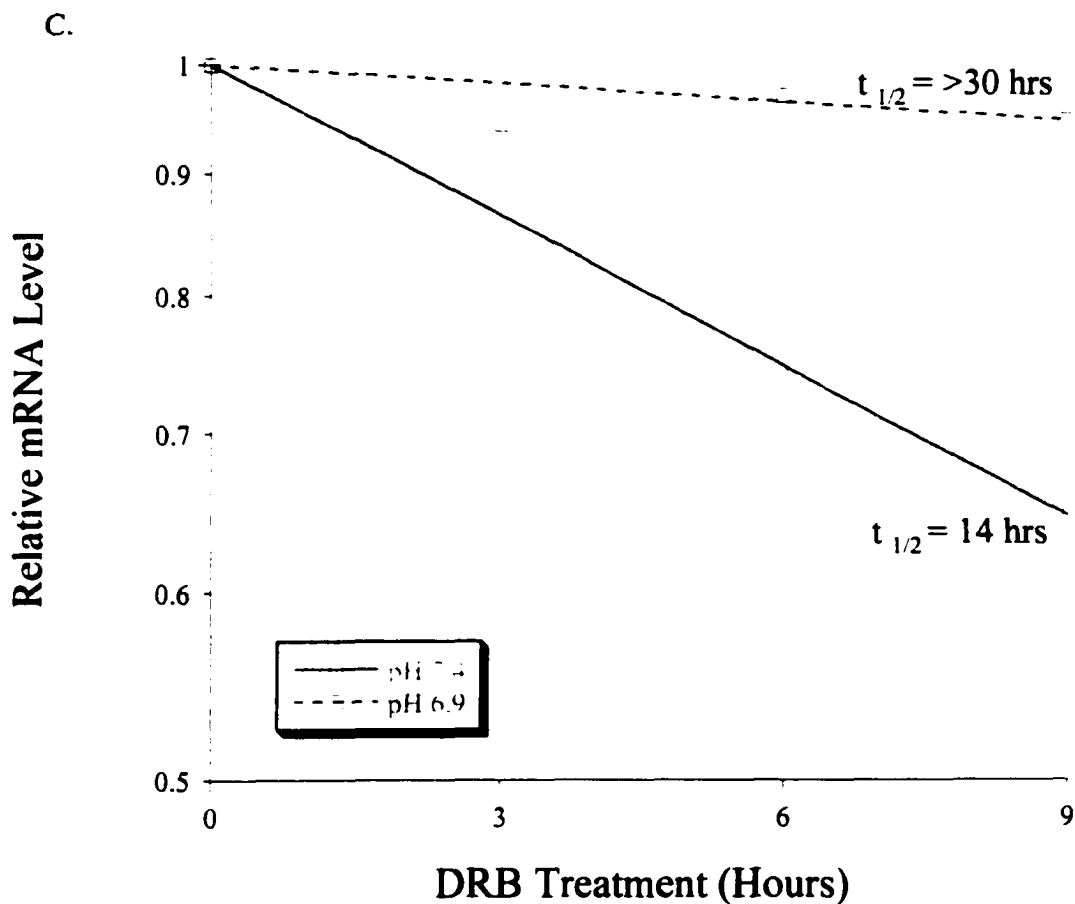
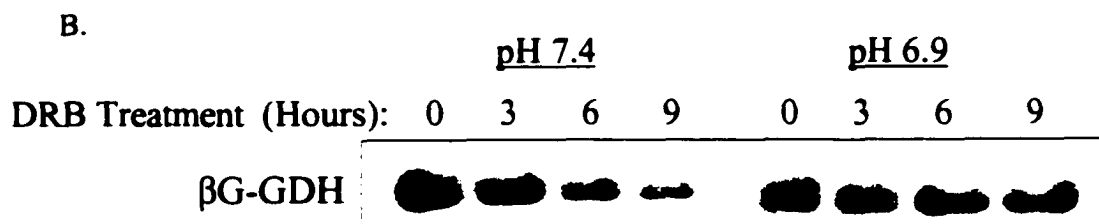
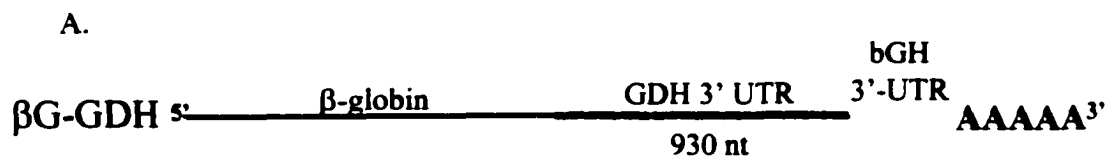
**Fig. 5.9.  $\beta$ G-GDH mRNA is stabilized in response to changes in pH.**

**Panel A.** A schematic of the  $\beta$ G-GDH mRNA.

**Panel B.** Northern blot of  $\beta$ G-GDH mRNA isolated from LLC-PK<sub>1</sub>-F<sup>+</sup> cells stably transfected with p $\beta$ G-GDH. Cells were either maintained in normal (pH 7.4) medium or transferred to acidic (pH 6.9) medium for 12 h and then treated with 65  $\mu$ M 5-6-dichloro-1- $\beta$ -ribofuranosylbenzimidazole (DRB) for 0, 3, 6, and 9 h.

**Panel C.** Relative levels of  $\beta$ G-GDH mRNA were determined by PhosphorImager analysis. The level of  $\beta$ G-GDH mRNA was divided by the corresponding level of 18S rRNA to correct for errors in sample loading. The log of normalized data was then plotted versus the time of treatment with DRB. Values are averages of data obtained from 2 separate determinations. The line represents the best-fit of the data points as determined by the KaleidaGraph program that weights each data point based upon its standard deviation.

## Half-life Analysis of $\beta$ G-GDH mRNA



mRNA was increased to over 30 h. Thus, this mRNA exhibits a pH-responsive stabilization (Fig. 5.9). This observation indicates that the 3'-UTR of the GDH mRNA contains one or more pHREs that impart selective stabilization to the GDH mRNA in response to acidosis.

## **5.2.5 Stability of mRNA containing the GDH4 ARE**

### **5.2.5.1 $\beta$ G-GDH4 mRNA is not sufficiently destabilized to observe a pH-response**

Due to the similarity in sequence and the fact that GDH AREs bind  $\zeta$ -crystallin it is possible that the GDH AREs also function as pH-response elements. The direct binding and competition analyses indicated that the GDH2 and GDH4 AREs bind  $\zeta$ -crystallin with the greatest affinity. The GDH4 sequence was cloned into p $\beta$ G to test whether a single GDH element could cause a pH-responsive stabilization of its mRNA.

The p $\beta$ G-GDH4 vector encodes the fourth 8-base ARE from the 3'-UTR of GDH (Fig. 4.2, Fig. 5.10.A). The  $t_{1/2}$  of the  $\beta$ G-GDH4 mRNA is over 30 h in cells maintained in either normal or acidic medium (Fig. 5.10). Thus, the 35-nt GDH4 sequence does not significantly destabilize the  $\beta$ G mRNA. Given the inherent stability of this construct, it could not be used to determine if the GDH4 sequence can function as a pH-responsive element.

### **5.2.5.2 GDH4 functions as a weak pHRE**

To assess whether the GDH4 sequence can function as a weak pHRE, the 3'-UTR of PEPCK was cloned downstream of the GDH4 element to produce the p $\beta$ G-GDH4-PEPCK plasmid (Fig. 5.11.A). The insertion of this sequence destabilizes the resulting  $\beta$ G-GDH4-PEPCK mRNA. The  $t_{1/2}$  of this mRNA in cells grown in pH 7.4 medium was

**Fig. 5.10.  $\beta$ G-GDH4 mRNA is not sufficiently destabilized to observe a pH-response.**

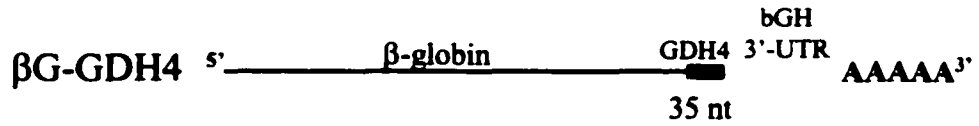
**Panel A.** A schematic of the  $\beta$ G-GDH4 mRNA.

**Panel B.** Northern blot of  $\beta$ G-GDH4 mRNA isolated from LLC-PK<sub>1</sub>-F<sup>+</sup> cells stably transfected with p $\beta$ G-GDH4. Cells were either maintained in normal (pH 7.4) medium or transferred to acidic (pH 6.9) medium for 12 h and then treated with 65  $\mu$ M 5-6-dichloro-1- $\beta$ -ribofuranosylbenzimidazole (DRB) for 0, 3, 6, and 9 h.

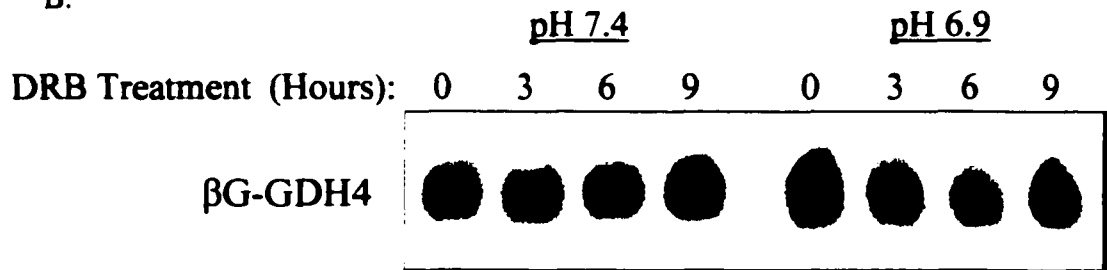
**Panel C.** Relative levels of  $\beta$ G-GDH4 mRNA were determined by PhosphorImager analysis. The level of  $\beta$ G-GDH4 mRNA was divided by the corresponding level of 18S rRNA to correct for errors in sample loading. The log of normalized data was then plotted versus the time of treatment with DRB. Values are averages of data obtained from 2 separate determinations. The line represents the best-fit line of the data points as determined by the KaleidaGraph program that weights each data point based upon its standard deviation.

## Half-life Analysis of $\beta$ G-GDH4 mRNA

A.



B.



C.

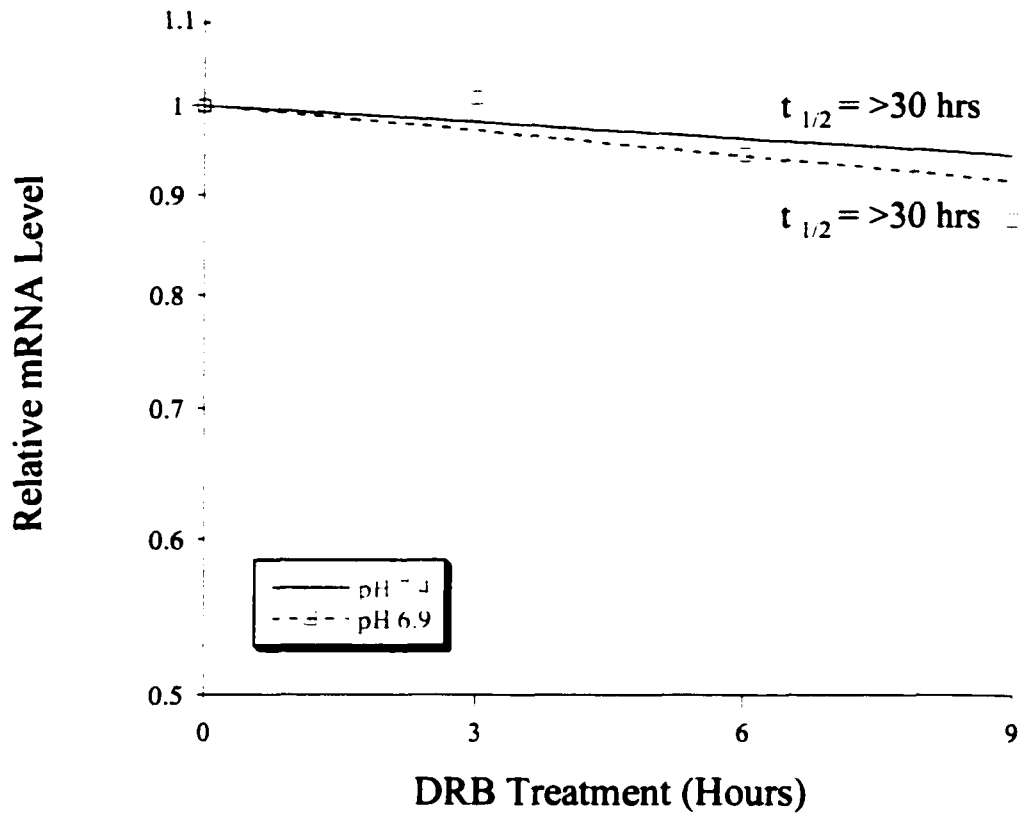


**Fig. 5.11. GDH4 functions as a weak pHRE in  $\beta$ G-GDH4-PEPCK mRNA.**

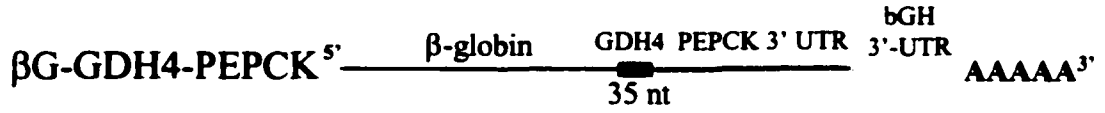
**Panel A.** A schematic of the  $\beta$ G-GDH4-PEPCK mRNA.

**Panel B.** Northern blot of  $\beta$ G-GDH4-PEPCK mRNA isolated from LLC-PK<sub>1</sub>-F<sup>+</sup> cells stably transfected with p $\beta$ G-GDH4-PEPCK. Cells were either maintained in normal (pH 7.4) medium or transferred to acidic (pH 6.9) medium for 12 h and then treated with 65  $\mu$ M 5-6-dichloro-1- $\beta$ -ribofuranosylbenzimidazole (DRB) for 0, 3, 6, and 9 h.

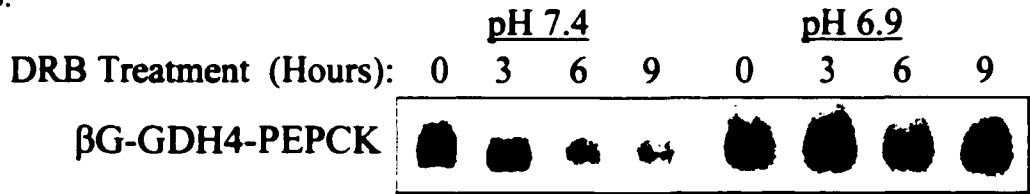
**Panel C.** Relative levels of  $\beta$ G-GDH4-PEPCK mRNA were determined by PhosphorImager analysis. The level of  $\beta$ G-GDH4-PEPCK mRNA was divided by the corresponding level of 18S rRNA to correct for errors in sample loading. The log of normalized data was then plotted versus the time of treatment with DRB. Values are averages of data obtained from 2 separate determinations. The line represents the best-fit of the data points as determined by the KaleidaGraph program that weights each data point based upon its standard deviation.

# Half-life Analysis of $\beta$ G-GDH4 -PEPCK mRNA

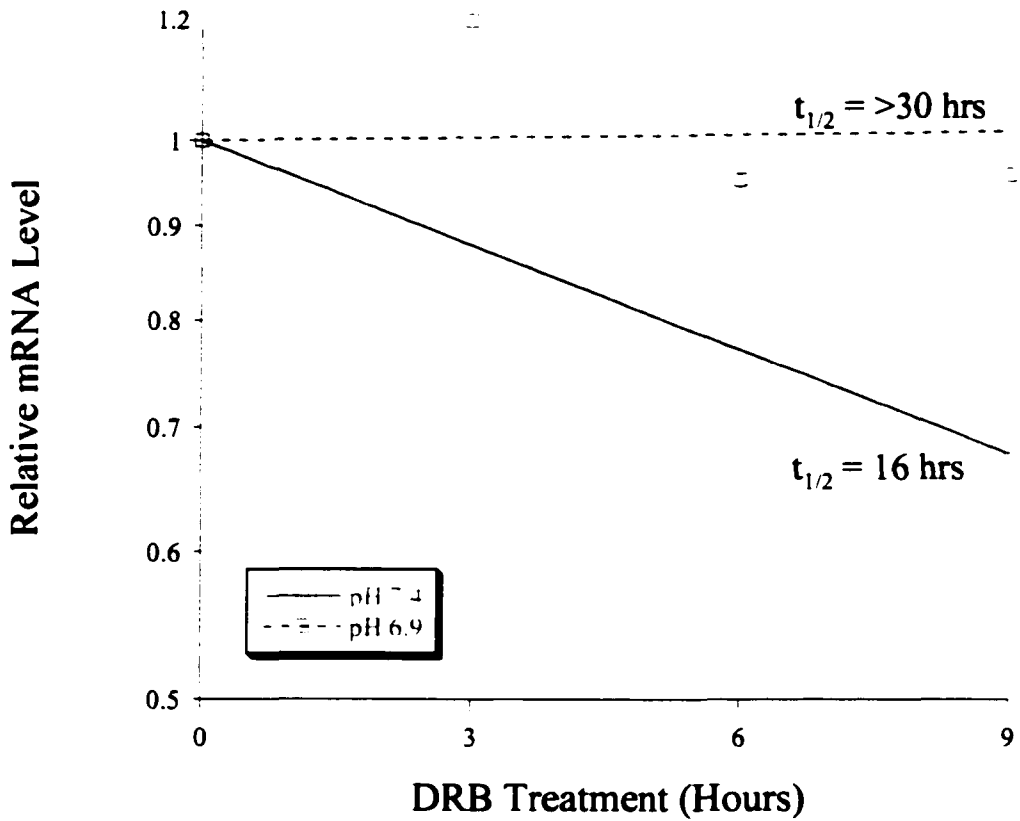
A.



B.



C.



16 h, and when the cells were treated with pH 6.9 medium, the  $t_{1/2}$  was increased to greater than 30 h (Fig. 5.11). These data indicate that GDH4 sequence functions as a pHRE. The three additional AREs in the GDH 3'-UTR may also function as weak pHREs that collectively impart a greater pH-responsive stabilization to the GDH mRNA.

The data for the functional analysis of the full-length 3'-UTRs and the individual elements is summarized in Table 5.1.

**Table 5.1. Summary of Half-life ( $t_{1/2}$ ) Values at pH 7.4 and 6.9 for Chimeric RNAs**

<u>mRNA</u>	<u><math>t_{1/2}</math> (Hours)</u> <u>at pH 7.4</u>	<u><math>t_{1/2}</math> (Hours)</u> <u>at pH 6.9</u>
$\beta$ G	>30	>30
$\beta$ G-GA	12	>30
$\beta$ G-GA(R2-I)	19	>30
$\beta$ G-GDH	14	>30
$\beta$ G-GDH4	>30	>30
$\beta$ G-GDH4-PCK	16	>30

## **6 mRNA Decay Studies using a Tetracycline-Responsive Expression System**

## **6.1 Tetracycline-responsive expression system**

The creation of a tetracycline-responsive expression system provides an important tool for studying mRNA decay and other biochemical events within the cell. The system provides a mechanism to activate or inhibit transcription of a single gene. In the previously discussed functional studies, DRB was used as an inhibitor to shut-off pol II transcription. However, with prolonged inhibition of general RNA transcription, the cells began to die. The tetracycline-responsive promoter system allows the *in vivo* decay of a specific mRNA to be studied without the occurrence of potential artifacts that may be caused by a general inhibition of pol II transcription (Xu et al 1998).

A tetracycline-responsive expression system consists of two important components that are transfected into LLC-PK<sub>1</sub>-F<sup>+</sup> cells. The first is the pTet-Off vector, which encodes for the regulatory protein tTA. tTA is a fusion protein consisting of the DNA binding domain of the Tet repressor (TetR) protein and the Herpes simplex virus virion protein 16 (VP16) activation domain. TetR normally functions as a negative regulator of the tetracycline-resistance operon genes of the Tn10 transposon by binding to a tetracycline operator sequence (tetO) in the absence of tetracycline. However, addition of the VP16 activation domain makes the tTA protein a transcriptional activator instead of a transcriptional repressor (CLONTECH Laboratories Inc. 1999; Gossen & Bujard 1992).

A stable cell line expressing high levels of the tTA protein must be generated in order to control the second component of the tetracycline-responsive system, the pTRE2 vector, which contains the gene and/or element to be studied. The pTRE2 vector contains

a tetracycline-responsive element (TRE) that has seven direct repeats of the tetO located upstream of a minimal cytomegalovirus (CMV) promoter (Fig. 4.3). Using a minimal CMV promoter minimizes “leaky” expression from the pTRE2 promoter, since the strong enhancers of the immediate early CMV promoter are missing. The gene or element of interest, such as Luciferase or  $\beta$ G-GA-bGH, can be cloned into this vector, so that its expression can be studied (CLONTECH Laboratories Inc. 1999; Gossen & Bujard 1992).

Transcription of an experimental pTRE2 construct is activated by the binding of the tTA protein to the TRE of the pTRE2 promoter. This protein can bind the pTRE2 promoter in the absence of Doxycycline (Dox), a tetracycline derivative, and transcription ensues. However, transcription is halted if Dox binds to tTA and prevents it from binding the TRE (Fig. 6.1). Therefore, an abrupt change in the level of Dox can cause a rapid turn-on or shut-off of transcription. The decay of a specific mRNA over time can then be monitored in order to determine the type of decay used by a specific RNA under varying conditions, such as those mimicking metabolic acidosis (Xu et al 1998).

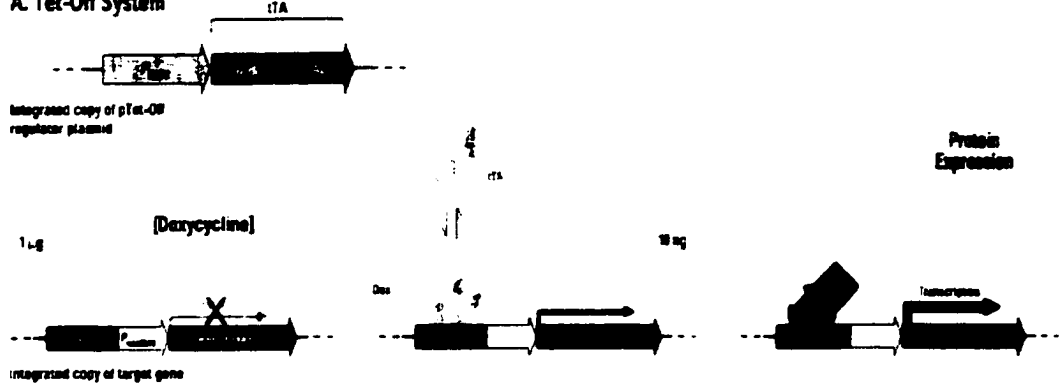
### **6.1.1 Creation and characterization of a tTA expressing LLC-PK<sub>1</sub>-F<sup>+</sup> cell line**

The pTet-Off vector was stably transfected into LLC-PK<sub>1</sub>-F<sup>+</sup> cells and twelve clonal cell lines expressing the tTA protein were isolated. The tetracycline-responsiveness of six of these cell lines was tested to determine the levels of transcriptional activation and inhibition in the absence or presence of Dox. The pTRE2-Luc vector that expresses the firefly luciferase protein was transiently transfected into the clonal cell lines and the cells were maintained in the presence or absence of 1  $\mu$ g/ml Dox

**Fig. 6.1. Schematic of the Tet-Off System for regulating gene expression.**

A stable cell line that expresses high levels of the tTA protein is selected. The chimeric tTA protein contains a Tet-binding domain fused to a strong transcriptional activation domain. The gene of interest is then cloned downstream of a promoter that contains a Tetracycline-responsive element (TRE) and a minimal immediate early promoter of cytomegalovirus ( $P_{\text{minCMV}}$ ). In the absence of Doxycycline (Dox), the tTA protein binds to the TRE and strongly activates transcription. In the presence of greater than 25 ng/ml Dox, the tTA protein no longer binds to the TRE and transcription is turned off. Thus, by adding and omitting Dox in the cell culture medium, a transcriptional pulse can be created. (CLONTECH Laboratories Inc. 1999)

### A. Tet-Off System



and then assayed for luciferase activity (Fig. 6.2). An optimal tTA-expressing cell line should show a strong fold induction (>20-fold) of the luciferase protein in the absence of Dox and very low levels of luciferase expression in the presence of Dox (CLONTECH Laboratories Inc. 1999).

The clonal cell lines that were tested showed varying levels of activation and inhibition of luciferase expression. The 8C line of LLC-PK<sub>1</sub>-F<sup>+</sup> cells showed the strongest tetracycline-responsive expression of the luciferase protein from pTRE2-Luc. This 8C LLC-PK<sub>1</sub>-F<sup>+</sup> cell line produced a 30-fold induction of the luciferase protein when compared to the expression levels in the presence of Dox (Fig. 6.2). Therefore, the 8C LLC-PK<sub>1</sub>-F<sup>+</sup> cell line was chosen for use in the subsequent experiments.

To optimize the luciferase assay conditions in order to find the best conditions for testing the tetracycline-responsive luciferase expression, varying amounts of lysates (5-40  $\mu$ l) were used in the luciferase assay. Five microliters of lysate gave the most consistent results (data not shown). In addition, increasing amounts of pTRE2-Luc (0.1-1.0  $\mu$ g) were transfected into the 8C LLC-PK<sub>1</sub>-F<sup>+</sup> cell line to determine what level of DNA produced the greatest response. Using 0.3  $\mu$ g of DNA resulted in a 200-fold induction. Thus, this level of DNA produced a high level of expression in the absence of Dox and a minimal level of expression in the presence of Dox (Fig. 6.3).

### **6.1.2 Creation and characterization of cell lines stably transfected with pTRE2- $\beta$ G-GA-bGH**

An experimental construct, pTRE2- $\beta$ G-GA-bGH, was designed that placed the  $\beta$ G-GA-bGH sequence from previous functional studies in front of a tetracycline-responsive promoter (Fig. 4.3). This made it possible to study the decay of the  $\beta$ G-GA

**Fig. 6.2. Characterization of stable LLC-PK<sub>1</sub>-F<sup>+</sup> transfectants expressing the tTA protein.**

Six stable tTA expressing LLC-PK<sub>1</sub>-F<sup>+</sup> cell lines (1C, 2B, 3C, 7B, 8C, and 11C) were cloned. The individual cell lines were transiently transfected with pTRE2-Luc.

Approximately 16 h after transfection, the medium was removed and fresh medium with or without 1  $\mu$ g/ml Doxycycline (Dox) was added. Cells were cultured for an additional 32 h and then extracts were prepared and assayed using the Luciferase Assay System (E1500, Promega). The protein concentration of the extracts was determined by Lowry assay and the firefly luciferase activity was standardized per  $\mu$ g of protein. The fold-induction of TRE2-Luc protein is calculated by dividing the -Dox values by the +Dox values. Values shown are the mean  $\pm$  S.D. of experiments done in triplicate.

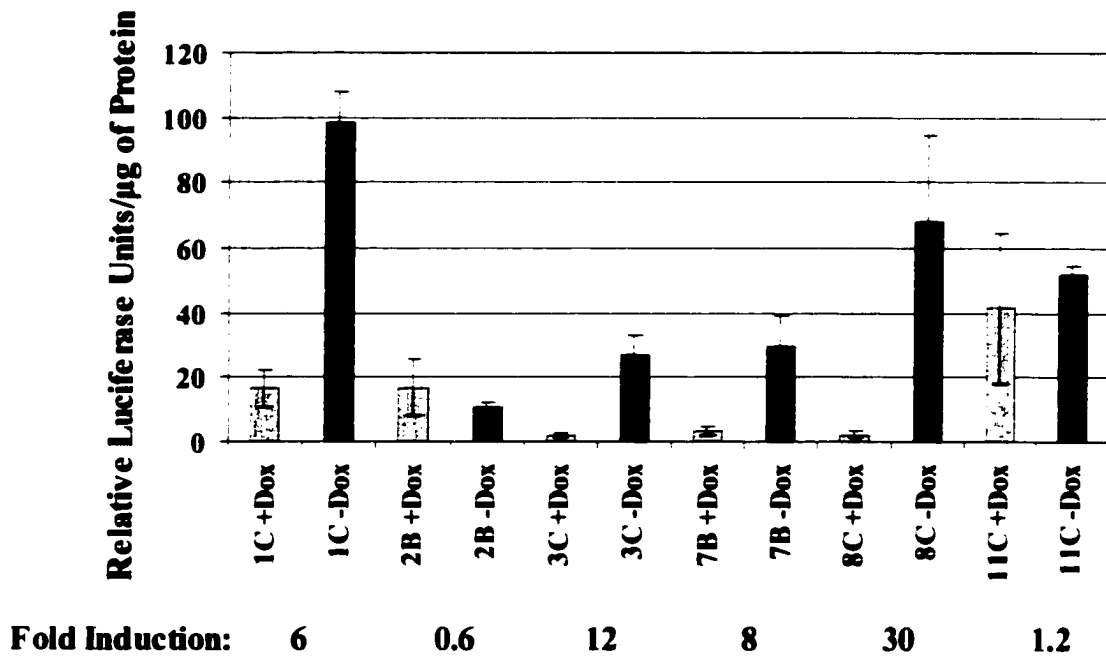


**Fig. 6.3. Optimization of tetracycline-responsive luciferase expression in 8C cells.**

Varying levels (0.1-1.0  $\mu\text{g}$ ) of pTRE2-Luc were transiently transfected into the 8C line of LLC-PK<sub>1</sub>-F<sup>+</sup> cells (tetracycline-responsive cell line). Approximately 16 h after transfection, the medium was removed and fresh medium with or without 1  $\mu\text{g}/\text{mL}$  Doxycycline (Dox) was added. Cells were cultured for an additional 32 h and then cell extracts were prepared and assayed using the Luciferase Assay System (E1500, Promega). The protein concentration of the extracts was determined by Lowry assay and the firefly luciferase activity was standardized per  $\mu\text{g}$  of protein. The fold-induction of TRE2-Luc protein is calculated by dividing the -Dox values by the +Dox values. Values shown are the mean  $\pm$  S.D. of experiments done in triplicate.



mRNA without effecting the levels of other mRNAs in the cell. Eight clonal cell lines (1A, 2A, 3A, 1B, 2B, 3B, 4B, and 5B) and two mixed cell lines (Mix and Dox Mix) were isolated from a stable transfection of pTRE2- $\beta$ G-GA-bGH into the 8C LLC-PK<sub>1</sub>-F<sup>+</sup> cell line. The cell lines were tested for tetracycline-responsive  $\beta$ G-GA expression by culturing the cells in the presence or absence of Dox and quantitating  $\beta$ G-GA mRNA expression by Northern analysis. Cell lines were judged based on whether  $\beta$ G-GA transcription was efficiently inhibited by the presence of Dox and whether in the absence of Dox there was a high level of transcription (Fig. 6.4).

The 2A sub-line of the 8C LLC-PK<sub>1</sub>-F<sup>+</sup> cells (8C/2A) showed the strongest tetracycline-responsive expression. The level of mRNA seen in the presence of Dox was almost undetectable but a high level of transcription was observed in the absence of Dox (Fig. 6.4.B). A 32-fold difference was seen in the levels of expression of  $\beta$ G-GA mRNA isolated from 8C/2A cells grown in the presence or absence of 0.5  $\mu$ g/ml Dox. This fold-change surpassed the levels observed for the other pTRE2- $\beta$ G-GA-bGH transfected cell lines and therefore the 8C/2A cell line was used in all further experiments (Fig. 6.4.A).

### **6.1.3 A pH-responsive stabilization of $\beta$ G-GA mRNA does not occur using Dox to inhibit transcription of the TRE- $\beta$ G-GA-bGH transgene**

A functional study was conducted using the tetracycline-responsive expression system to more accurately determine the half-life of  $\beta$ G-GA mRNA. This analysis used the same experimental conditions developed for previous functional studies except that Dox was added to turn-off  $\beta$ G-GA mRNA transcription instead of using DRB to inhibit pol II transcription. In this experiment, 8C/2A cells were grown for 12 h in either normal (pH 7.4) or acidic (pH 6.9) medium. At this point, Dox was added to inhibit  $\beta$ G-GA

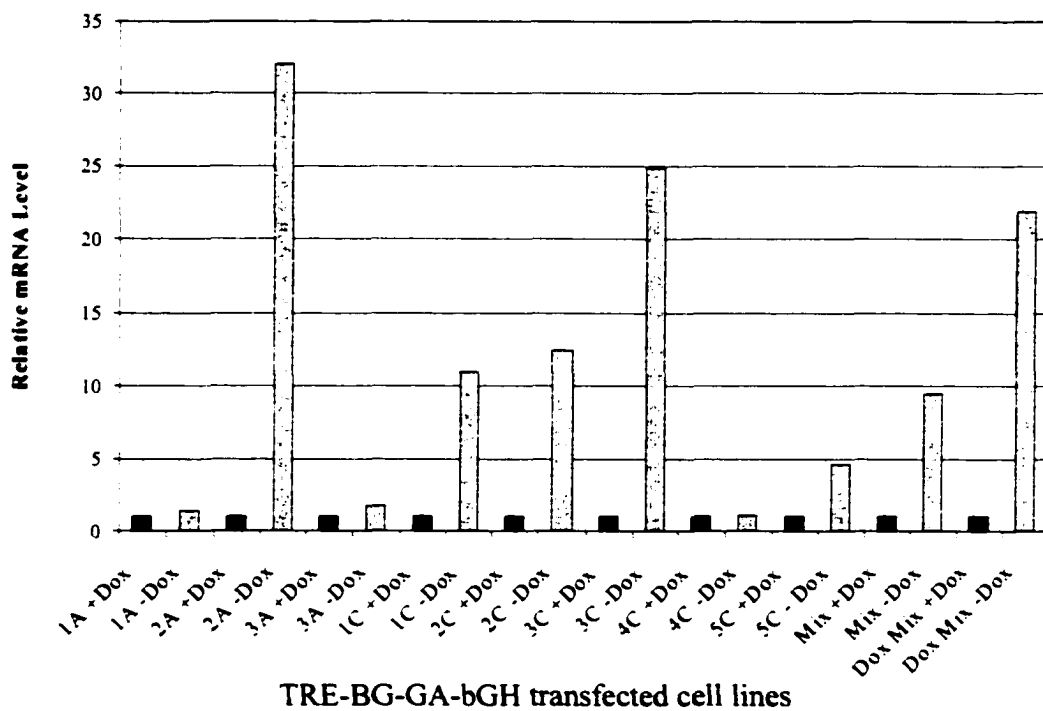
**Fig. 6.4. Characterization of 8C LLC-PK<sub>1</sub>-F<sup>+</sup> cells stably transfected with pTRE2-βG-GA-bGH.**

**Panel A.** Eight clonal cell lines (1A, 2A, 3A, 1B, 2B, 3B, 4B, and 5B) and two mixed cell lines (Mix and Dox Mix) were made by stable transfection of pTRE2-βG-GA-bGH into 8C LLC-PK<sub>1</sub>-F<sup>+</sup> cells. The lines were characterized by growing the cells for 48 h in pH 7.4 medium in the presence or absence of 0.5 μg/ml Doxycycline (Dox). Total RNA was harvested from the cells and used in a Northern blot. The level of βG-GA mRNA was divided by the corresponding level of 18S rRNA to correct for errors in sample loading. For each cell line, the reported data were normalized to the +Dox values.

**Panel B.** Northern blot analysis of the βG-GA mRNA levels expressed in the 8C/2A LLC-PK<sub>1</sub>-F<sup>+</sup> cell line maintained in the presence or absence of Dox.

A.

**Fold Induction: 1.4 32 1.7 11 13 25 1.1 4.7 9.5 22**



B.

[Dox]  $\mu\text{g/mL}$ : 0.5 0



Example of 8C/2A

mRNA transcription and RNA was isolated at 0, 3, 6, and 9 h after treatment with Dox. This analysis indicated that the  $\beta$ G-GA mRNA turned over with a half-life of 2 h in cells maintained in either normal or acidic conditions (Fig. 6.5). No pH-responsive stabilization of the message was observed (Fig. 6.5). An explanation was needed to determine why the results of this experiment did not mirror the results seen in previous functional studies (Fig. 5.6).

The most obvious difference between the two experiments was the promoter used to transcribe the  $\beta$ G-GA mRNA. The previous studies used a Rous sarcoma virus long terminal repeat (RSV) promoter to drive transcription (Fig. 4.2), whereas the current experiments used a tetracycline-responsive promoter (Fig. 4.3).

Therefore, levels of the  $\beta$ G-GA mRNAs from the cell lines were compared on a Northern blot. The level of the  $\beta$ G-GA mRNA transcribed from the tetracycline-responsive promoter in the absence of Dox was far greater than the level of mRNA synthesized from the RSV promoter (Fig. 6.6). The high level of  $\beta$ G-GA mRNA that is transcribed from the tetracycline-responsive promoter may exceed the level of the cellular factors that are responsible for a pH-responsive stabilization of the mRNA. In such a case, the mRNA would not be stabilized under acidic conditions since there is not a sufficient level of stabilizing factors present in the cell.

In order to create a level of  $\beta$ G-GA transcription with which a pH-responsive stabilization could be seen, a short pulse of transcription was generated.  $\beta$ G-GA transcription was turned off by maintaining 8C/2A cells in the presence of Dox for 48 h. Dox was then removed from the cells for 3 h to create a pulse of transcription and the resulting RNA was harvested. The level of  $\beta$ G-GA mRNA produced by a 3 h

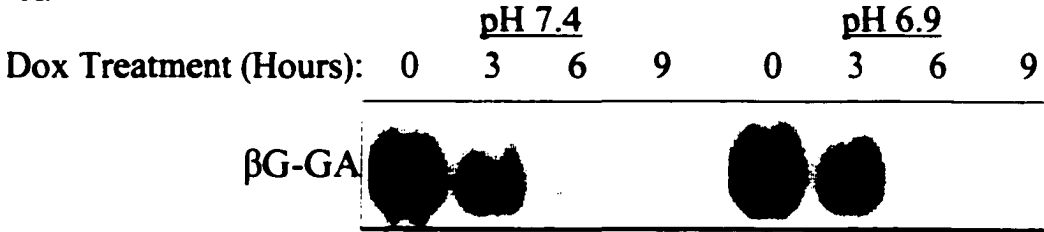
**Fig. 6.5. A pH-responsive stabilization of  $\beta$ G-GA mRNA does not occur using Dox to inhibit transcription of the TRE- $\beta$ G-GA-bGH transgene.**

**Panel A.** Northern blot analysis of  $\beta$ G-GA mRNA levels in 8C/2A (tetracycline-responsive/TRE- $\beta$ G-GA-bGH) LLC-PK<sub>1</sub>-F<sup>+</sup> cells. Cells were cultured in either normal (pH 7.4) medium or acidic (pH 6.9) medium minus Dox for 12 h and then treated with 1  $\mu$ g/ml Dox for 0, 3, 6, and 9 h.

**Panel B.** Relative levels of  $\beta$ G-GA mRNA were determined by PhosphorImager analysis. The level of  $\beta$ G-GA mRNA was divided by the corresponding level of 18S rRNA to correct for errors in sample loading. The log of normalized data was then plotted versus time of treatment with Dox. Values are averages of data obtained from 3 separate determinations. The line represents the best-fit of the data points as determined by the KaleidaGraph program that weights each data point based upon its standard deviation.

# Half-life Analysis Using Dox to Inhibit Transcription of TRE- $\beta$ G-GA-bGH Transgene

A.



B.

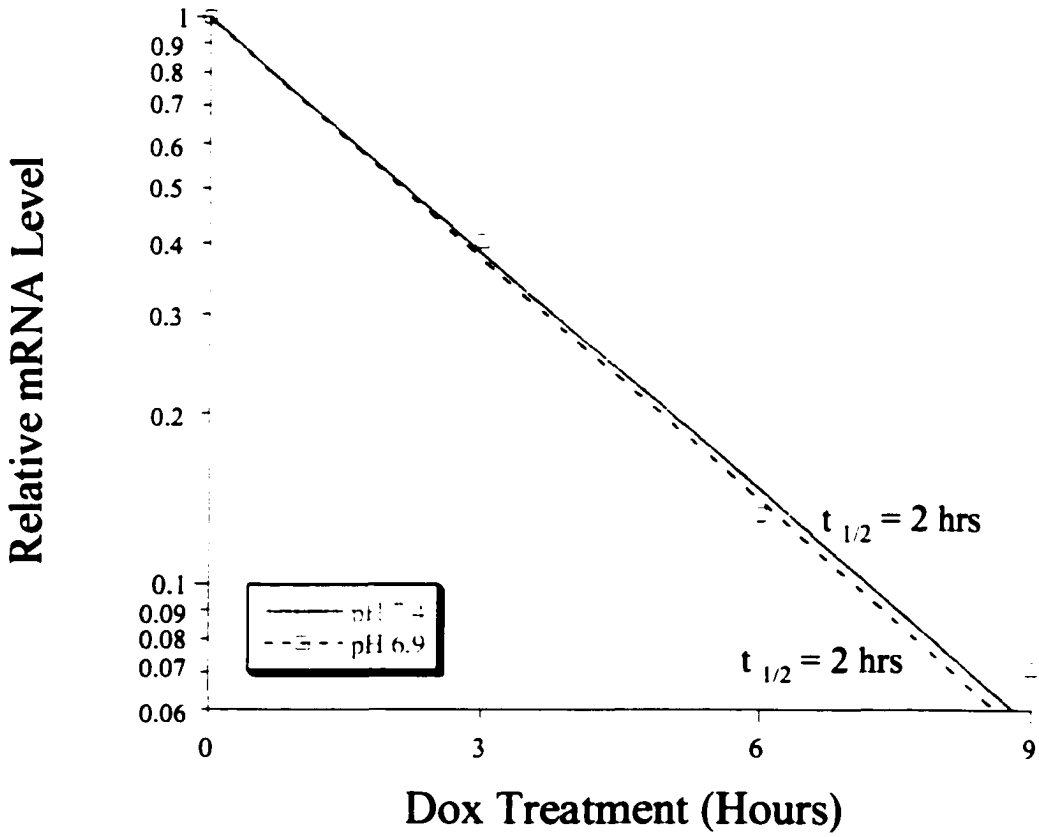
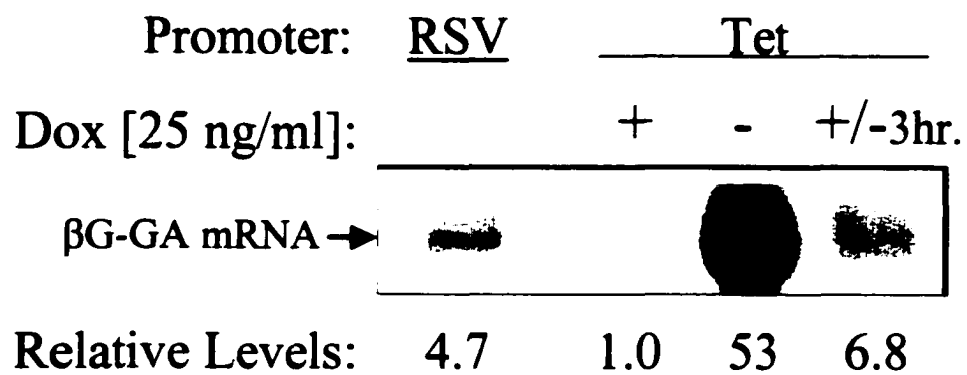


**Fig. 6.6.  $\beta$ G-GA mRNA is expressed at higher levels using a tetracycline-responsive promoter compared to a RSV promoter.**

RNA was isolated from LLC-PK<sub>1</sub>-F<sup>+</sup> cells that were stably transfected with the p $\beta$ G-GA plasmid that is driven by a Rous sarcoma virus long terminal repeat promoter (RSV).

RNA was also isolated from 8C/2A (tetracycline-responsive/TRE- $\beta$ G-GA-bGH) LLC-PK<sub>1</sub>-F<sup>+</sup> cells that were grown in the presence or absence of 25 ng/mL Doxycycline (Dox) for 48 h and from cells that were grown in the presence of Dox, washed with PBS, and then grown for 3 h in medium minus Dox. The isolated RNAs were subjected to Northern blot analysis and the levels of  $\beta$ G-GA mRNA were determined by PhosphorImager analysis. The relative mRNA levels were calculated by normalizing the data to the levels of  $\beta$ G-GA mRNA observed for the 8C/2A LLC-PK<sub>1</sub>-F<sup>+</sup> cells for 48 h in the presence of Dox.



transcriptional pulse was comparable to the level of  $\beta$ G-GA mRNA produced by the RSV promoter (Fig. 6.6). Therefore, a 3 h transcriptional pulse should provide a level of  $\beta$ G-GA mRNA expression where a pH-responsive stabilization would be observed since the stabilizing factors present in the cell should no longer being overwhelmed.

#### **6.1.4 Creating a transcriptional pulse of $\beta$ G-GA**

A transcriptional pulse was further developed to study the decay of  $\beta$ G-GA mRNA. The conditions for the pulse needed to be studied in order to find the optimal Dox concentrations and length of pulse needed to create a homogeneous population of  $\beta$ G-GA mRNA. First, the level of Dox needed to completely turn off transcription, but that could still be rapidly washed from the cells in order to activate transcription, needed to be determined. Increasing amounts of Dox (10-1000 ng/ml) were used to treat 8C/2A cells for 48 h. The percentage of  $\beta$ G-GA mRNA present in the cell after treatment with Dox was determined by quantifying the mRNA levels on a Northern blot. As the amount of Dox was increased, the level of transcription decreased, though all levels of Dox that were used, generally inhibited transcription. The decrease in the percentage of mRNA remaining in the cell began to plateau between 20 and 30 ng/ml of Dox. The further addition of Dox beyond 30 ng/ml did not significantly decrease the amount of  $\beta$ G-GA mRNA remaining (Fig. 6.7). Therefore, 25 ng/ml of Dox was used to inhibit transcription of  $\beta$ G-GA mRNA in further experiments.

The next condition that needed to be optimized was the length of the transcriptional pulse. An optimal pulse length provides a population of mRNA that is large enough to be easily visualized on a Northern blot, but is still homogeneous in length. This optimal pulse length generally is seen when the RNA population reaches

**Fig. 6.7. The inhibition of TRE- $\beta$ G-GA-bGH transcription using various concentrations of Doxycycline (Dox).**

**Panel A.** Northern blot of  $\beta$ G-GA mRNA from 8C/2A (tetracycline-responsive/TRE- $\beta$ G-GA-bGH) LLC-PK<sub>1</sub>-F<sup>-</sup> cells grown in the presence or absence of 25 ng/ml Dox for 48 h.

**Panel B.** Table showing the percent of  $\beta$ G-GA mRNA remaining after treating 8C/2A LLC-PK<sub>1</sub>-F<sup>-</sup> cells with 10-1000 ng/ml Dox for 48 h.

## Dox Addition for 48h

**A.**

25 ng/mL

Dox:

-

+



← βG-GA

**B.**

<u>ng/ml Dox</u>	<u>% mRNA remaining</u>
10	2.9
20	2.1
30	1.8
40	1.7
50	1.5
100	1.5
1000	1.4

a level that is at least 5% of full expression in the absence of Dox (Xu et al 1998). The amount of transcription that is seen 1 h after Dox removal (2%) does not reach a level of transcription that is significantly different from the level of transcription seen after 48 h of Dox treatment. While a 2 h pulse, provides a sufficient level of transcription (6%), it is close enough to the minimum level of transcription needed, so that a longer pulse is preferred. An appropriate level of transcription (21%) was consistently produced by using a 3 h pulse. Furthermore, this pulse length still yields a more homogeneous population of  $\beta$ G-GA mRNA than experiments conducted without a pulse (Fig. 6.8).

The optimized conditions for creating a transcriptional pulse of  $\beta$ G-GA mRNA begin with culturing 8C/2A cells in 25 ng/ml Dox for 48 h. Then, removing the Dox and allowing for 3 h of transcription, at which point high levels of Dox (1000 ng/ml) are added into the medium to rapidly inhibit transcription of the TRE2- $\beta$ G-GA-bGH gene, so that mRNA decay can be monitored over time.

### **6.1.5 $\beta$ G-GA mRNA synthesized during a three hour transcriptional pulse is stabilized under acidic conditions**

The transcriptional pulse described above was used to determine the half-life of  $\beta$ G-GA mRNA without disrupting the transcription of other mRNAs in the cell. The 8C/2A cells were maintained in either normal or acidic medium and in the presence of Dox for 48 h. This was followed by a 3 h pulse, that was stopped with the addition of Dox and RNA was isolated at 0, 3, 6, and 9 h. The half-life of  $\beta$ G-GA mRNA cultured in normal conditions was 3 h. However, when the cells were maintained in acidic conditions, the half-life of the  $\beta$ G-GA mRNA was stabilized to a level greater than 30 h (Fig. 6.9). This experiment confirms the results of the previous functional studies

**Fig. 6.8. Reinitiation of  $\beta$ G-GA mRNA expression after removal of Doxycycline (Dox) from tetracycline-responsive cells.**

RNA was isolated from 8C/2A (tetracycline-responsive/TRE-BG-GA-bGH) LLC-PK<sub>1</sub>-F<sup>-</sup> cells that were grown in pH 7.4 medium for 48 h in the presence or absence of 25 ng/ml Dox and from cells that were grown in the presence of Dox, washed with PBS, and then grown for 1-3 h in fresh medium without Dox. The isolated RNAs were subjected to Northern blot analysis and the relative levels of  $\beta$ G-GA mRNA were determined by PhosphorImager analysis. mRNA levels are expressed as a percentage of the level expressed in the absence of Dox. Values are averages of data obtained from 2 separate determinations.

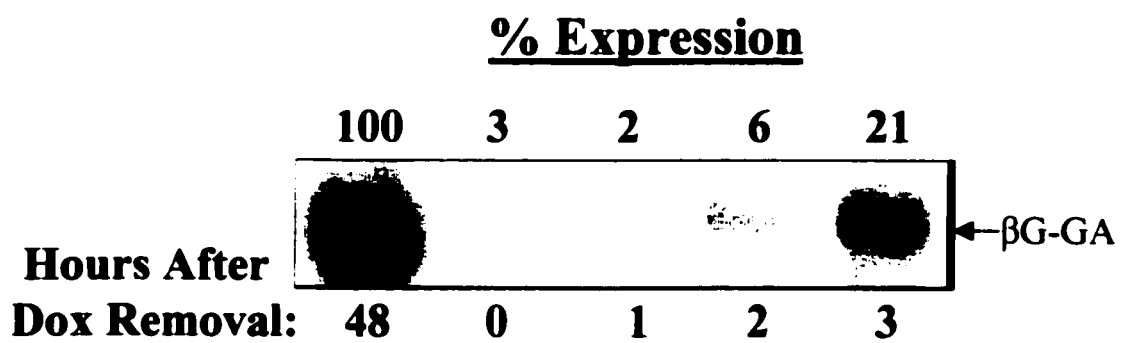


**Fig. 6.9.  $\beta$ G-GA mRNA synthesized during a three hour transcriptional pulse is stabilized under acidic conditions.**

**Panel A.** Northern blot of  $\beta$ G-GA mRNA isolated from 8C/2A (tetracycline-responsive/TRE-BG-GA-bGH) LLC-PK<sub>1</sub>-F<sup>+</sup> cells. Cells were maintained in either normal (pH 7.4) medium or acidic (pH 6.9) medium containing 25 ng/ml Doxycycline (Dox) for 48 h. The cells were washed with PBS and incubated in medium minus Dox for 3 h to create a transcriptional pulse. Then, fresh medium containing 1  $\mu$ g/ml Dox was added and RNA was isolated at 0, 3, 6, and 9 h after Dox readdition.

**Panel B.** Relative levels of  $\beta$ G-GA mRNA were determined by PhosphorImager analysis. The level of  $\beta$ G-GA mRNA was divided by the corresponding level of 18S rRNA to correct for errors in sample loading. The log of normalized data was then plotted versus the time of treatment with Dox. Values are averages of data obtained from 3 separate determinations. The line represents the best-fit of the data points as determined by the KaleidaGraph program that weights each data point based upon its standard deviation.



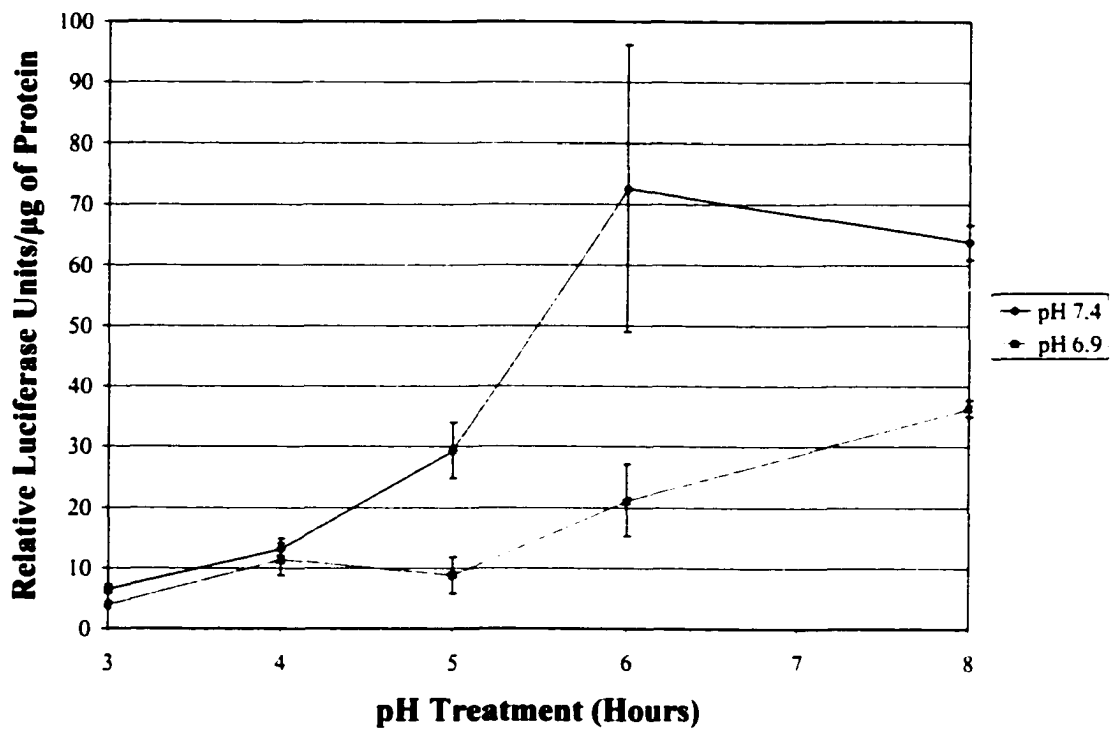
using the GA 3'-UTR in which a pH-responsive stabilization was observed.  $\beta$ G-GA mRNA, isolated in experiments using the tetracycline-responsive expression system, exhibits a shorter half-life at pH 7.4 compared to the previous studies which used DRB to inhibit transcription (Fig. 5.6 and Fig. 6.9). This could be explained by the fact that only a homogeneous population of a single mRNA is being studied with the tetracycline-responsive system. Furthermore, the efficiency of the cellular decay machinery is not compromised by a gradual loss of essential proteins due to inhibition of their synthesis.

### **6.1.6 Transcription of the TRE2- $\beta$ G-GA-bGH transgene in 8C LLC-PK<sub>1</sub>-F<sup>+</sup> cells is effected by changes in the pH of the medium**

In the half-life experiment using the transcriptional pulse, the relative level of the  $\beta$ G-GA mRNA was less in the cells that had been treated with pH 6.9 medium compared to the levels in cells treated at pH 7.4. Therefore, the 8C LLC-PK<sub>1</sub>-F<sup>+</sup> cell line was transiently transfected with pTRE2-Luc in the presence of Dox to determine whether the cell line or the TRE promoter activity was affected by changes in extracellular pH. After 12 h, Dox was removed and cells were treated with either pH 7.4 or pH 6.9 medium. Cell extracts were prepared at 3 to 8 h after the treatments and assayed using the Luciferase Assay System. It was determined that the rate of increase of luciferase activity was less in cells grown in pH 6.9 medium compared to pH 7.4 cells (Fig. 6.10). This indicates that less luciferase protein is being synthesized at pH 6.9, which is consistent with differences in  $\beta$ G-GA mRNA levels observed in the transcriptional pulse study (Fig. 6.9). The combined results indicate that the tetracycline-responsive promoter or the general rate of transcription is slightly less active in the 8C LLC-PK<sub>1</sub>-F<sup>+</sup> cells treated with the acidic medium. However, this result should not affect the decay studies using the

**Fig. 6.10. Transcription of the TRE2-  $\beta$ G-GA-bGH transgene in 8C LLC-PK<sub>1</sub>-F<sup>+</sup> cells is effected by changes in the pH of the medium.**

8C LLC-PK<sub>1</sub>-F<sup>+</sup> cells were transiently transfected with pTRE2-Luc in pH 7.4 medium containing 25 ng/ml Doxycycline (Dox). After 12 h, the transfection medium and Dox were washed from the cells and pH 7.4 or pH 6.9 medium was added. Cell extracts were prepared at 3-8 h after pH treatment and assayed using the Luciferase Assay System (E1500, Promega). The protein concentration of the extracts was determined by Lowry assay and the firefly luciferase activity was standardized per  $\mu$ g of protein. Values shown are the mean +/- the standard error of experiments done in triplicate.



8C LLC-PK<sub>1</sub>-F<sup>+</sup> cell line, since the rate of mRNA decay should be independent of slight differences in the rates of transcription observed in cells treated with normal or acidic medium.

### **6.1.7 RNase H Treatment of $\beta$ G-GA mRNA**

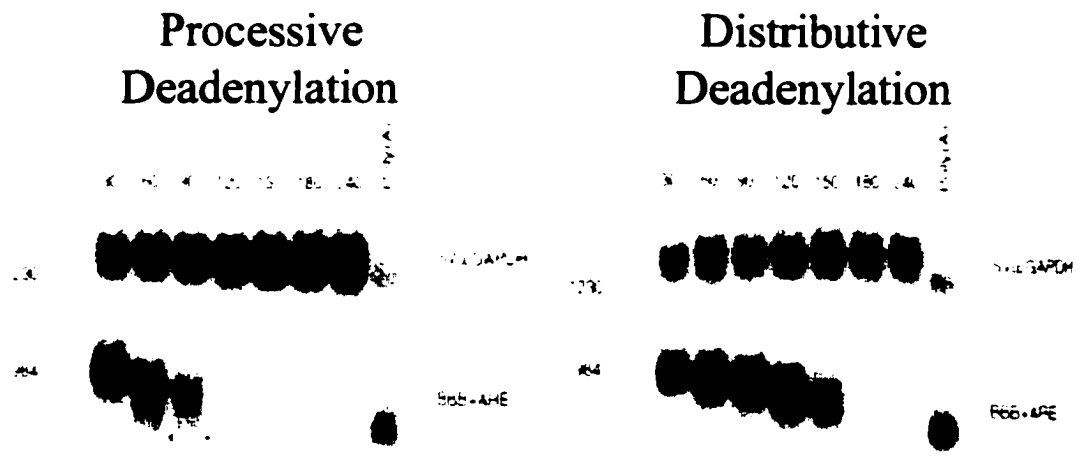
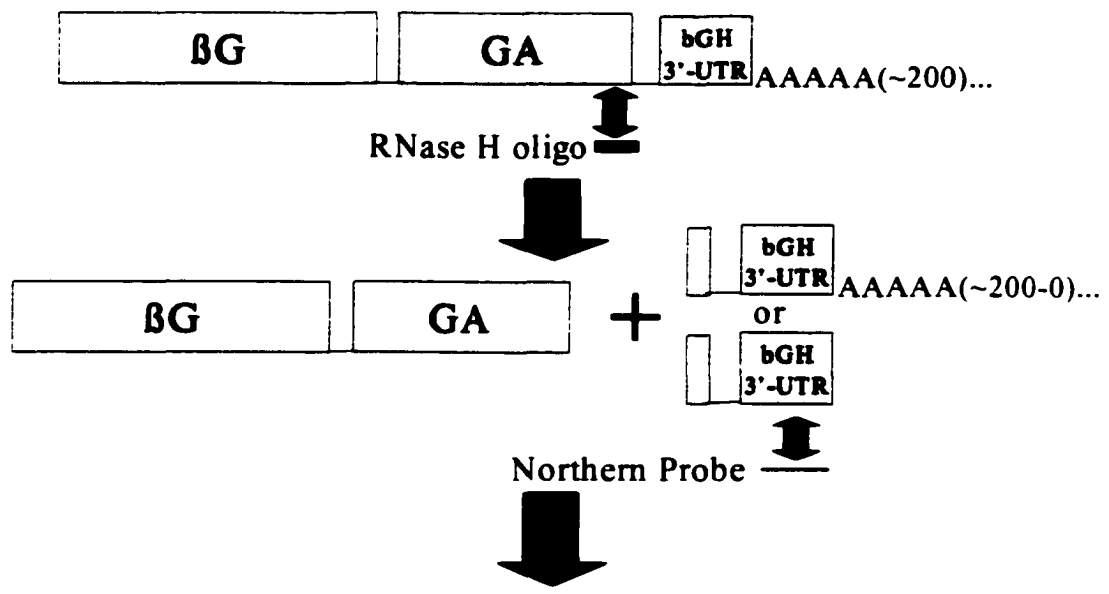
Knowledge of the mechanism of  $\beta$ G-GA mRNA decay is important in order to determine how a pH-responsive stabilization of the mRNA occurs. Since deadenylation is often the first step of mRNA decay, it was important to determine whether deadenylation was a part of the decay mechanism for  $\beta$ G-GA mRNA and whether this mechanism is effected by changes in extracellular pH that mimic a metabolic acidosis. The  $\beta$ G-GA mRNA is approximately 2.0 kb in length. It is difficult to monitor the loss of 100-300 adenine residues from the poly (A) tail of this size of mRNA. However, RNase H treatment can be used to obtain a shorter RNA for which deadenylation can be easily monitored.

#### **6.1.7.1 Testing of RNase H treatment on $\beta$ G-GA mRNA**

To shorten the  $\beta$ G-GA mRNA to a reasonable length that allows the visualization of deadenylation, a 26-nt deoxyoligonucleotide (GA oligo) was designed that specifically hybridizes to the 3'-end of the GA sequence. The  $\beta$ G-GA mRNA hybridized to the GA oligo is cleaved by RNase H into two RNA fragments. A 30-mer of oligo dT can also be added to the reaction to remove the poly (A) tail from the 3'-end of the  $\beta$ G-GA mRNA, creating a 330-nt deadenylated RNA fragment. The 3'-fragments can then be detected on a Northern blot using a [<sup>32</sup>P]-CTP labeled cDNA probe that specifically hybridizes to the bGH sequence found at the 3'-end of the  $\beta$ G-GA mRNA (Fig. 6.11).

**Fig. 6.11. Schematic of RNase H digestion of  $\beta$ G-GA mRNA.**

A deoxyoligonucleotide (oligo) that specifically binds the 3'-end of the glutaminase (GA) sequence is incubated with the  $\beta$ G-GA mRNA and RNase H. The RNase H degrades the RNA that is hybridized to the specific oligo. If a 30-mer of oligo dT is also added, the poly (A) tail is also removed from the mRNA. A [<sup>32</sup>P]-CTP labeled DNA oligo that specifically binds the 3'-RNA fragment is then used as probe in a Northern blot. The two Northern blots shown are representative of two types of deadenylation: processive deadenylation (GM-CSF) or distributive deadenylation (c-fos). The Northern blots are from the Shyu laboratory (Xu et al 1997).



(Xu et al., MCB 1997:4611-4621)

The  $\beta$ G-GA RNA fragment created by RNase H digestion with the GA oligo is significantly shorter than the untreated  $\beta$ G-GA mRNA. When both the GA oligo and oligo dT were added, the RNase H digestion resulted in a 3'-fragment that had a significantly greater mobility. Thus, the adenylated and the fully deadenylated RNA fragments were easily resolved, making it feasible to monitor the extent of deadenylation of the  $\beta$ G-GA mRNA (Fig. 6.12).

#### **6.1.7.2 $\beta$ G-GA mRNA is deadenylated as part of a biphasic decay mechanism**

The RNAs that were analyzed in the previous  $\beta$ G-GA mRNA half-life experiments using a transcriptional pulse were treated with RNase H. The 3'-ends of the  $\beta$ G-GA mRNAs harvested from cells maintained in normal medium showed a rapid degradation similar to that observed with the full-length mRNA (Fig. 6.13.A). In addition, the 3'-ends of  $\beta$ G-GA mRNAs harvested from cells treated with acidic medium were significantly stabilized and decayed at a rate similar to that observed for the full-length mRNA (Fig. 6.13). Thus, analysis of the 3'-ends mirror the pH-responsive stabilization seen using  $\beta$ G-GA mRNAs (Fig. 6.9).

At pH 7.4, the  $\beta$ G-GA mRNA exhibited a synchronous deadenylation that precedes the decay of the mRNA body. This pattern is consistent with a distributive deadenylation mechanism (Fig. 6.13.A). This synchronous deadenylation is observed with class I and class III AREs (Xu et al 1997).

The mechanism of decay for  $\beta$ G-GA mRNA harvested from cells treated with acidic medium is more difficult to ascertain. It appears to follow the synchronous deadenylation mechanism seen at pH 7.4, which indicates that distributive deadenylation is occurring (Fig. 6.13.B). However, further time points need to be taken in order to

**Fig. 6.12. RNase H treatment shortens  $\beta$ G-GA mRNA.**

RNA isolated from 8C/2A LLC-PK<sub>1</sub>-F<sup>+</sup> cells (tetracycline-responsive/TRE- $\beta$ G-GA-bGH) is either untreated (lane 1) or treated with RNase H and an oligonucleotide that is complementary to the 3'-end of the GA sequence (GA oligo) (lane 2) or the GA oligo and a 30-mer of oligo dT (lane 3). The RNAs were subjected to Northern blot analysis and hybridized with a [<sup>32</sup>P]-labeled cDNA probe that specifically hybridizes to the bGH sequence. The RNA fragment resulting from a reaction with both the GA oligo and oligo dT is 330 nt.

<b>GA oligo</b>	-	+	+
<b>Oligo dT (30 Ts)</b>	-	-	+

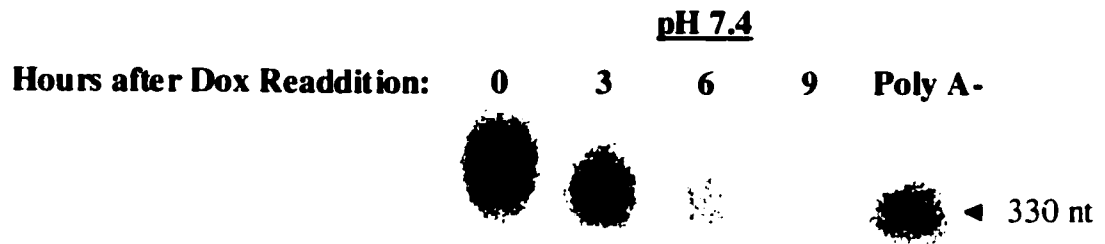


**Fig. 6.13.  $\beta$ G-GA mRNA is deadenylated as part of a biphasic decay mechanism.**

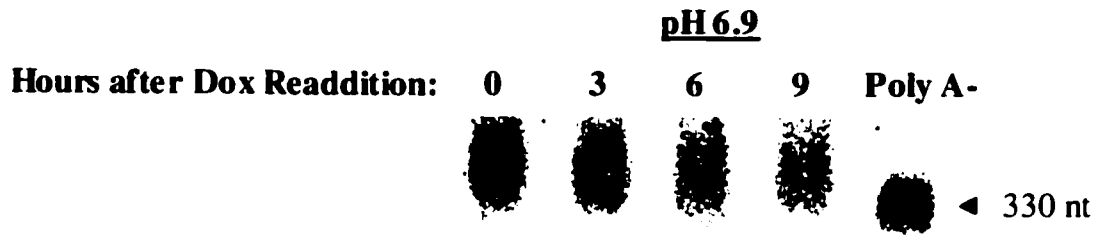
**Panel A.** 8C/2A LLC-PK<sub>1</sub>-F<sup>+</sup> cells were maintained in normal (pH 7.4) medium containing 25 ng/ml Doxycycline (Dox) for 48 h. The Dox was removed and the cells were maintained in medium minus Dox for 3 h, then fresh medium containing 1  $\mu$ g/ml Dox was added and cell extracts were prepared at 0, 3, 6, and 9 h after Dox readdition. The isolated RNAs were treated with RNase H using a specific GA oligo that shortens the message to 330 nt plus the poly (A) tail or the GA oligo and oligo dT to create an RNA fragment 330 nt in length.

**Panel B.** Same experiment as above except cells were maintained in pH 6.9 medium.

A.



B.



truly elucidate this mechanism. The use of distributive deadenylation at both pHs is logical due to the presence of the GA pHRE in the 3'-UTR of the mRNA, which falls into the class III non-AUUUA category of AREs that effect mRNA stability.

## **7 Discussion and Future Directions**

## **7.1 $\zeta$ -crystallin binding to GA and GDH AREs**

Addition of the 3'-UTR of the GA mRNA is sufficient to impart a pH-responsive stabilization to the chimeric  $\beta$ G-GA mRNA (Hansen et al 1996). The GA 3'-UTR was also observed to bind a rat renal cytosolic protein (Laterza et al 1997) that was later identified as  $\zeta$ -crystallin (Tang & Curthoys 2001). The binding element was mapped to a region, GA(R2-I), that contains a direct repeat of two AREs that were 88% identical (Laterza et al 1997). The 3'-UTRs of other mRNAs that encode enzymes that are part of the ammonogenic and gluconeogenic pathways were examined for similar AREs. Four AREs were found in the 3'-UTR of the GDH mRNA that are 88% identical to one of the elements in GA (Das et al 1989). This similarity coupled with the finding that the GA and GDH are induced with similar kinetics following the onset of metabolic acidosis (Kaiser et al 1992), created an interest in determining whether the 3'-UTR of GDH also binds  $\zeta$ -crystallin. Binding studies indicated that  $\zeta$ -crystallin binds to the GDH 3'-UTR and that the resulting RNA/protein complex had a similar mobility to the GA(R2-I)/protein complex. However, due to the length of the complete 3'-UTR of the GDH RNA, it was difficult to determine whether the GDH elements bound  $\zeta$ -crystallin as strongly as the GA(R2-I) segment. Since the GDH elements are distributed throughout the 3'-UTR, vectors were constructed that expressed a single GDH element within a 30-nt length of RNA. Binding studies were then done to determine whether an individual element from the GDH mRNA could function as well as a direct repeat of elements from the GA mRNA. To make this comparison, it was important to also determine the level of protein binding exhibited by the individual GA elements. The individual GA elements showed a similar level of protein binding. However, the affinity of  $\zeta$ -crystallin binding to

a single element was not as great as the binding affinity observed when the elements were present in a direct repeat. The individual GDH elements also bound  $\zeta$ -crystallin, but with even less affinity than was observed for the individual GA elements. It is important to note that not all of the GDH elements bound by  $\zeta$ -crystallin with the same affinity. The GDH2 and GDH4 sequences showed a greater binding affinity than the GDH1 and GDH3 elements.

The specificity of binding to the individual AREs was determined by competition studies. The binding of  $\zeta$ -crystallin to labeled GA(R2-I) was specifically competed by the addition of unlabeled individual AREs. All of the GA and GDH elements acted as effective competitors of  $\zeta$ -crystallin/GA(R2-I) binding, indicating that the binding of an element to  $\zeta$ -crystallin is specific. In these experiments, the GA elements were found to be stronger competitors than the GDH elements and the GDH2 and GDH4 segments were the best competitors among the GDH AREs. These results further established that all of the AREs serve as functional  $\zeta$ -crystallin binding elements. The ability of  $\zeta$ -crystallin to bind to the GDH elements provides further evidence that the increase in the level of GDH mRNA during metabolic acidosis is due to a pH-responsive stabilization of the GDH mRNA.

The greater affinity of  $\zeta$ -crystallin binding to the GA AREs compared to the GDH AREs is consistent with the observation that the increase in the level of GA mRNA during acidosis is significantly greater than the increase observed for GDH mRNA. Thus, the fold stabilization of GDH mRNA should be less than the degree of stabilization observed for the GA mRNA. Therefore, less binding of  $\zeta$ -crystallin may be required to achieve the observed level of stabilization of the GDH mRNA.

## **7.2 pH-responsive stabilization of the GDH mRNA**

To establish the function of the observed binding of  $\zeta$ -crystallin to the AREs within the 3'-UTRs of GDH, it was necessary to determine whether the 3'-UTR of GDH also confers a pH-responsive stabilization to a chimeric reporter mRNA. This was accomplished by inserting the DNA encoding the 3'-UTR of GDH into the p $\beta$ G plasmid and demonstrating that the resulting mRNA was stabilized in a pH-responsive manner.

The next logical step was to test whether an individual ARE from the GDH 3'-UTR could function as a pH-responsive element. However, initially it was necessary to determine whether a single ARE inserted in the p $\beta$ G plasmid would sufficiently destabilize the  $\beta$ G mRNA so that a pH-responsive stabilization of the mRNA could be observed.

Previous experiments established that the  $\zeta$ -crystallin binding site within the GA mRNA functioned as a pHRE. For example, when the binding element within the  $\beta$ G-GA mRNA was mutated, the pH-responsive stabilization was abolished. Since the 3'-UTR of GDH mRNA contained four well-spaced pHREs, it would have been difficult to perform the comparable experiment with the  $\beta$ G-GDH construct. In a second experiment, a 76-nt segment of the GA cDNA containing the  $\zeta$ -crystallin binding site was cloned into the  $\beta$ G-PEPCK vector. This vector produces a chimeric mRNA that contains a non-pH-responsive destabilizing element from the 3'-UTR of the PEPCK mRNA. The resulting  $\beta$ G-GA(R2-H)-PEPCK mRNA was stabilized in cells transferred to acidic medium (Laterza & Curthoys 2000). To utilize this approach for small elements, a control experiment was initially performed to determine if the GA(R2-I) segment encoding the pHRE of the GA mRNA was sufficient to both destabilize the  $\beta$ G mRNA at

pH 7.4 and stabilize it at pH 6.9. The  $\beta$ G-GA(R2-I) mRNA was seen to fulfill both of these requirements, though the destabilization at pH 7.4 was not as strong as the destabilization of the  $\beta$ G-GA mRNA. Thus, the 3'-UTR of GA mRNA may contain additional destabilizing elements.

The GDH4 ARE was chosen for functional studies, because of the four GDH elements, it showed strong  $\zeta$ -crystallin binding and competition. However, the GDH4 ARE did not destabilize the  $\beta$ G-GDH4 mRNA sufficiently to determine if a pH-responsive stabilization occurred. This result was not altogether unexpected given that the GA(R2-I) element was less effective than the GA 3'-UTR in destabilizing the  $\beta$ G mRNA and the GDH4 RNA bound  $\zeta$ -crystallin with lower affinity than GA(R2-I) RNA.

To test the pH-responsiveness conferred by the GDH4 element, the 3'-UTR of PEPCK was inserted downstream of the GDH4 sequence in the  $\beta$ G-GDH4 plasmid. The resulting  $\beta$ G-GDH4-PEPCK mRNA was sufficiently unstable at pH 7.4 that a pH-responsive stabilization of the mRNA could be observed in cells transferred to pH 6.9 medium. This experiment illustrated that the GDH4 ARE and possibly the three other GDH AREs function as pHREs within the GDH mRNA.

The combined binding and functional studies illustrate that the GA and GDH mRNAs are stabilized in response to the onset of metabolic acidosis. It was also determined that the individual GA and GDH AREs are responsible, at least in part, for this stabilization. Since these pHREs also bind  $\zeta$ -crystallin, it is probable that the  $\zeta$ -crystallin/mRNA complex acts to stabilize the mRNA during metabolic acidosis. It is also probable that at pH 7.4, the mRNAs bind less  $\zeta$ -crystallin and are no longer protected from ribonucleases.

### **7.3 The decay of GA mRNA**

The stabilization of GA mRNA under acidic conditions is thought to occur by the enhanced binding of  $\zeta$ -crystallin that protects the GA mRNA from an endoribonuclease. Therefore, it was interesting to determine the mechanism by which the GA mRNA is degraded. The most common mechanism for the decay of ARE-containing mRNAs is a biphasic process that involves the initial deadenylation of an mRNA followed by a rapid degradation of the body of the mRNA.

A tetracycline-responsive expression system was created to determine if deadenylation precedes the degradation of the GA mRNA and if so, to identify the mechanism of deadenylation. This system was used to more accurately characterize the half-life of the GA mRNA. Monitoring the decay of a specific mRNA is possible since the transcription of a single chimeric mRNA can be rapidly activated or inactivated by modulating the level of Dox in the medium, without effecting the transcription of other mRNAs in the cell.

A tetracycline-responsive LLC-PK<sub>1</sub>-F<sup>+</sup> cell line was created by the stable transfection of a plasmid encoding a tetracycline-responsive protein, tTA. The tetracycline-responsiveness of several of the clonal cell lines was tested and the 8C line of LLC-PK<sub>1</sub>-F<sup>+</sup> cells was chosen since it showed the strongest activation of the tetracycline-responsive promoter. The experimental pTRE2- $\beta$ G-GA-bGH plasmid, containing a tetracycline-responsive promoter and the  $\beta$ G-GA-bGH sequence used in previous studies, was stably transfected into the 8C line of LLC-PK<sub>1</sub>-F<sup>+</sup> cells. The 2A line of the 8C LLC-PK<sub>1</sub>-F<sup>+</sup> cells was chosen since it showed the greatest increase in

mRNA levels in the absence of Dox and an efficient shut-off of transcription in the presence of Dox.

Therefore, the proposed functional studies were performed using Dox to specifically inhibit the synthesis of the  $\beta$ G-GA mRNA, instead of using DRB as a general inhibitor of pol II transcription. Using this approach,  $\beta$ G-GA mRNA was found to be unstable in cells grown at both pH 7.4 and 6.9. To explain this observation, the levels of transcription using either the RSV promoter or the tetracycline-responsive promoter were compared. A significantly greater level of transcript was produced from the tetracycline-responsive promoter. Thus, the very high level of  $\beta$ G-GA mRNA may exceed the level of  $\zeta$ -crystallin and/or other factors needed to accomplish a pH responsive stabilization. This condition could explain the lack of stabilization observed in the functional studies using the tetracycline-responsive expression system.

To determine if lower levels of  $\beta$ G-GA mRNA were needed to conduct functional studies in the tetracycline-responsive system, the conditions necessary to create a transcriptional pulse were established. By culturing 8C/2A LLC-PK<sub>1</sub>-F<sup>+</sup> cells with low levels of Dox, transcription of the  $\beta$ G-GA mRNA was inhibited. Dox was then washed from the cells to initiate transcription. After a 3 h pulse, transcription was rapidly inhibited by the addition of high levels of Dox into the medium. Thus, the decay of a homogenous population of  $\beta$ G-GA mRNA could be monitored over time.

Using this approach, a pH-responsive stabilization of the  $\beta$ G-GA mRNA was observed. Therefore data obtained using the less intrusive assay confirms the previous conclusion that the 3'-UTR of GA confers stability to the  $\beta$ G-GA mRNA under acidic conditions.

The total RNAs isolated from the transcriptional pulse analysis were further studied to determine the mechanism of decay. It was hypothesized that deadenylation of the  $\beta$ G-GA mRNA would precede its decay since the 3'-UTR of GA contains an ARE which exhibits moderate instability at pH 7.4. Therefore, the RNAs from the functional studies were digested with RNase H and a specific GA oligo to cleave the  $\beta$ G-GA mRNA to yield a reasonable length of RNA for monitoring deadenylation. The deadenylation of the  $\beta$ G-GA mRNA was observed to be synchronous under both normal and acidic conditions although the  $\beta$ G-GA mRNA was deadenylated at a slower rate when cells were treated with acidic medium. The body of the mRNA was degraded following the deadenylation. Synchronous deadenylation is consistent with a distributive or non-processive ribonucleolytic removal of the poly (A) tail. Synchronous deadenylation has been observed to occur for mRNAs containing a Class I or Class III ARE (Chen & Shyu 1995). Since it lacks an AUUUA sequence, the GA pHRE is a Class III ARE. Thus, the observation of distributive deadenylation by the  $\beta$ G-GA mRNA is consistent with the previous classification.

The data illustrating that the pHRE from the GA 3'-UTR binds  $\zeta$ -crystallin and that the pHRE is responsible for the pH-responsive stabilization of the  $\beta$ G-GA mRNA are consistent with the data indicating that the  $\beta$ G-GA mRNA is deadenylated at a slower rate under acidic conditions. Thus, these data expand our previous model and indicate that  $\zeta$ -crystallin binds to the GA pHRE under acidic conditions and protects the mRNA from both deadenylation and degradation. However, when  $\zeta$ -crystallin is not bound to the pHRE, the mRNA is no longer protected and the pHRE recruits a deadenylase that

initiates the degradation of the GA mRNA. It is likely that this same model also applies to the pH-responsive stabilization of the GDH mRNA.

#### **7.4 Expanding the model of GA and GDH mRNA stabilization**

The proposed model discussed in Chapter 1.8.4 (Fig. 1.2) can be expanded with the new discoveries made in this research. The putative model can be applied to both the GA and GDH mRNAs since both of the mRNAs are stabilized in response to acidic conditions. Phosphorylation of a stabilizing mRNA-binding protein is a common mechanism in the stabilization of an mRNA. Therefore, it is possible that  $\zeta$ -crystallin is phosphorylated to enhance the binding of  $\zeta$ -crystallin to the AREs during metabolic acidosis (See Chapter 7.5 for future experiments on this topic). The binding of  $\zeta$ -crystallin alone to the AREs in order to protect the mRNA during metabolic acidosis could be an oversimplification. Other proteins, such as the pHRE-BP2 protein (See Appendix), or protein complexes may bind the mRNA or  $\zeta$ -crystallin to stabilize the mRNA.

The GA and GDH mRNAs are protected by the binding of  $\zeta$ -crystallin. However, under conditions in which the mRNA is not protected by  $\zeta$ -crystallin binding, such as normal acid-base balance, the ARE(s) may recruit a deadenylase to the mRNA that removes the poly (A) tail. The ARE may also recruit an exosome or an exoribonuclease to complete the degradation of the mRNA. At this point, the remaining 5' -cap and mRNA body are rapidly degraded. Thus, the new data obtained in these studies are consistent with the previously proposed model and has provided further insight into the stabilization of GA and GDH mRNA with additional information about the mechanism of mRNA degradation.

## **7.5 Future Directions**

Significant progress has been made in determining the mechanism of stabilization of the GA and GDH mRNAs during metabolic acidosis in renal cells. However, there are still many questions that remain. These questions include: Is  $\zeta$ -crystallin part of a protective complex that prevents degradation of an mRNA and if so what other proteins are involved?; What changes in  $\zeta$ -crystallin are required for its stabilization of the GA and GDH mRNAs?; Do the GA and GDH AREs recruit a ribonuclease or does an ARE-binding protein, that binds to the pHRE in the absence of  $\zeta$ -crystallin, recruit the ribonuclease?; and What is the ribonuclease? Many other questions will arise as our knowledge of this process expands. Some of these questions can be answered by utilizing the tetracycline-responsive expression system, while others will require the use of other tools such as an in vitro decay system.

The finding that the tetracycline-responsive promoter synthesizes a level of  $\beta$ G-GA mRNA that apparently overwhelms the stabilization machinery creates an opportunity to test our proposed mechanism in intact cells. The overexpression of the  $\beta$ G-GA mRNA should create a dominant negative effect in the cells that should also prevent the pH-responsive increase of the endogenous GA mRNA. This could be tested using the 8C/2A LLC-PK<sub>1</sub>-F<sup>+</sup> cells grown in the presence and absence of Dox to determine the effect of extracellular pH on expression of the endogenous GA mRNA. If the pH-responsive increase in GA mRNA requires the binding of proteins to its 3'-UTR to mediate its stabilization, then the increase in endogenous GA mRNA will be blocked when the  $\beta$ G-GA mRNA is overexpressed.

The tetracycline-responsive expression system can be used to determine whether the GDH mRNA utilizes the same biphasic decay mechanism as observed for the GA mRNA. It is also important to use this system to determine whether the pHREs found in the GA and GDH 3'-UTRs contribute to the biphasic decay mechanism. It is possible that the pHREs function only in the binding of  $\zeta$ -crystallin and the pH-responsive stabilization of the mRNA but do not contribute directly to the deadenylation and decay of the mRNA. The additional pTRE2 constructs developed in this thesis will be useful in answering these questions.

An in vitro decay system is being developed in the laboratory to study the factors involved in the stabilization and decay of the GA and GDH mRNAs. Factors that are identified as part of this mechanism can then be tested in vivo using the tetracycline-responsive expression system to affect expression of these factors and to determine their function in intact cells.

Experiments can also use the tetracycline-responsive expression system to determine if the pH-responsive mRNA stabilization is mediated by the p38 stress-activated protein kinase (SAPK) signaling pathway. The transfer of LLC-PK<sub>1</sub>-F<sup>+</sup> cells to acidic medium leads to a dual phosphorylation and activation of p38 SAPK. The activated kinase mediates the phosphorylation and activation of ATF-2, a transcription factor that can bind to the CRE-1 element of the PEPCK promoter to activate its transcription. Anisomycin is a known inhibitor of protein synthesis and an activator of the p38 SAPK pathway. When LLC-PK<sub>1</sub>-F<sup>+</sup> cells are treated with anisomycin, PEPCK transcription is activated in a manner that mimics the effects of acidic medium. In

addition, SB203580, a specific p38 SAPK inhibitor, blocks both the acid- and anisomycin-mediated inductions of PEPCK mRNA (Feifel et al 2002).

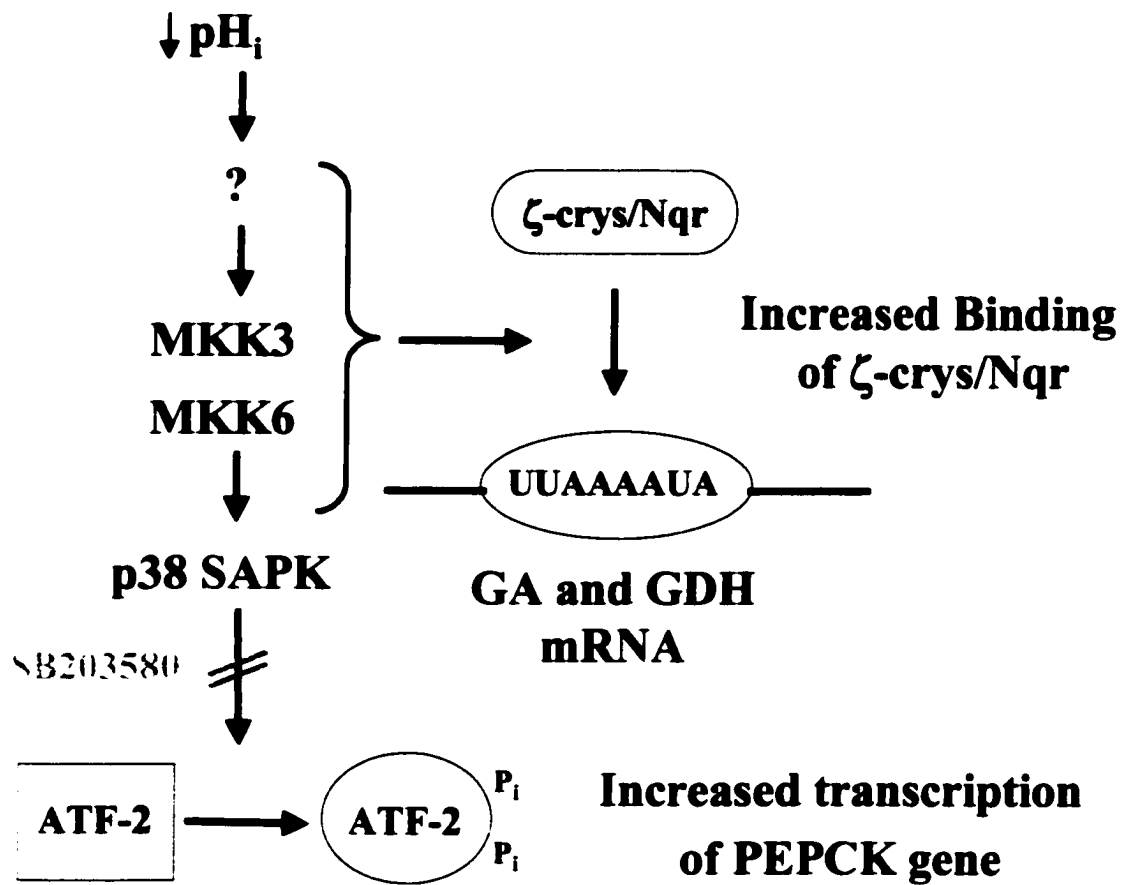
Since the stabilization of the GA mRNA occurs coordinately with the activated transcription of the PEPCK mRNA during metabolic acidosis, it is possible that both pH-responsive adaptations are initiated by the same signal transduction mechanism that senses a change in the acid-base balance of the cell. Therefore, it is possible that  $\zeta$ -crystallin is phosphorylated during metabolic acidosis to facilitate its binding to the GA pHRE. However, the addition of SB203580 to LLC-PK<sub>1</sub>-F<sup>+</sup> cells had no effect on the pH-responsive stabilization of the GA mRNA (Curthoys & Gstraunthaler 2001). Thus, a kinase upstream of p38 SAPK, such as MKK3 or MKK6, may be responsible for the pH-responsive stabilization of the GA and GDH mRNAs (Fig. 7.1). This hypothesis can be tested by expressing constitutively active and dominant negative forms of MKK3 and MKK6 in the tetracycline-responsive expression system and monitoring their effects on the stability of GA mRNA. If specific phosphorylation does not enhance  $\zeta$ -crystallin binding to the pHRE, it is possible that  $\zeta$ -crystallin is modified in another manner. Possible modifications could include a pH-induced conformational change, covalent modifications other than phosphorylation, or the binding of other molecules to  $\zeta$ -crystallin.

Thus, the experimental tools that have been created and the experiments that have been completed provide a foundation for future research of the renal pH-response and its effect on GA and GDH. Future experiments will continue to provide insight into the regulation of acid-base balance in the kidneys. This work may one day provide insight

**into pharmacological approaches for stimulating ammoniogenesis and/or gluconeogenesis to more effectively treat various forms of chronic metabolic acidosis.**

**Fig. 7.1. A model for the coordinate induction of GA, GDH, and PEPCK gene expression during metabolic acidosis through the activation of the p38 SAPK signaling pathway.**

Activation of the p38 SAPK signaling pathway occurs when there is a decrease in intracellular pH ( $\text{pH}_i$ ). The activation of this pathway leads to the phosphorylation and subsequent activation of ATF-2.  $\zeta$ -crys/Nqr may be modified by a kinase upstream of p38 SAPK to enhance the binding of  $\zeta$ -crys/Nqr to a pHRE within the 3'-UTR of the GA and GDH mRNAs. MKK, mitogen-activated protein kinase kinase.



## **8 Appendix: Preliminary Characterization of pHRE-BP2**

## **8.1 FPLC affinity purification of a second pHRE binding protein**

During the affinity purification of the 36-kDa  $\zeta$ -crystallin, a second protein (pHRE-BP2) was eluted from the GA RNA affinity ligand with the final elution buffer. The RNA affinity ligand is a 52-b nucleic acid containing two deoxythymidines at the 5'-end, 44 ribonucleotides of the GA 3'-UTR including the GA pHRE, and six deoxyribonucleotides including two biotinylated thymidines at the 3'-end. The unidentified protein was termed, pHRE-BP2. It has an approximate subunit molecular weight of 45-kDa. The original FPLC affinity purification protocol developed by A. Tang, collected 14-0.5 ml fractions from a linear gradient of increasing salt concentration between 4X and 20X (Tang & Curthoys 2001). No fractions contained solely  $\zeta$ -crystallin or pHRE-BP2 since some of each protein was present in most of the fractions (Fig. 8.1).

Therefore, the elution profile was changed so that relatively pure fractions of  $\zeta$ -crystallin and pHRE-BP2 could be collected. Since a large part of the pHRE-BP2 protein is eluted at a higher salt concentration than  $\zeta$ -crystallin, a steeper 4X to 20X salt gradient was used to separate the two proteins. Using the new elution profile, only nine fractions were collected from 4X to 20X salt and five fractions were collected at a 20X salt concentration. pHRE-BP2 was partially eluted from the FPLC column as the salt gradient increases from 4X to 20X, but the majority of the protein is eluted at a 20X salt concentration (Fig. 8.2). Using the new purification scheme, a slight overlap of protein fractions remains. However, when fractions 4-6 are pooled, the majority of protein is  $\zeta$ -crystallin and when fractions 12-14 are pooled, the vast majority of protein is pHRE-BP2. The same protein elution profile was observed when  $\zeta$ -crystallin and pHRE-BP2 were purified from renal cortical cytosolic extracts from acidotic rats (Data not shown).

**Fig. 8.1. Original protein elution profile from an FPLC affinity column for  $\zeta$ -crys/Nqr.**

Fractions 1-14 were collected during a gradient elution from 4X to 20X salt concentration. The fractions were dialyzed overnight against 1X binding buffer and then separated by 10% SDS-PAGE and stained with 0.1% silver nitrate.

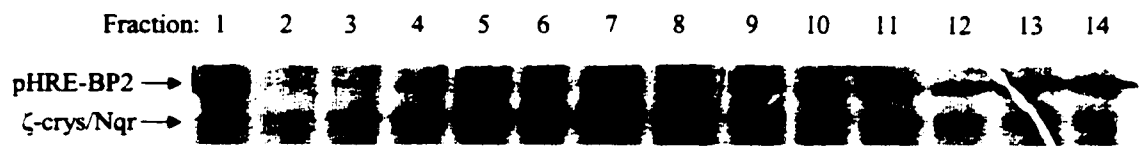
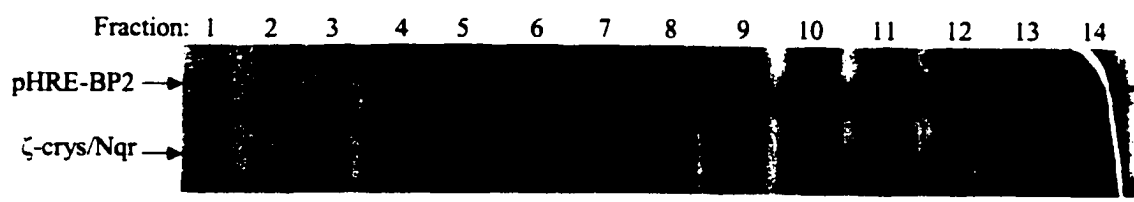


**Fig. 8.2. Protein elution profile from an FPLC affinity column.**

Fractions 1-9 were collected during a gradient elution from 4X to 20X salt concentration.

Fractions 10-14 were collected during elution at 20X salt concentration. The fractions were dialyzed overnight against 1X binding buffer and then separated by 10% SDS-PAGE and stained with 0.1% silver nitrate.



## **8.2 Preliminary studies of pHRE-BP2 binding**

### **8.2.1 $\zeta$ -crystallin and pHRE-BP2 bind GA(R2-I)**

Binding studies were conducted to test whether the purified pHRE-BP2 bound GA(R2-I) RNA, a 25-nt RNA encoding the GA pHRE, in an EMSA. When increasing amounts of purified  $\zeta$ -crystallin were incubated with the GA(R2-I) RNA, an increase in the amount of protein/RNA complex was observed (Fig. 8.3). GA(R2-I) RNA incubated with increasing amounts of purified pHRE-BP2 also produced an increased level of a protein/RNA complex that had slightly different mobility. The extent of protein/RNA complex formation was not as great using the purified pHRE-BP2 as was observed with purified  $\zeta$ -crystallin (Fig. 8.3). Protein/RNA complexes of the same mobility were observed when the two proteins were purified from renal cortical cytosolic extracts isolated from acidotic rats (Fig. 8.4).

The binding of purified  $\zeta$ -crystallin and pHRE-BP2 to GA(R2-I) RNA was compared to the protein binding observed using rat renal cortical cytosolic extracts. Both a  $\zeta$ -crystallin/RNA complex and a pHRE-BP2/RNA complex were observed when GA(R2-I) RNA was incubated with cytosolic extracts. The complexes observed using cytosolic extracts had similar mobility to those obtained using the purified proteins (Fig. 8.3).

To determine whether there was a synergistic binding of  $\zeta$ -crystallin and pHRE-BP2 to GA(R2-I) RNA, equal amounts of the two proteins were incubated either separately or together with the RNA. The level of  $\zeta$ -crystallin/RNA complex formation was not increased in the presence of pHRE-BP2. However, the level of pHRE-BP2/RNA complex may be increased slightly (1.25-fold) in the presence of  $\zeta$ -crystallin (Fig. 8.4).

**Fig. 8.3.  $\zeta$ -crys/Nqr and pHRE-BP2 bind GA(R2-I).**

[<sup>32</sup>P]-labeled GA(R2-I) RNA was incubated in the absence of protein (lane 1) or in the presence of a protein from rat renal cortical cytosolic extracts. Lane 2 contains 0.1  $\mu$ l of unpurified cytosolic extract. Lanes 3-5 contain increasing amounts of purified  $\zeta$ -crys/Nqr and lanes 6-8 contain increasing amounts of purified pHRE-BP2. The samples were resolved on a non-denaturing polyacrylamide gel. The gel was then dried and imaged with a PhosphorImager screen.

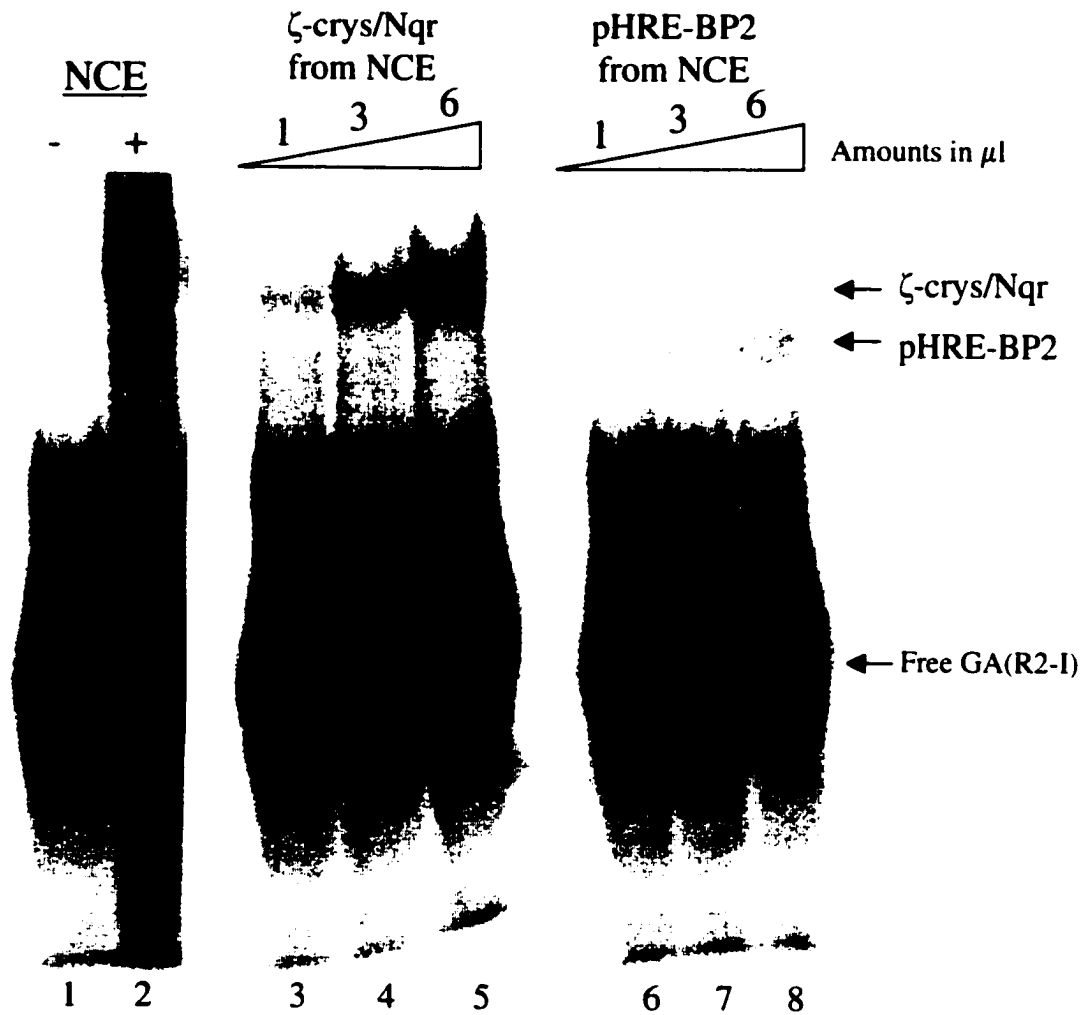
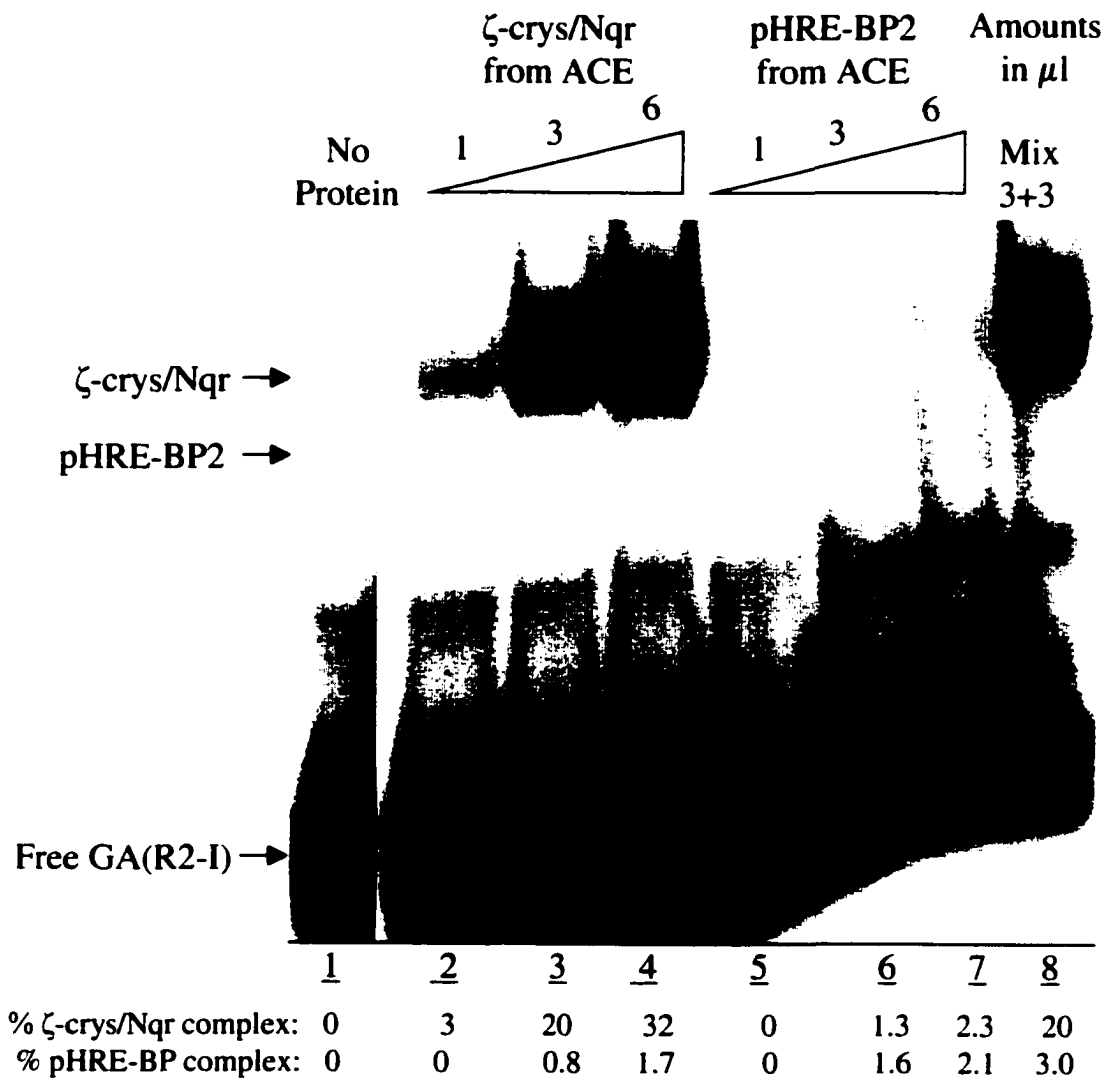


**Fig. 8.4. Analysis of binding synergism between  $\zeta$ -crys/Nqr and pHRE-BP2 to GA(R2-I).**

[<sup>32</sup>P]-labeled GA(R2-I) RNA was incubated in the absence of protein (lane 1). Increasing amounts of  $\zeta$ -crys/Nqr (lanes 2-4) and pHRE-BP2 (lanes 5-7) were incubated with the labeled GA(R2-I). Equal amounts of  $\zeta$ -crys/Nqr and pHRE-BP2 were incubated together with GA(R2-I) (lane 8). The samples were resolved on a non-denaturing gel polyacrylamide gel. The gel was then dried and imaged with a PhosphorImager screen.



## **8.2.2 Antibody analysis of pHRE-BP2**

Preliminary experiments were conducted to determine whether pHRE-BP2 is an isoform of  $\zeta$ -crystallin. When pHRE-BP2 was incubated with GA(R2-I) RNA, a shifted complex was formed. Neither the position of the shifted complex, nor the presence of the shifted complex was changed when an antibody towards  $\zeta$ -crystallin was added into the reaction mixture (Fig. 8.5). This data indicates that pHRE-BP2 is probably not an isoform of  $\zeta$ -crystallin. It is possible that pHRE-BP2 is a unique RNA binding protein or it could be a protein precursor or a modified form of  $\zeta$ -crystallin that is not in an appropriate conformation for antibody binding.

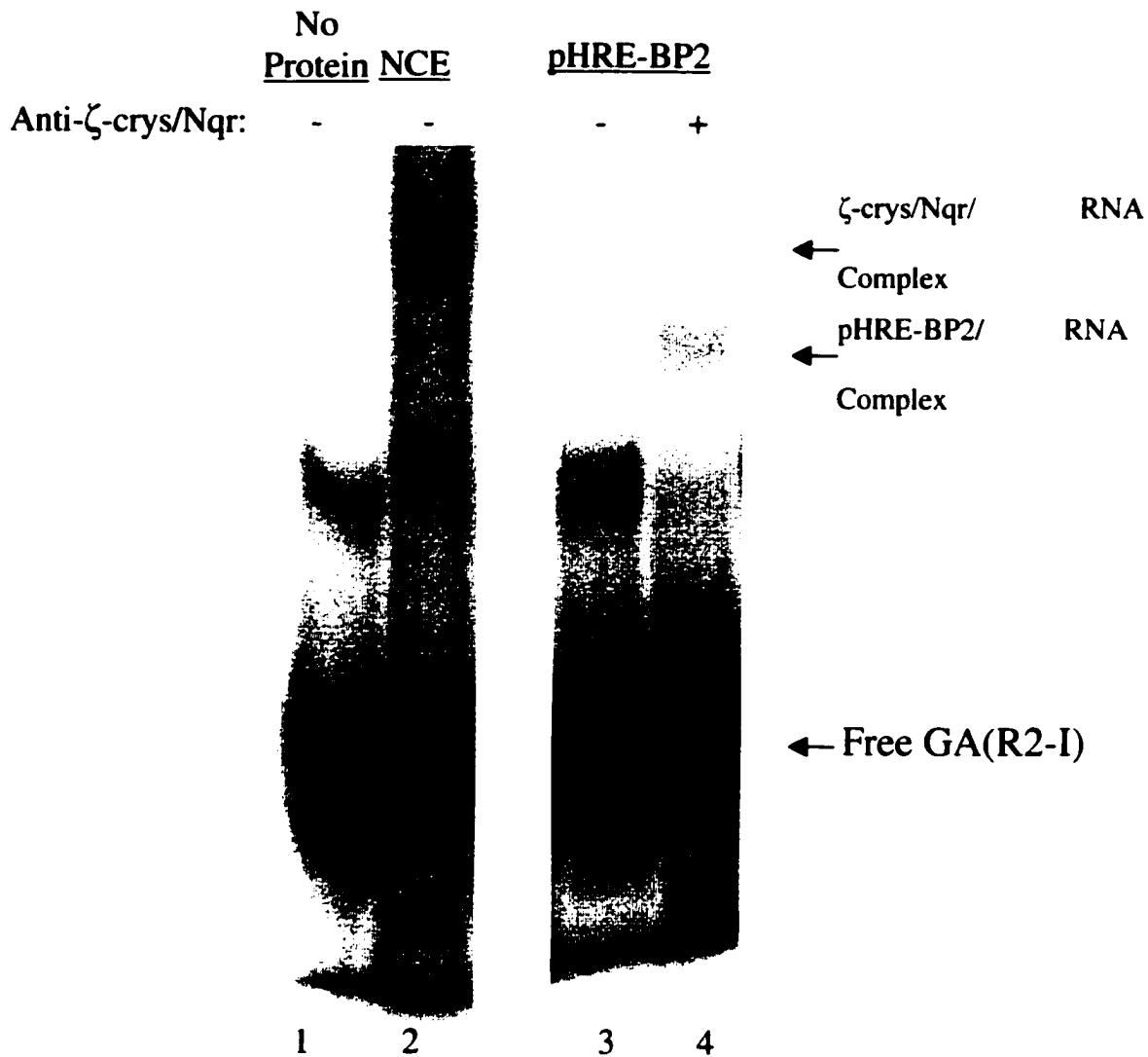
## **8.2.3 GA(R2-I) versus GA(R2-H) binding to pHRE-BP2**

The lower apparent binding affinity of GA(R2-I) to pHRE-BP2 compared to  $\zeta$ -crystallin was surprising since pHRE-BP2 appeared to bind to the RNA ligand with greater affinity than  $\zeta$ -crystallin (Fig. 8.3). A possible explanation is that the RNA affinity ligand contains a longer RNA sequence than the GA(R2-I) RNA, suggesting that there may be a second protein binding site adjacent to the GA(R2-I) region. Therefore, binding studies were conducted using the 76-nt GA(R2-H) RNA, which contains the full sequence of the RNA affinity ligand, plus an extra 22 ribonucleotides from the GA 3'-UTR.

It is important to note that when the purified pHRE-BP2 was concentrated to increase the amount of shifted complex, some  $\zeta$ -crystallin/GA(R2-H) complex was observed. Residual  $\zeta$ -crystallin in the pHRE-BP2 fractions bound about 2% of the GA(R2-H) RNA without RNase T1 treatment and 9% of the RNA in RNase T1-treated

**Fig. 8.5. Anti- $\zeta$ -crys/Nqr antibodies do not effect pHRE-BP2 binding to GA(R2-I).**

[<sup>32</sup>P]-labeled GA(R2-I) RNA was incubated in the absence (lane 1) or presence of normal rat renal cortical cytosolic extracts (NCE) (lane 2). In the remaining lanes (3-4), the GA(R2-I) RNA was incubated with purified pHRE-BP2, in the absence (lane 3) or presence (lane 4) of an anti- $\zeta$ -crys/Nqr antibody. The samples were resolved on a non-denaturing polyacrylamide gel. The gel was dried and imaged with a PhosphorImager screen.



samples. This data indicates that pHRE-BP2 was not completely purified from  $\zeta$ -crystallin. The percentage of RNA bound to purified  $\zeta$ -crystallin from  $\zeta$ -crystallin fractions is 15% in non-RNase T1 treated reactions and 35% in RNase T1 treated fractions (Fig. 8.6). The silver stained polyacrylamide gel of the eluted column fractions indicates that there is a low level of pHRE-BP2 present in the  $\zeta$ -crystallin fractions (Fig. 8.2). However, when the purified  $\zeta$ -crystallin samples were used in EMSAs, a significant level of pHRE-BP2/RNA complex was not observed (Fig. 8.6). The presence of residual  $\zeta$ -crystallin in the pHRE-BP2 fractions does not create a sufficient amount of shifted complex to account for the results discussed below.

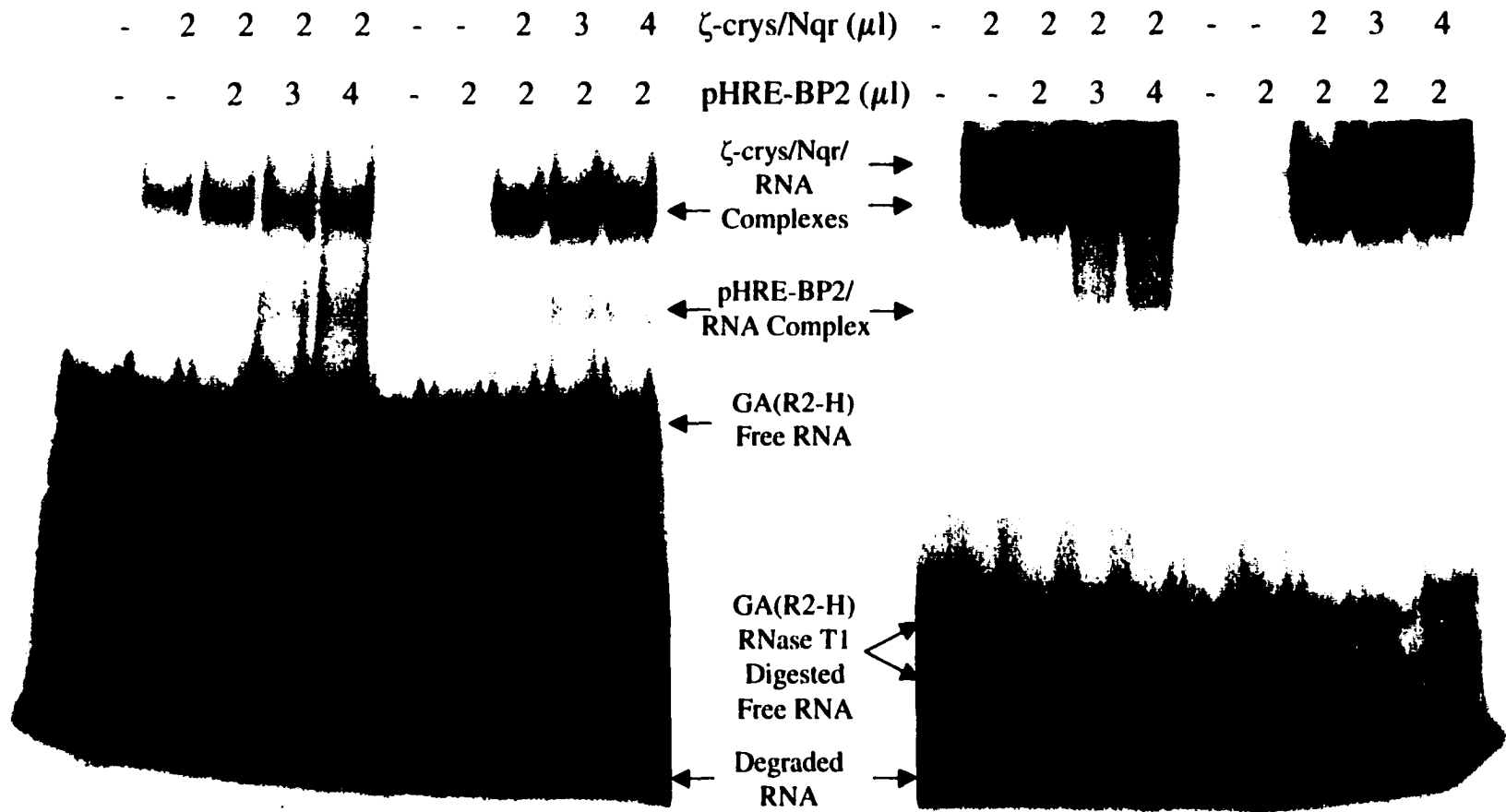
The binding of  $\zeta$ -crystallin and pHRE-BP2 to GA(R2-I) and GA(R2-H) was compared. Due to the increased length of the GA(R2-H), RNase T1 was added to the binding reactions to digest RNA not directly associated with a binding protein. Controls, in which RNA was either untreated or treated with RNase T1, were done to determine whether the addition of RNase T1 to the binding reaction had any effect on protein binding to the RNA.

Binding of  $\zeta$ -crystallin to GA(R2-I) RNA or untreated GA(R2-H) RNA produced similarly-sized protein/RNA complexes. The protein/RNA complex formed through the binding of GA(R2-I) or untreated GA(R2-H) to pHRE-BP2 were also similar in mobility to one another. However, the GA(R2-H) RNA/protein complexes were observed to migrate slightly faster than the GA(R2-I) RNA/protein complexes (Fig. 8.7). It is interesting to note that when RNase T1 is added to the reaction, the GA(R2-H) RNA/protein complexes show the same mobility observed using a GA(R2-I) RNA, indicating that the RNA digested by RNase T1 is responsible for the slight change

**Fig. 8.6. Synergistic binding to GA(R2-H) to  $\zeta$ -crys/Nqr and pHRE-BP2 and the effect of RNase T1 treatment on binding.**

[<sup>32</sup>P]-labeled GA(R2-H) RNA is incubated in the absence of binding proteins (lanes 1 and 11), or with  $\zeta$ -crys/Nqr and/or pHRE-BP2 (lanes 2-10 and 12-20). 2  $\mu$ l of  $\zeta$ -crys/Nqr was added to several reactions (lanes 2-5 and 12-15) with increasing amounts of pHRE-BP2 added to the reactions (lanes 3-5 and 13-15). 2  $\mu$ l of pHRE-BP2 was added to several reactions (lanes 6-10 and 16-20) with increasing amounts of pHRE-BP2 added to the reactions (lanes 7-10 and 17-20). Lanes 11-20 were treated with RNase T1 after the RNA/protein incubation. The samples were resolved on a non-denaturing polyacrylamide gel. The gel was dried and imaged with a PhosphorImager screen.

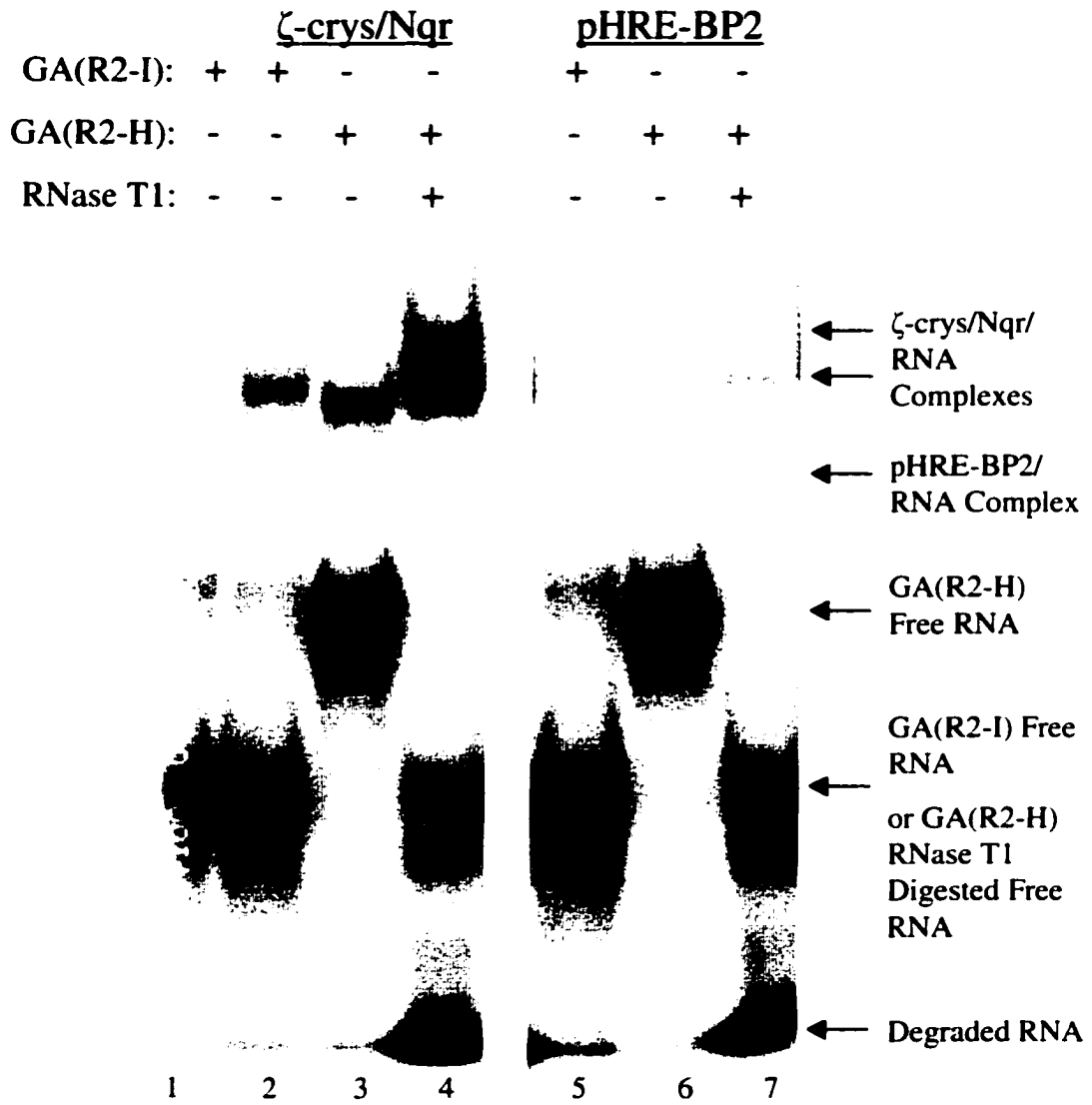
173



No RNase T1 Treatment										RNase T1 Treatment										
<u>1</u>	<u>2</u>	<u>3</u>	<u>4</u>	<u>5</u>	<u>6</u>	<u>7</u>	<u>8</u>	<u>9</u>	<u>10</u>		<u>11</u>	<u>12</u>	<u>13</u>	<u>14</u>	<u>15</u>	<u>16</u>	<u>17</u>	<u>18</u>	<u>19</u>	<u>20</u>
0	15	22	18	19	0	2.4	26	32	29	% ζ-crys/Nqr complex	0	35	54	55	61	0	9	55	72	76
0	2.1	6.1	10	12	0	3.9	8.3	10	8.3	% pHRE-BP complex	0	0	5.3	10	14	0	2.7	6.2	10	9.0

**Fig. 8.7. Comparison of  $\zeta$ -crys/Nqr and pHRE-BP2 binding to GA(R2-I) and GA(R2-H).**

[<sup>32</sup>P]-labeled GA(R2-I) RNA was used in lanes 1, 2, and 5, while [<sup>32</sup>P]-labeled GA(R2-H) RNA was used in lanes 3-4 and 6-7. The RNA was incubated with purified  $\zeta$ -crys/Nqr (lanes 2-4) or with purified pHRE-BP2 (lanes 5-7). Lanes 4 and 7 were treated with RNase T1 after RNA/protein incubation. The samples were resolved on a non-denaturing polyacrylamide gel. The gel was dried and imaged with a PhosphorImager screen.



in RNA/protein complex mobility. This data is consistent with the binding of both  $\zeta$ -crystallin and pHRE-BP2 to the pHRE sequence contained within GA(R2-I) RNA. It also illustrates that the remaining 50-nt of GA(R2-H) RNA does not contain an additional protein binding site.

The addition of RNase T1 to binding reactions containing GA(R2-H) caused another change in  $\zeta$ -crystallin binding. Two shifted complexes were formed, one migrating in the previously observed pattern and another complex migrating with slower mobility (Fig. 8.7). This could be indicative of multiple  $\zeta$ -crystallin molecules binding to the pHRE.

Another interesting difference arises between GA(R2-H) RNA/protein complexes that are either treated or untreated with RNase T1. There is an approximately two-fold increase in both  $\zeta$ -crystallin and pHRE-BP2 binding to GA(R2-H) when RNase T1 is added to the binding reaction (Fig. 8.7). The reason for this increased binding is uncertain.

The addition of  $\zeta$ -crystallin to binding reactions containing pHRE-BP2 and GA(R2-H) causes a two-fold increase in the formation of the pHRE-BP2/GA(R2-H) RNA complex formation (Fig. 8.6, lanes 7-8 and 17-18). When the converse experiment was conducted, in which pHRE-BP2 was added into the  $\zeta$ -crystallin/GA(R2-H) RNA binding reaction, there was no significant increase in the formation of the  $\zeta$ -crystallin/GA(R2-H) RNA complex that was not treated with RNase T1 (Fig. 8.6, lanes 3), but there was a 1.5-fold increase in complex formation when the reactions were treated with RNase T1 (Fig. 8.6, lanes 13). This indicates that synergistic binding occurs when both  $\zeta$ -crystallin and pHRE-BP2 are added into a binding reaction.

When increasing amounts of  $\zeta$ -crystallin were titrated into the pHRE-BP2/GA(R2-H), no additional increase in complex formation was observed (Fig. 8.6, lanes 9-10 and 19-20). Additionally, when increasing amounts of pHRE-BP2 were added into  $\zeta$ -crystallin/GA(R2-H) RNA binding reactions, no additional complex formation was observed (Fig. 8.6, lanes 4-5 and 14-15). The plateau in RNA/protein binding that occurs when increasing amounts of a second binding protein are added to the reaction could be due to saturation of the protein binding sites with RNA.

### **8.3 Future Directions**

One of the first steps in completing this project is to increase the level of pHRE-BP2/RNA complex that is formed. The most efficient method of accomplishing this is to further concentrate purified pHRE-BP2. An increased level of complex formation will make competition studies easier to perform and interpret. The results obtained in a competition study will indicate whether pHRE-BP2 binding to the GA pHRE is specific. Previous attempts to conduct competition studies provided no significant data due to the low level of protein/RNA complexes (Data not shown). The specificity of binding is especially important to determine since the GA(R2-H) RNA appears to bind pHRE-BP2 with less affinity than the slightly shorter RNA affinity ligand used during protein purification on an FPLC column. A possible explanation is that the 12-nt of pBSSK from the T7 promoter through the Asp718 at the start of the GA sequence adds four guanine, two cytosine, three adenine, and three thymidine residues to the DNA template, which could affect protein binding to the GA pHRE.

Once the specificity of pHRE-BP2 binding has been determined, it will be important to determine whether pHRE-BP2 and  $\zeta$ -crystallin interact with one another to

bind the GA pHRE. It should also be determined what role, if any, that pHRE-BP2 plays in the stabilization of GA mRNA during metabolic acidosis.

In order to answer these questions, the identity of pHRE-BP2 must be elucidated. This can be accomplished through micro-sequencing of the purified protein, as was done for the identification of  $\zeta$ -crystallin. An alternative approach is to use antibodies to known RNA binding proteins to determine whether a specific antibody recognizes pHRE-BP2 in a western blot analysis.

The data presented here provides preliminary results regarding pHRE-BP2 binding. However, further work must be conducted in order to complete the picture of how and why pHRE-BP2 binds to the GA pHRE sequence. The identification of pHRE-BP2 will, hopefully, provide further insight into how GA mRNA is stabilized during metabolic acidosis.

## References

- Adam, W., Simpson, D. P. 1974. Glutamine transport in rat kidney mitochondria in metabolic acidosis. *J Clin Invest* 54:165-74.
- Alberta, J. A., Rundell, K., Stiles, C. D. 1994. Identification of an activity that interacts with the 3'-untranslated region of c-myc mRNA and the role of its target sequence in mediating rapid mRNA degradation. *J Biol Chem* 269:4532-8.
- Amasino, R. M. 1986. Acceleration of nucleic acid hybridization rate by polyethylene glycol. *Anal Biochem* 152:304-7.
- Banner, C., Silverman, S., Thomas, J. W., Lampel, K. A., Vitkovic, L., et al. 1987. Isolation of a human brain cDNA for glutamate dehydrogenase. *J Neurochem* 49:246-52.
- Brennan, C. M., Gallouzi, I. E., Steitz, J. A. 2000. Protein ligands to HuR modulate its interaction with target mRNAs in vivo. *J Cell Biol* 151:1-14.
- Brosnan, J., Vinay, P., Gougoux, A., Halperin, R. 1988. Renal ammonia production and its implications for acid-base balance. In *pH Homeostasis-Mechanism and Control*, ed. H. D. pp. 281-304. New York: Academic
- Burch, H. B., Narins, R. G., Chu, C., Fagioli, S., Choi, S., et al. 1978. Distribution along the rat nephron of three enzymes of gluconeogenesis in acidosis and starvation. *Am J Physiol* 235:F246-53.
- Chen, C., Okayama, H. 1987. High-efficiency transformation of mammalian cells by plasmid DNA. *Mol Cell Biol* 7:2745-52.
- Chen, C. Y., Chen, T. M., Shyu, A. B. 1994. Interplay of two functionally and structurally distinct domains of the c-fos AU-rich element specifies its mRNA-destabilizing function. *Mol Cell Biol* 14:416-26.
- Chen, C. Y., Gherzi, R., Ong, S. E., Chan, E. L., Rajmakers, R., et al. 2001. AU binding proteins recruit the exosome to degrade ARE-containing mRNAs. *Cell* 107:451-64.

- Chen, C. Y., Shyu, A. B. 1994. Selective degradation of early-response-gene mRNAs: functional analyses of sequence features of the AU-rich elements. *Mol Cell Biol* 14:8471-82.
- Chen, C. Y., Shyu, A. B. 1995. AU-rich elements: characterization and importance in mRNA degradation. *Trends Biochem Sci* 20:465-70.
- Chen, C. Y., Xu, N., Shyu, A. B. 1995. mRNA decay mediated by two distinct AU-rich elements from c-fos and granulocyte-macrophage colony-stimulating factor transcripts: different deadenylation kinetics and uncoupling from translation. *Mol Cell Biol* 15:5777-88.
- Chomczynski, P., Sacchi, N. 1987. Single-step method of RNA isolation by acid guanidinium thiocyanate-phenol-chloroform extraction. *Anal Biochem* 162:156-9.
- CLONTECH Laboratories Inc. 1999. Tet-Off and Tet-On Gene Expression Systems User Manual. In *Protocol #PT3001-1* www.clontech.com
- Cunningham, K. S., Hanson, M. N., Schoenberg, D. R. 2001. Polysomal ribonuclease 1 exists in a latent form on polysomes prior to estrogen activation of mRNA decay. *Nucleic Acids Res* 29:1156-62.
- Curthoys, N. P., Gstraunthaler, G. 2001. Mechanism of increased renal gene expression during metabolic acidosis. *Am J Physiol Renal Physiol* 281:F381-90.
- Curthoys, N. P., Lowry, O. H. 1973. The distribution of glutaminase isoenzymes in the various structures of the nephron in normal, acidotic, and alkalotic rat kidney. *J Biol Chem* 248:162-8.
- Curthoys, N. P., Watford, M. 1995. Regulation of glutaminase activity and glutamine metabolism. *Annu Rev Nutr* 15:133-59
- D'Alessio, J. M., Harris, G. H., Perna, P. J., Paule, M. R. 1981. Ribosomal ribonucleic acid repeat unit of *Acanthamoeba castellanii*: cloning and restriction endonuclease map. *Biochemistry* 20:3822-7.
- Das, A. T., Moerer, P., Charles, R., Moorman, A. F., Lamers, W. H. 1989. Nucleotide sequence of rat liver glutamate dehydrogenase cDNA. *Nucleic Acids Res* 17:2355.
- Decker, C. J., Parker, R. 1993. A turnover pathway for both stable and unstable mRNAs in yeast: evidence for a requirement for deadenylation. *Genes Dev* 7:1632-43.
- Dubois, M. F., Bellier, S., Seo, S. J., Bensaude, O. 1994. Phosphorylation of the RNA polymerase II largest subunit during heat shock and inhibition of transcription in HeLa cells. *J Cell Physiol* 158:417-26.

- Fan, X. C., Steitz, J. A. 1998. Overexpression of HuR, a nuclear-cytoplasmic shuttling protein, increases the in vivo stability of ARE-containing mRNAs. *Embo J* 17:3448-60.
- Feifel, E., Obexer, P., Andratsch, M., Euler, S., Taylor, L., et al. 2002. p38 MAPK mediates acid-induced transcription of PEPCK in LLC-PK(1)-FBPase(+) cells. *Am J Physiol Renal Physiol* 283:F678-88.
- Gagna, C. E., Chen, J. H., Kuo, H. R., Lambert, W. C. 1998. Binding properties of bovine ocular lens zeta-crystallin to right-handed B-DNA, left-handed Z-DNA, and single-stranded DNA. *Cell Biol Int* 22:217-25
- Gao, M., Fritz, D. T., Ford, L. P., Wilusz, J. 2000. Interaction between a poly(A)-specific ribonuclease and the 5' cap influences mRNA deadenylation rates in vitro. *Mol Cell* 5:479-88.
- Gao, M., Wilusz, C. J., Peltz, S. W., Wilusz, J. 2001. A novel mRNA-decapping activity in HeLa cytoplasmic extracts is regulated by AU-rich elements. *Embo J* 20:1134-43.
- Garland, D., Rao, P. V., Del Corso, A., Mura, U., Zigler, J. S., Jr. 1991. zeta-Crystallin is a major protein in the lens of *Camelus dromedarius*. *Arch Biochem Biophys* 285:134-6.
- Gonzalez, P., Hernandez-Calzadilla, C., Rao, P. V., Rodriguez, I. R., Zigler, J. S., Jr., Borras, T. 1994a. Comparative analysis of the zeta-crystallin/quinone reductase gene in guinea pig and mouse. *Mol Biol Evol* 11:305-15.
- Gonzalez, P., Rao, P. V., Zigler, J. S., Jr. 1994b. Organization of the human zeta-crystallin/quinone reductase gene (CRYZ). *Genomics* 21:317-24.
- Goodman, A. D., Fuisz, R. E., Cahill, G. F., Jr. 1966. Renal gluconeogenesis in acidosis, alkalosis, and potassium deficiency: its possible role in regulation of renal ammonia production. *J Clin Invest* 45:612-9.
- Gorman, C., Padmanabhan, R., Howard, B. H. 1983. High efficiency DNA-mediated transformation of primate cells. *Science* 221:551-3.
- Gossen, M., Bujard, H. 1992. Tight control of gene expression in mammalian cells by tetracycline-responsive promoters. *Proc Natl Acad Sci U S A* 89:5547-51.
- Grosset, C., Chen, C. Y., Xu, N., Sonenberg, N., Jacquemin-Sablon, H., Shyu, A. B. 2000. A mechanism for translationally coupled mRNA turnover: interaction between the poly(A) tail and a c-fos RNA coding determinant via a protein complex. *Cell* 103:29-40.
- Gstraunthaler, G., Handler, J. S. 1987. Isolation, growth, and characterization of a gluconeogenic strain of renal cells. *Am J Physiol* 252:C232-8.

- Haile, D. J., Rouault, T. A., Harford, J. B., Kennedy, M. C., Blondin, G. A., et al. 1992. Cellular regulation of the iron-responsive element binding protein: disassembly of the cubane iron-sulfur cluster results in high-affinity RNA binding. *Proc Natl Acad Sci U S A* 89:11735-9.
- Hansen, W. R., Barsic-Tress, N., Taylor, L., Curthoys, N. P. 1996. The 3'-nontranslated region of rat renal glutaminase mRNA contains a pH- responsive stability element. *Am J Physiol* 271:F126-31
- Hanson, M. N., Schoenberg, D. R. 2001. Identification of in vivo mRNA decay intermediates corresponding to sites of in vitro cleavage by polysomal ribonuclease 1. *J Biol Chem* 276:12331-7.
- Hanson, R. W., Reshef, L. 1997. Regulation of phosphoenolpyruvate carboxykinase (GTP) gene expression. *Annu Rev Biochem* 66:581-611
- Hentze, M. W. 1994. Enzymes as RNA-binding proteins: a role for (di)nucleotide-binding domains? *Trends Biochem Sci* 19:101-3.
- Holcomb, T., Curthoys, N. P., Gstraunthaler, G. 1995. Subcellular localization of PEPCK and metabolism of gluconeogenic substrains of renal cell lines. *Am J Physiol* 268:C449-57.
- Hsu, C. L., Stevens, A. 1993. Yeast cells lacking 5'→3' exoribonuclease 1 contain mRNA species that are poly(A) deficient and partially lack the 5' cap structure. *Mol Cell Biol* 13:4826-35.
- Hughey, R. P., Rankin, B. B., Curthoys, N. P. 1980. Acute acidosis and renal arteriovenous differences of glutamine in normal and adrenalectomized rats. *Am J Physiol* 238:F199-204.
- Hwang, J. J., Curthoys, N. P. 1991. Effect of acute alterations in acid-base balance on rat renal glutaminase and phosphoenolpyruvate carboxykinase gene expression. *J Biol Chem* 266:9392-6.
- Hwang, J. J., Perera, S., Shapiro, R. A., Curthoys, N. P. 1991. Mechanism of altered renal glutaminase gene expression in response to chronic acidosis. *Biochemistry* 30:7522-6.
- Kaiser, S., Hwang, J. J., Smith, H., Banner, C., Welbourne, T. C., Curthoys, N. P. 1992. Effect of altered acid-base balance and of various agonists on levels of renal glutamate dehydrogenase mRNA. *Am J Physiol* 262:F507-12.
- Krebs, H. 1935. Metabolism of amino-acids. IV. The synthesis of glutamine from glutamic acid and ammonia, and the enzymic hydrolysis of glutamine in animal tissues. *Biochem J* 29:1951-69

- Lai, W. S., Carballo, E., Strum, J. R., Kennington, E. A., Phillips, R. S., Blackshear, P. J. 1999. Evidence that tristetraprolin binds to AU-rich elements and promotes the deadenylation and destabilization of tumor necrosis factor alpha mRNA. *Mol Cell Biol* 19:4311-23.
- Laterza, O. F., Curthoys, N. P. 2000. Specificity and functional analysis of the pH-responsive element within renal glutaminase mRNA. *Am J Physiol Renal Physiol* 278:F970-7.
- Laterza, O. F., Hansen, W. R., Taylor, L., Curthoys, N. P. 1997. Identification of an mRNA-binding protein and the specific elements that may mediate the pH-responsive induction of renal glutaminase mRNA. *J Biol Chem* 272:22481-8
- Lee, D. C., Gonzalez, P., Wistow, G. 1994. Zeta-crystallin: a lens-specific promoter and the gene recruitment of an enzyme as a crystallin. *J Mol Biol* 236:669-78.
- Loflin, P., Chen, C. Y., Shyu, A. B. 1999. Unraveling a cytoplasmic role for hnRNP D in the in vivo mRNA destabilization directed by the AU-rich element. *Genes Dev* 13:1884-97.
- Loflin, P., Lever, J. E. 2001. HuR binds a cyclic nucleotide-dependent, stabilizing domain in the 3' untranslated region of Na(+)/glucose cotransporter (SGLT1) mRNA. *FEBS Lett* 509:267-71.
- Lowell, J. E., Rudner, D. Z., Sachs, A. B. 1992. 3'-UTR-dependent deadenylation by the yeast poly(A) nuclease. *Genes Dev* 6:2088-99.
- Lowry, O. H., Rosebrough, N. J., Farr, A. L., Randall, R. J. 1951. Protein measurement with Folin phenol reagent. *J Biol Chem* 193:265-275
- Meister, A. 1975. Function of glutathione in kidney via the gamma-glutamyl cycle. *Med Clin North Am* 59:649-66.
- Melton, D. A., Krieg, P. A., Rebagliati, M. R., Maniatis, T., Zinn, K., Green, M. R. 1984. Efficient in vitro synthesis of biologically active RNA and RNA hybridization probes from plasmids containing a bacteriophage SP6 promoter. *Nucleic Acids Res* 12:7035-56.
- Min, H., Turck, C. W., Nikolic, J. M., Black, D. L. 1997. A new regulatory protein, KSRP, mediates exon inclusion through an intronic splicing enhancer. *Genes Dev* 11:1023-36.
- Ming, X. F., Kaiser, M., Moroni, C. 1998. c-jun N-terminal kinase is involved in AUUUA-mediated interleukin-3 mRNA turnover in mast cells. *Embo J* 17:6039-48.

- Ming, X. F., Stoecklin, G., Lu, M., Looser, R., Moroni, C. 2001. Parallel and independent regulation of interleukin-3 mRNA turnover by phosphatidylinositol 3-kinase and p38 mitogen-activated protein kinase. *Mol Cell Biol* 21:5778-89.
- Muhrad, D., Decker, C. J., Parker, R. 1994. Deadenylation of the unstable mRNA encoded by the yeast MFA2 gene leads to decapping followed by 5'→3' digestion of the transcript. *Genes Dev* 8:855-66.
- Mukherjee, D., Gao, M., O'Connor, J. P., Raijmakers, R., Pruijn, G., et al. 2002. The mammalian exosome mediates the efficient degradation of mRNAs that contain AU-rich elements. *Embo J* 21:165-74.
- Nakatani, Y., Banner, C., von Herrath, M., Schneider, M. E., Smith, H. H., Freese, E. 1987. Comparison of human brain and liver glutamate dehydrogenase cDNAs. *Biochem Biophys Res Commun* 149:405-10.
- Nakatani, Y., Schneider, M., Banner, C., Freese, E. 1988. Complete nucleotide sequence of human glutamate dehydrogenase cDNA. *Nucleic Acids Res* 16:6237.
- Neu, J., Shenoy, V., Chakrabarti, R. 1996. Glutamine nutrition and metabolism: where do we go from here ? *Faseb J* 10:829-37.
- Nissim, I. 1999. Newer aspects of glutamine/glutamate metabolism: the role of acute pH changes. *Am J Physiol* 277:F493-7.
- Peng, S. S., Chen, C. Y., Shyu, A. B. 1996. Functional characterization of a non-AUUUA AU-rich element from the c- jun proto-oncogene mRNA: evidence for a novel class of AU-rich elements. *Mol Cell Biol* 16:1490-9.
- Peng, S. S., Chen, C. Y., Xu, N., Shyu, A. B. 1998. RNA stabilization by the AU-rich element binding protein, HuR, an ELAV protein. *Embo J* 17:3461-70.
- Perera, S. Y., Chen, T. C., Curthoys, N. P. 1990. Biosynthesis and processing of renal mitochondrial glutaminase in cultured proximal tubular epithelial cells and in isolated mitochondria. *J Biol Chem* 265:17764-70.
- Perera, S. Y., Voith, D. M., Curthoys, N. P. 1991. Biosynthesis and processing of mitochondrial glutaminase in HTC hepatoma cells. *Biochem J* 273:265-70.
- Porter, D., Curthoys, N. P. 1997. Use of thermostable and Escherichia coli RNase H in RNA mapping studies. *Anal Biochem* 247:279-86.
- Preisig, P. A., Alpern, R. J. 1988. Chronic metabolic acidosis causes an adaptation in the apical membrane Na/H antiporter and basolateral membrane Na(HCO<sub>3</sub>)<sub>3</sub> symporter in the rat proximal convoluted tubule. *J Clin Invest* 82:1445-53.
- Rao, P. V., Gonzalez, P., Persson, B., Jornvall, H., Garland, D., Zigler, J. S., Jr. 1997. Guinea pig and bovine zeta-crystallins have distinct functional characteristics

- highlighting replacements in otherwise similar structures. *Biochemistry* 36:5353-62.
- Rao, P. V., Krishna, C. M., Zigler, J. S., Jr. 1992. Identification and characterization of the enzymatic activity of zeta-crystallin from guinea pig lens. A novel NADPH:quinone oxidoreductase. *J Biol Chem* 267:96-102.
- Rao, P. V., Zigler, J. S., Jr. 1992. Purification and characterization of zeta-crystallin/quinone reductase from guinea pig liver. *Biochim Biophys Acta* 1117:315-20.
- Richter, J. D. 1999. Cytoplasmic polyadenylation in development and beyond. *Microbiol Mol Biol Rev* 63:446-56.
- Ross, J. 1995. mRNA stability in mammalian cells. *Microbiol Rev* 59:423-50.
- Sachs, A. B. 1993. Messenger RNA degradation in eukaryotes. *Cell* 74:413-21.
- Sambrook, J., Fritsch, E. F., Manniatis, T. 1989. *Molecular Cloning: A Laboratory Manual*. 2nd ed. Cold Spring Harbor, NY: Cold Spring Harbor Laboratory Press. 6.1-6.48 pp.
- Schousboe, A., Westergaard, N., Waagepetersen, H. S., Larsson, O. M., Bakken, I. J., Sonnewald, U. 1997. Trafficking between glia and neurons of TCA cycle intermediates and related metabolites. *Glia* 21:99-105.
- Seyama, S., Saeki, T., Katunuma, N. 1973. Comparison of properties and inducibility of glutamate dehydrogenases in rat kidney and liver. *J Biochem (Tokyo)* 73:39-45.
- Shapiro, R. A., Farrell, L., Srinivasan, M., Curthoys, N. P. 1991. Isolation, characterization, and in vitro expression of a cDNA that encodes the kidney isoenzyme of the mitochondrial glutaminase. *J Biol Chem* 266:18792-6.
- Shapiro, R. A., Haser, W. G., Curthoys, N. P. 1987. Immunoblot analysis of glutaminase peptides in intact and solubilized mitochondria isolated from various rat tissues. *Biochem J* 242:743-7.
- Shyu, A. B., Wilkinson, M. F. 2000. The double lives of shuttling mRNA binding proteins. *Cell* 102:135-8.
- Sonnewald, U., Westergaard, N., Schousboe, A. 1997. Glutamate transport and metabolism in astrocytes. *Glia* 21:56-63.
- Souba, W. 1993. *Glutamine: Physiology, Biochemistry, and Nutrition in Critical Illness* Austin: R.G. Landes. 110 pp.
- Squires, E. J., Hall, D. E., Brosnan, J. T. 1976. Arteriovenous differences for amino acids and lactate across kidneys of normal and acidotic rats. *Biochem J* 160:125-8.

- Srinivasan, M., Kalousek, F., Curthoys, N. P. 1995. In vitro characterization of the mitochondrial processing and the potential function of the 68-kDa subunit of renal glutaminase. *J Biol Chem* 270:1185-90.
- Stoecklin, G., Ming, X. F., Looser, R., Moroni, C. 2000. Somatic mRNA turnover mutants implicate tristetraprolin in the interleukin-3 mRNA degradation pathway. *Mol Cell Biol* 20:3753-63.
- Tang, A., Curthoys, N. P. 2001. Identification of zeta-crystallin/NADPH:quinone reductase as a renal glutaminase mRNA pH response element-binding protein. *J Biol Chem* 276:21375-80.
- Tannen, R. 1993. Renal ammonia production and excretion. In *Handbook of Physiology . Renal Physiology*. pp. 1017-1059. Vol. I, sect 8, ch 23. Bethesda: Am Physiol Soc
- Tong, J., Harrison, G., Curthoys, N. P. 1986. The effect of metabolic acidosis on the synthesis and turnover of rat renal phosphate-dependent glutaminase. *Biochem J* 233:139-44.
- Tong, J., Shapiro, R. A., Curthoys, N. P. 1987. Changes in the levels of translatable glutaminase mRNA during onset and recovery from metabolic acidosis. *Biochemistry* 26:2773-7.
- van Hoof, A., Parker, R. 1999. The exosome: a proteasome for RNA? *Cell* 99:347-50.
- van Hoof, A., Parker, R. 2002. Messenger RNA degradation: beginning at the end. *Curr Biol* 12:R285-7.
- Wang, Z., Kiledjian, M. 2000. The poly(A)-binding protein and an mRNA stability protein jointly regulate an endoribonuclease activity. *Mol Cell Biol* 20:6334-41.
- Wang, Z., Kiledjian, M. 2001. Functional link between the mammalian exosome and mRNA decapping. *Cell* 107:751-62.
- Wells, S. E., Hillner, P. E., Vale, R. D., Sachs, A. B. 1998. Circularization of mRNA by eukaryotic translation initiation factors. *Mol Cell* 2:135-40.
- Wilson, G. M., Brewer, G. 1999. Identification and characterization of proteins binding A + U-rich elements. *Methods* 17:74-83.
- Wilson, T., Treisman, R. 1988. Removal of poly(A) and consequent degradation of c-fos mRNA facilitated by 3' AU-rich sequences. *Nature* 336:396-9.
- Winzen, R., Kracht, M., Ritter, B., Wilhelm, A., Chen, C. Y., et al. 1999. The p38 MAP kinase pathway signals for cytokine-induced mRNA stabilization via MAP kinase-activated protein kinase 2 and an AU-rich region-targeted mechanism. *Embo J* 18:4969-80.

- Wright, P. A., Knepper, M. A. 1990. Glutamate dehydrogenase activities in microdissected rat nephron segments: effects of acid-base loading. *Am J Physiol* 259:F53-9.
- Wright, P. A., Packer, R. K., Garcia-Perez, A., Knepper, M. A. 1992. Time course of renal glutamate dehydrogenase induction during NH<sub>4</sub>Cl loading in rats. *Am J Physiol* 262:F999-1006.
- Xu, N., Chen, C. Y., Shyu, A. B. 1997. Modulation of the fate of cytoplasmic mRNA by AU-rich elements: key sequence features controlling mRNA deadenylation and decay. *Mol Cell Biol* 17:4611-21.
- Xu, N., Chen, C. Y., Shyu, A. B. 2001. Versatile role for hnRNP D isoforms in the differential regulation of cytoplasmic mRNA turnover. *Mol Cell Biol* 21:6960-71.
- Xu, N., Loflin, P., Chen, C. Y., Shyu, A. B. 1998. A broader role for AU-rich element-mediated mRNA turnover revealed by a new transcriptional pulse strategy. *Nucleic Acids Res* 26:558-65
- Zhang, W., Wagner, B. J., Ehrenman, K., Schaefer, A. W., DeMaria, C. T., et al. 1993. Purification, characterization, and cDNA cloning of an AU-rich element RNA-binding protein, AUF1. *Mol Cell Biol* 13:7652-65.
- Zhao, Z., Chang, F. C., Furneaux, H. M. 2000. The identification of an endonuclease that cleaves within an HuR binding site in mRNA. *Nucleic Acids Res* 28:2695-701.